Oncology and Translational Medicine

Volume 5 • Number 1 • February 2019

Oncology and Translational Medicine Volume 5 • Number 1 • February 2019 pp 1–51

邮发代号：38-121
ISSN 2095-9621

GENERAL INFORMATION
≫otm.tjh.com.cn

ISSN 2095-9621
CN 42-1865/R

Oncology and Translational Medicine

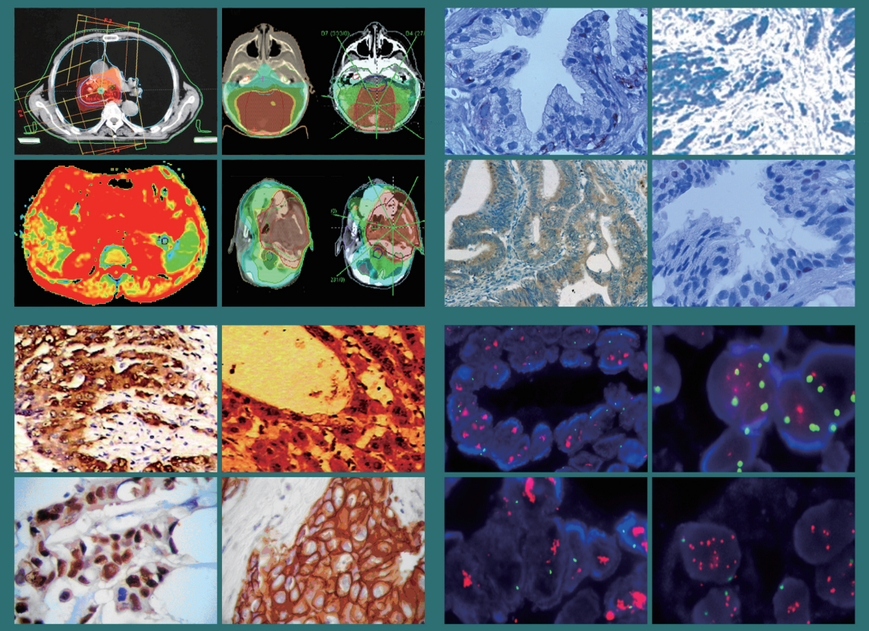

Volume 5
Number 1
February 2019

Oncology and Translational Medicine

Oncology and Translational Medicine
February 2019 Volume 5 Number 1

Contents

Call For Papers
Oncology and Translational Medicine

(CN 42-1865/R, ISSN 2095-9621)

Dear Authors,

Oncology and Translational Medicine (OTM), a peer-reviewed open-access journal, is very interested in your study. If you have unpublished papers in hand and have the idea of making our journal a vehicle for your research interests, please feel free to submit your manuscripts to us via the Paper Submission System.

Aims & Scope

- Lung Cancer
- Liver Cancer
- Pancreatic Cancer
- Gastrointestinal Tumors
- Breast Cancer
- Thyroid Cancer
- Bone Tumors
- Genitourinary Tumors
- Brain Tumor
- Blood Diseases
- Gynecologic Oncology
- ENT Tumors
- Skin Cancer
- Cancer Translational Medicine
- Cancer Imageology
- Cancer Chemotherapy
- Radiotherapy
- Tumors Psychology
- Other Tumor-related Contents

Contact Us
Editorial office of Oncology and Translational Medicine
Tongji Hospital
Tongji Medical College
Huazhong University of Science and Technology
Jie Fang Da Dao 1095
430030 Wuhan, China
Tel.: 86-27-69378388
Email: dmedizin@tjh.tjmu.edu.cn;
dmedizin@sina.com

Oncology and Translational Medicine (OTM) is sponsored by Tongji Hospital, Tongji Medical College, Huazhong University of Science and Technology, China (English, bimonthly).

OTM mainly publishes original and review articles on oncology and translational medicine. We are working with the commitment to bring the highest quality research to the widest possible audience and share the research work in a timely fashion.

Manuscripts considered for publication include regular scientific papers, original research, brief reports and case reports. Review articles, commentaries and letters are welcome.

About Us

- Peer-reviewed
- Rapid publication
- Online first
- Open access
- Both print and online versions

For more information about us, please visit:
http://otm.tjh.com.cn

Oncology and Translational Medicine
DOI 10.1007/s10330-018-0313-3
February 2019, Vol. 5, No. 1, P1–P5

ORIGINAL ARTICLE

Intravenous injection of AAV-PHP.eB across the blood-brain barrier in the adult mouse for central nervous system gene therapy*

Yongwei Shu[1], Jie Yao[2] (Co-first author), Yang Qu[1], Jing Zheng[2], Jing Ding[1], Lina Zhang[1], Yefan Wang[2], Linlin Zhao[1], Jingyu Zhang[1] (✉), Siqi Tang[2] (✉)

[1] Department of Neurology, The Fourth Hospital of Harbin Medical University, Heilongjiang 150001, China
[2] Laboratory of Molecular Neuropharmacology, School of Pharmacy, East China University of Science and Technology, Shanghai 200237, China

Abstract

Objective To verify the neurotypicality of AAV-PHP.eB after tail vein injection in adult mice and its efficiency in crossing the blood-brain barrier (BBB).

Methods The rAAV-SYN-GFP plasmid was constructed, and adult C57BL mice were injected with AAV-PHP.eB: SYN-GFP in the tail vein (300 nL, virus titer 3×10^9 vg) and in the prefrontal lobe (50 L, virus titer 5×10^{11} vg). The green fluorescent protein (GFP) signal in the brain was observed at two weeks, while the GFP signal in the peripheral organs was observed at four weeks.

Results Two weeks after tail vein injection, GFP expression was observed throughout the brain, especially in the cortex, hippocampus, and geniculate nucleus. No GFP signal was observed or detected by western blotting in the peripheral organs after four weeks. GFP signal was observed mainly at the local site after prefrontal lobe injection.

Conclusion AAV-PHP.eB: SYN-GFP can effectively cross the BBB in adult mice. Using a neuron-specific promoter allows exogenous gene expression in neurons; therefore, AAV-PHP.eB can be used as an effective carrier for studying diseases in the central nervous system (CNS).

Received: 24 October 2018
Revised: 23 December 2018
Accepted: 17 January 2019

Key words: gene therapy; AAV-PHP.eB; blood-brain barrier; regulatory element; noninvasive viral injection

Over the past 20 years, gene therapy has been developed greatly [1]. In particular, recombinant adeno-associated Viruses (rAAV) are commonly used for delivering genes and vaccines. Safety and efficacy have been evaluated in the clinical trials of therapies for different diseases, including Leber's congenital amaurosis type 2, Duchenne muscular dystrophy, and hemophilia B [2–5].

AAVs are a kind of non-enveloped single-stranded DNA virus classified as a parvovirus, and their replication depends on the presence of adenoviruses or herpes simplex viruses (also called helper viruses) [6]. They can establish a latent infection in different cell types while having no association with any human disease, making them potential vectors for carrying exogenous transgenes. With genetic engineering, genomes as big as 4.7 kilobases can be loaded and inserted in a region flanked by two inverted terminal repeats, rep for AAV replication and cap for structure proteins and helper genes, and therapeutic rAAV can be produced.

Variant AAV capsid sequences generate different serotypes, and currently the 11 most common AAV variants (AAV1–AAV11) have been elucidated from human and non-human tissues [7]. Most serotypes show neuron tropism, including AAV1, AAV2, AAV5, and AAV9 [8–10]. These neurotropic viral vectors are promising candidates for the treatment of central nervous system

✉ Correspondence to: Jingyu Zhang. Email: zhangjingyuyx@163.com
Siqi Tang. Email: tangsiqi1@hotmail.com

* Supported by grants from the Innovation of Science and Technology Talents in Harbin (No. 2017RAXQJ045) and the Fundamental Research Funds for the Central Universities.

(CNS) diseases.

With increasing interests in gene therapy for CNS diseases, more basic research and pre-clinical trials are currently being conducted. A key issue is finding efficient vector delivery strategies to overcome limited rAAV transduction efficiency due to the blood-brain barrier (BBB). Though direct intracranial injection is effective for diseases with a localized lesion such as Parkinson's disease, other diseases such as glioblastoma multiforme (GBM), lysosomal storage diseases (LSDs), Alzheimer's disease, and Canavan's disease require widespread vector delivery to systematically manipulate pathological changes [11–14]. Under these circumstances, a better approach is to administer the vectors through vasculature injections for global delivery [15]. In addition, in contrast to intracranial injections that can cause brain injury, relatively noninvasive intravenous or intra-arterial injections can lower surgical risks.

Among the mentioned neurotropic characteristic of AAV serotype variants, AAV9 is the only serotype that can efficiently get through the BBB after intravenous injection in adult murine models [16], which makes it practical for further studies on noninvasive viral injection targeting the CNS [17]. According to a review in 2017, AAV-PHP.eB has been applied in clinical trials on neurodegenerative disorders including Parkinson's disease [19–20] and Alzheimer's disease [15].

Besides neurotropic serotypes, strong expression promoters like cytomegalovirus (CMV), CMV early enhancer/chicken β-actin (CAG), and phosphoglycerate kinase promoters are also considered and are the most widely used in AAV vectors for robust transgene expression, both in neurons and non-neuronal cells such as motor neurons, astrocytes, and Purkinje cells [21, 16]. Different neurons in the CNS form circuits involved in relative independent functions; thus, how to target a gene to a particular area and how it performs under expected conditions are big challenges for AAV clinical application, driving us to carefully consider expression patterns after AAV transduction. Cell type-specific transgene expression can provide a more tailored expression pattern by targeting certain cell types during pathogenesis. Human synapsin (hSyn) is a commonly used promoter to limit expression in neurons [22].

According to an updated report, AAV-PHP.eB performs as the most efficient serotype that can cross the BBB and rapidly diffuse in the CNS after intravenous administration. We want to establish a noninvasive delivery strategy with a high transduction efficiency and tissue specificity. Here, we report that, by applying the Syn promoter with the regulatory element WPRE that can improve GFP expression, we observed high neuronal specificity of expression and high efficiency of delivery of the exogenous gene in the nervous system, demonstrating the tissue specificity and the potential for wider usage of this gene delivery strategy.

Materials and Methods

Animals

C57BL mice were bought from Shanghai Jiesijie Laboratory Animal Technology Company.

Vector design and virus production

Vector information containing the hSyn promoter was obtained on Addgene (No.50465), and the gene vector hSyn-EGFP is as follows (Fig.1).

Plasmid AAV-PHP.eB was purchased from PackGene Biotech, LLC. The vector genome, the helper plasmid containing cap9 sequences, and adenovirus genes were transfected into 293 cells, and the virus was harvested from lytic 293 cells and culture supernatants. A dose of 1×10^{13} vector genomes (vg) virus was obtained for animal injection.

Virus administration

Virus injections were carried out in 8-week-old male C57BL mice with body weight of 250–300 g. In order to find the vessel, two white mice were injected in the tail vein, while the virus was delivered through the prefrontal lobe in two black mice assisted with a brain stereotaxic apparatus (Olympus, Japan).

Tissue preparation

At two and at four weeks after administration, one mouse of each injection route was obtained for cardiac perfusion. Phosphate-buffered saline (PBS) was kept running, followed by treatment with 4% paraformaldehyde (wt/vol) until the limbs of the mouse became stiff. Then, the brain and the internal organs, including the heart, liver, kidney, and lungs, were immersed in 4% paraformaldehyde and stored at 4 °C overnight. After dehydration by 15% and 30% (wt/vol) sucrose, tissues were embedded in Optimal Cutting Temperature compound and frozen at –80 °C for cryostat sectioning (Thermo).

Immunohistochemistry

Tissue slices (50 μm) were obtained for fluorescent staining. Briefly, slides were incubated at room temperature and washed with 10 μM PBS (pH 7.4) three times before blocking with 5% bovine serum albumin (BSA) and 0.3% Triton X-100 in 10 μM PBS for two hours. After washing with PBS three times, the slices were incubated with primary rabbit-derived GFP antibody (1:1000; Vector, USA) overnight at 4°C. Slices were subsequently washed with PBS, incubated with fluorescent dye labeled with donkey anti-rabbit IgG (488,

1:1000; Alexa Fluor, Invitrogen) for 30 mins, and then stained with DAPI (1:400; Haoran Biotech, Shanghai) for 20 mins to label the nuclei. After washing with PBS, the slides were mounted with non-fluorescent mounting media (Hydromount). Images were captured through a confocal microscope (Nikon-TIE-A1, Japan).

Western blotting

Tissue sections obtained from the brain, heart, kidney, lung, and stomach of intravenously injected mice were homogenized for western blotting. Primary antibodies of mouse anti-GFP (1:3000; Abcam, USA) and mouse anti-actin (1:5000; ProteinTech, USA) were added. Peroxidase-conjugated goat anti-mouse IgG secondary antibody (1:5000; Yeasen, China) was used. Protein bands were visualized by western blotting substrate (Tanon, China) and imaged using the chemiluminescence instrument (Tanon, China).

Results

First, we constructed a plasmid in which the AAV-PHP.eB sequence mediated the expression of EGFP under the control of the Syn promoter (Fig. 1). Then, virus was harvested from 293 cells and supernatants. Finally, we got 1×10^{13} vector genomes (vg) high-titer viral preparations.

In order to compare the transduction efficacy of different routes of administration, we separately employed tail vein injection and intracranial injection in 8-week-old non-transgenic mice (C57BL), as demonstrated in Fig. 2a. Two weeks after tail vein AAV-SYN-GFP administration, the global-scale nervous system was labeled by GFP fluorescence (Fig. 2b). GFP was particularly and strongly expressed in the cerebral cortex, hippocampus, geniculate nucleus, and cerebellar Purkinje fibers (Fig. 2d, 2e). Strong GFP fluorescence was also observed near the area of vector delivery two weeks after intracranial injection (Fig. 2c); beyond that area, GFP signal was sparsely observed. These results showed the global expression pattern of the target gene delivered by tail vain administration and that its efficacy is greater than that by prefrontal lobe injection. As previously described, we also further confirmed that these vectors can cross the BBB.

As GFP was driven by the neuron-specific promoter Syn, we clarified the GFP fluorescence in the internal organs four weeks after intravenous delivery. Though the background signal was high, we found scarce punctiform GFP signals in other tissues, including the kidney, lung, heart, stomach, and liver (Fig. 3). The result demonstrated high CNS specificity using AAV-PHP.eB with a neuron-specific promoter. In the liver, we observed different sectioned areas with high fluorescent background, but observed limited GFP signal. In order to further clarify the neurotropic characteristic of AAV vectors, tissues from different organs, including the midbrain, heart, kidney, lung, and stomach, were homogenized for western blotting (Fig. 4). Results further confirmed that GFP was only expressed in the brain, demonstrating the tissue-specific expression pattern of AAV vectors.

Discussion

Here, we demonstrated the capability of the new AAV capsid AAV-PHP.eB vector for specific targeting driven by a specific promoter with a substantial dose. We clarified that AAV-PHP.eB has two important advantages for application in gene therapy: First, the low required

Fig. 1 Schematic view of gene vector

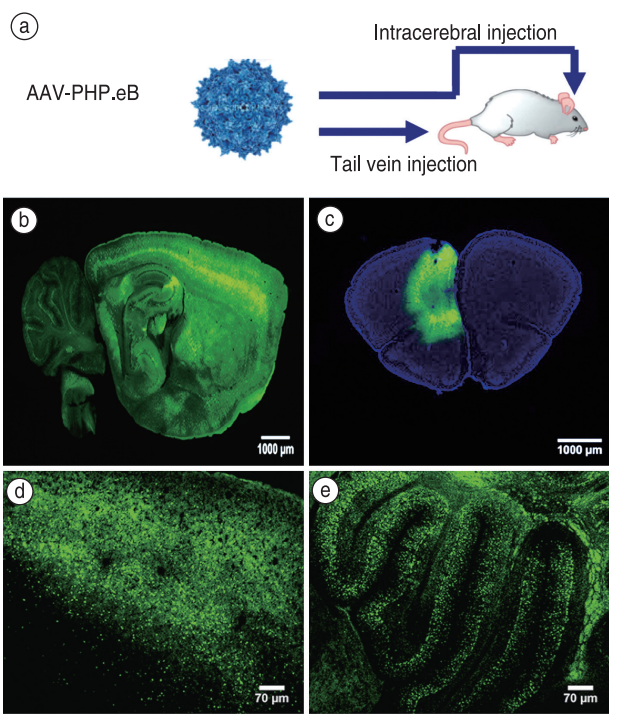

Fig. 2 Global GFP expression in the central nervous system after AAV-PHP.eB: SYN-GFP intravenous injection. (a) Schematic view depicting the operation of AAV-PHP.eB injection into the tail vein and the prefrontal lobe of an adult C57BL mouse; (b) After virus injection through the tail vein at 5×10^{11} vg per viral vector, the whole brain area showed strong GFP expression, especially in the cortex, hippocampus, and geniculate nucleus; (c) The virus was directly injected into the prefrontal lobe at 3×10^{9} vg per viral vector. The GFP fluorescence of the entire brain tissue was mainly concentrated around the injection site; (d) GFP-positive local area of cerebral cortex via tail vein injection; (e) GFP-positive local area of cerebellar Purkinje fibers

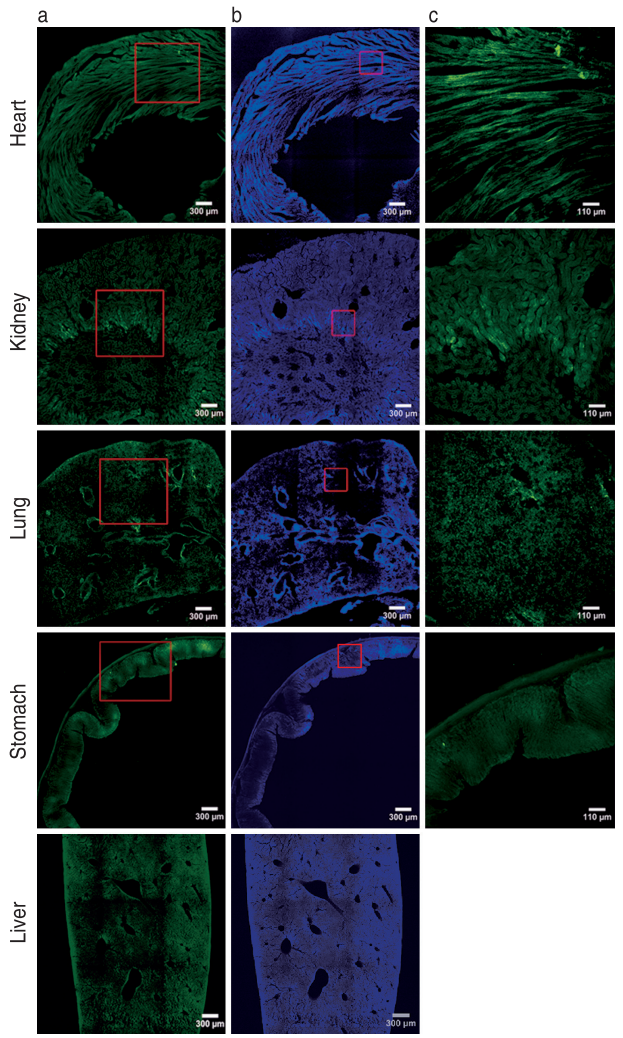

Fig. 3 No GFP signal was observed in the internal organs with AAV-PHP.eB: SYN-GFP intravenous injection after 4 weeks. Images show fluorescence expression by 2 different channels. Representative images of GFP channel (column a, green) and DAPI channel (column b, blue). (c) Amplified tissue images in red frame of column a. Scale bars were 300 μm (a, b) and 110 μm (c)

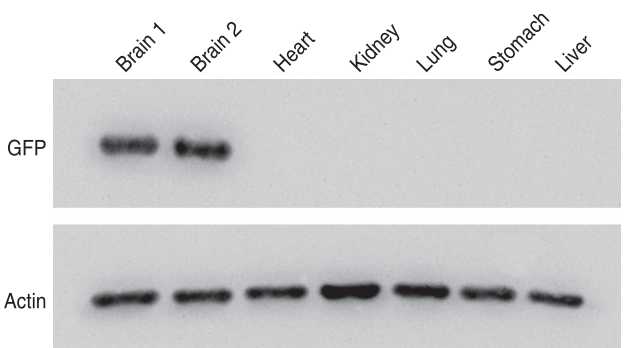

Fig. 4 No GFP expression in the internal organ tissues with AAV-PHP.eB: SYN-GFP intravenous injection after 4 weeks. The results further confirmed that GFP was expressed only in midbrain tissues

viral dose of AAV-PHP.eB (~10^{11} vg) that can cross the BBB and achieve effective expression in the target area via a tissue-specific promoter. Second, intravenous administration of AAV-PHP.eB: SYN showed little off-target effects on the liver, lung, and other peripheral organs.

It was previously reported that, after intravenous injection of AAV9, infected cells can be found in the CNS and in the peripheral nervous system (PNS) in neonatal mice, and in astrocytes and some hippocampal neurons during adulthood [23–24]. This initiated the development of various noninvasive viral delivery systems for the treatment of diseases of the CNS. To date, noninvasive gene delivery systems targeting the CNS have been widely increasing. It was reported that three fluorescent proteins were separately packed into AAV-PHP.eB with hSyn1 promoter and mixed vectors showed the multicolor hues in the cortex, striatum, and cerebellum after intravenous administration in non-transgenic mice. This indicated efficient transduction, and that AAV-PHP.eB with a neuron-specific promoter can be a promising tool for gene delivery to specific cell types in the brain. More interestingly, another type of AAV-PHP.S capsid was also reported to specifically transduce dorsal root ganglia, as well as cardiac and enteric neurons [25].

For viral gene therapy targeting CNS diseases in the future, it should be carefully considered if the goal is to express the target gene in as many cells systemically, or to express the gene in target cells of a local region. In the brain, rAAV9 delivery can initially transduce neurons and astrocytes using a strong CBA promoter, though the ratios varied across studies [23, 26].

Our experiment used the most common neuron-specific promoter hSyn. We clearly observed GFP expression in many regions, including the cortex and hippocampus, the two most studied areas for brain function. We observed a wider GFP expression pattern in the substantia nigra pars reticulata, motor cortex, and hippocampus by neonatal intracerebroventricular injection of rAAV9 [27], which is consistent with our observation, demonstrating that intravascular injection in adult mice also shows efficient transduction results like that in neonatal mice. Since rAAV9 reduces neurotropism and favors astroglial transduction as mice grow up, using a cell type-specific promoter can avoid this change; however, how the transduction efficiency is affected at different stages still requires further study. In addition, whether engineered AAV-PHP.eB shows a different transduction efficiency compared with that of rAAV9 also requires further clarification. All these studies are critical for determining the best injection window and load in treating long-term progressive diseases.

In order to study the function of genes in different brain diseases, as well as to find therapeutic targets, more

tissue-specific promoters like CamkIIα for excitatory neurons and strong promoters like CMV and CAG should be tested [28–29]. This will promote further studies and applications of AAV gene therapy in CNS diseases in the future.

No current clinical treatments can prevent the progression of CNS diseases; however, gene therapy has a strong potential to "permanently" cure disease by replacing a dysfunctional copy of a gene with a normal one [24]. Though many challenges from basic research to technical application remain to be addressed, clinical gene delivery trials with AAV-PHP.eB are increasing, and we believe that these will push viral gene therapy forward.

Conflicts of interest

The authors declare no potential conflicts of interest.

References

1. Saraiva J, Nobre RJ, Pereira de Almeida L. Gene therapy for the CNS using AAVs: The impact of systemic delivery by AAV9. J Control Release, 2016, 241: 94–109.
2. Bainbridge JW, Mehat MS, Sundaram V, *et al*. Long-term effect of gene therapy on Leber's congenital amaurosis. N Engl J Med, 2015, 372: 1887–1897.
3. Cideciyan AV, Hauswirth WW, Aleman TS, *et al*. Human RPE65 gene therapy for Leber congenital amaurosis: persistence of early visual improvements and safety at 1 year. Hum Gene Ther, 2009, 20: 999–1004.
4. Nathwani AC, Tuddenham EG, Rangarajan S, *et al*. Adenovirus-associated virus vector-mediated gene transfer in hemophilia B. N Engl J Med, 2011, 365: 2357–2365.
5. Testa F, Maguire AM, Rossi S, *et al*. Three-year follow-up after unilateral subretinal delivery of adeno-associated virus in patients with Leber congenital Amaurosis type 2. Ophthalmology, 2013, 120: 1283–1291.
6. Schaffer DV, Koerber JT, Lim KI. Molecular engineering of viral gene delivery vehicles. Annu Rev Biomed Eng, 2008, 10: 169–194.
7. Wu Z, Asokan A, Samulski RJ. Adeno-associated virus serotypes: vector toolkit for human gene therapy. Mol Ther, 2006, 14: 316–327.
8. Bartlett JS, Samulski RJ, McCown TJ. Selective and rapid uptake of adeno-associated virus type 2 in brain. Hum Gene Ther, 1998, 9: 1181–1186.
9. Mandel RJ, Burger C. Clinical trials in neurological disorders using AAV vectors: promises and challenges. Curr Opin Mol Ther, 2004, 6: 482–490.
10. Cearley CN, Wolfe JH. A single injection of an adeno-associated virus vector into nuclei with divergent connections results in widespread vector distribution in the brain and global correction of a neurogenetic disease. J Neurosci, 2007, 27: 9928–9940.
11. Meijer DH, Maguire CA, LeRoy SG, *et al*. Controlling brain tumor growth by intraventricular administration of an AAV vector encoding IFN-beta. Cancer Gene Ther, 2009, 16: 664–671.
12. Samaranch L, Salegio EA, San Sebastian W, *et al*. Strong cortical and spinal cord transduction after AAV7 and AAV9 delivery into the cerebrospinal fluid of nonhuman primates. Hum Gene Ther, 2013, 24: 526–532.
13. Chang M, Copper JD, Sleat DE, *et al*. Intraventricular enzyme replacement improves disease phenotypes in a mouse model of late infantile neuronal ceroid lipofuscinosis. Mol Ther, 2008, 16: 649–656.
14. Zhuang X, Xiang X, Gizzle W, *et al*. Treatment of brain inflammatory diseases by delivering exosome encapsulated anti-inflammatory drugs from the nasal region to the brain. Mol Ther, 2011, 19: 1769–1779.
15. Hocquemiller M, Giersch L, Audrain M, *et al*. Adeno-associated virus-based gene therapy for CNS diseases. Hum Gene Ther, 2016, 27: 478–496.
16. Zhang H, Yang B, Mu X, *et al*. Several rAAV vectors efficiently cross the blood-brain barrier and transduce neurons and astrocytes in the neonatal mouse central nervous system. Mol Ther, 2011, 19: 1440–1448.
17. Pulicherla N, Shen S, Yadav S, *et al*. Engineering liver-detargeted AAV9 vectors for cardiac and musculoskeletal gene transfer. Mol Ther, 2011, 19: 1070–1078.
18. Deverman BE, Pravdo PL, Simpson BP, *et al*. Cre-dependent selection yields AAV variants for widespread gene transfer to the adult brain. Nat Biotechnol, 2016, 34: 204–209.
19. Bartus RT, Baumann TL, Siffert J, *et al*. Safety/feasibility of targeting the substantia nigra with AAV2-neurturin in Parkinson patients. Neurology, 2013, 80: 1698–1701.
20. Mittermeyer G, Christine CW, Rosenbluth KH, *et al*. Long-term evaluation of a phase 1 study of AADC gene therapy for Parkinson's disease. Hum Gene Ther, 2012, 23: 377–381.
21. Ilieva H, Polymenidou M, Cleveland DW. Non-cell autonomous toxicity in neurodegenerative disorders: ALS and beyond. J Cell Biol, 2009, 187: 761–772.
22. Kügler S, Kilic E, Bähr M. Human synapsin 1 gene promoter confers highly neuron-specific long-term transgene expression from an adenoviral vector in the adult rat brain depending on the transduced area. Gene Ther, 2003, 10: 337–347.
23. Foust KD, Nurre E, Montgomery CL, *et al*. Intravascular AAV9 preferentially targets neonatal neurons and adult astrocytes. Nat Biotechnol, 2009, 27: 59–65.
24. Ojala DS, Amara DP, Schaffer DV. Adeno-associated virus vectors and neurological gene therapy. Neuroscientist, 2015, 21: 84–98.
25. Chan KY, Jang MJ, Yoo BB, *et al*. Engineered AAVs for efficient noninvasive gene delivery to the central and peripheral nervous systems. Nat Neurosci, 2017, 20: 1172–1179.
26. Gray SJ, Matagne V, Bachaboina L, *et al*. Preclinical differences of intravascular AAV9 delivery to neurons and glia: a comparative study of adult mice and nonhuman primates. Mol Ther, 2011, 19: 1058–1069.
27. McLean JR, Smith GA, Rocha EM, *et al*. Widespread neuron-specific transgene expression in brain and spinal cord following synapsin promoter-driven AAV9 neonatal intracerebroventricular injection. Neurosci Lett, 2014, 576: 73–78.
28. Li DP, Zhou JJ, Zhang J, *et al*. CaMKII regulates synaptic NMDA receptor activity of hypothalamic presympathetic neurons and sympathetic outflow in hypertension. J Neurosci, 2017, 37: 10690–10699.
29. Chira S, Jackson CS, Oprea I, *et al*. Progresses towards safe and efficient gene therapy vectors. Oncotarget, 2015, 6: 30675–30703.

DOI 10.1007/s10330-018-0313-3
Cite this article as: Shu YW, Yao J, Qu Y, *et al*. Intravenous injection of AAV-PHP.eB across the blood-brain barrier in the adult mouse for central nervous system gene therapy. Oncol Transl Med, 2019, 5: 1–5.

Oncology and Translational Medicine
DOI 10.1007/s10330-018-0317-7

February 2019, Vol. 5, No. 1, P6–P11

ORIGINAL ARTICLE

Analyzing proteins in colonic tissues from mice with ulcerative colitis using the iTRAQ technology*

Na Chen, Zhongyin Zhou (✉)

Department of Gastroenterology, Renmin Hospital of Wuhan University, Hubei Key Laboratory of Digestive Disease, Wuhan 430060, China

Abstract

Objective The aim of the study was to investigate the expression of proteins in colonic tissues of mice with ulcerative colitis (UC) by using isobaric tags for relative and absolute quantitation (iTRAQ), probe into the pathogenesis of UC, and find potential biomarkers of UC.

Methods Forty C57 mice were randomly divided into the control and model groups (20 mice in each group). The mice in the model group were administered dextran sulphate sodium (DSS) for 7 consecutive days ad libitum to induce acute colitis, and the colon tissue was extracted on the 8th day after the successful establishment of the UC model. Proteins were identified by the iTRAQ and tandem mass spectrometry techniques,and the identified proteins were analyzed by bioinformatics.

Results A total of 4019 proteins were identified among the two groups. Among them, 317 significant differentially expressed proteins (DEPs) were detected according to the screening criteria for selecting DEPs, i.e. fold change ratios ≥ 1.5 or ≤ 0.67 and *P*-values < 0.05, of which 156 were upregulated and 161 were downregulated. In the Gene Ontology (GO) analysis, the DEPs were classified into 48 functional categories, which contained biological process, cellular component, and molecular function. Based on the 317 DEPs, the KEGG pathway analysis identified 160 vital pathways.

Conclusion DEPs in colonic tissues of mice with UC were screened using the iTRAQ technique, which laid a foundation for further studies regarding the pathogenesis of UC.

Received: 13 November 2018
Revised: 15 December 2018
Accepted: 27 December 2018

Key words: ulcerative colitis (UC); isobaric tags for relative and absolute quantitation (iTRAQ); colonic tissue; differentially expressed proteins (DEPs)

Ulcerative colitis (UC) is a chronic non-specific inflammatory bowel disease with an unclear etiology and pathogenesis; it mainly affects the colon and is characterized by the inflammation of the colorectal mucosa and submucosa. The alternating periods of the relapse and remission of mucosal inflammation can have a serious impact on the life quality of the patients. The main clinical manifestations of UC are abdominal pain, diarrhea, and hematochezia [1–2]. In recent years, the incidence of UC is on the rise, and patients with UC are at an increased risk for colorectal cancer with the extension of the course of UC [3]. The risk of carcinogenesis 10 years after the onset of UC is higher; hence, UC is considered an intractable disease [4]. Most scholars believe that its pathogenesis is the result of the interaction of immune system disorders, genetic factors, environmental factors, microbial infection and so on [5]. Although new drugs and treatments have been emerging, their efficacy is not satisfactory. Therefore, there is an urgent need for a better understanding of the mechanism of UC and to find more effective and alternative molecular targets for treatment of this disease in clinical practice.

With the rapid development of proteomic techniques, isobaric tags for relative and absolute quantitation (iTRAQ) coupled with liquid chromatography-tandem mass spectrometry (LC-MS/MS) serves asa more powerful methodology for quantitative proteomics [6]. The iTRAQ technique is a quantitative technique involving isotope labeling that can simultaneously study up to eight different samples with good accuracy and repeatability; it has been applied in proteomics research very well [7–8]. In the present study, iTRAQ coupled with LC-MS/MS was

✉ Correspondence to: Zhongyin Zhou. Email: 13871029766@163.com
* Supported by a grant from the Natural Science Foundation of Hubei Province (No. 2011CHB025).

used to analyze the expression of proteins in the colonic tissue of mice with UC, and to explore the mechanism of UC, which laid a foundation for further studies on UC.

Materials and methods

Experimental animals

Forty wild-type male C57BL/6 mice that weighed 18–22 g (6–8 weeks old) and were of specific pathogen-free (SPF) grade were purchased from Vital River Laboratory Animal Technology Co., Ltd. (Beijing, China). They were housed in a pathogen-free-grade animal room under standard conditions [room temperature: (21 ± 2) °C, room relative humidity: 40%–60%, 12 h day/night cycle with lights], and fed with standard chow diet and water ad libitum for one week to adapt to the environment. All procedures involving animals were approved by the Animal Care Committee of the University of Wuhan, China (certificate No. SYXK(E)2015-0027).

Grouping and model preparation

Forty C57 mice were randomly divided into the control and model groups (n = 20 in each group) after 7 days of adaptive feeding. The mice in the control group were fed standard chow diet and water ad libitum for a week, while those in the model group were fed with drinking water containing 3% dextran sodium sulfate (DSS, molecular weight 36 000–50 000; MP Bio, Santa Ana, CA, USA) for 7 consecutive days to induce acute colitis. At day 8 of the experiment, the mice were sacrificed following isoflurane (GeneCreate Biological Engineering Co., Ltd., Wuhan, China) inhalation and cervical dislocation, and their colons were dissected. Then, the colon tissues were frozen in liquid nitrogen immediately and stored in a refrigerator at –80 ℃ for future use.

Protein extraction and quantification

The colonic tissues of mice from the control and model groups were randomly divided into two groups each, namely control 1, control 2, model 1, and model 2 (n = 10 each group). Then, the four samples were ground into a powder after being frozen in liquid nitrogen. The powder was dissolved with lysis buffer (containing 7 M urea, 2 M thiourea, 4% SDS, 40 mMtris-HCl, 1 mM PMSF, 2 mM EDTA, all which were procured from Sinopharm Chemical Reagent Co., Ltd, China). After five minutes, 10 mM DTT (Solarbio Science & Technology Co., Ltd, Beijing, China) was added to the samples. The suspension was sonicated for 15 minutes and then centrifuged at 4 ℃ and 13 000 rpm for 20 minutes. The precipitate was collected with chilled acetone (Sinopharm Chemical Reagent Co., Ltd, China) and incubated at –20 °C overnight. The precipitate was collected by treatment with a solution of 10 mM DTT for 1 hour at 56 ℃. Centrifugation was performed again, at 13 000 rpm for 20 min at 4 ℃; then, the precipitate was collected and dried. Protein concentrations were measured using the Bradford method [9]. All samples were stored at –80 ℃ prior to further analysis.

Protein digestion and iTRAQ labeling

First, 100 μg of each protein sample was reduced, alkylated, and then digested with trypsin (GeneCreate Biological Engineering Co., Ltd., Wuhan, China) overnight at 37 ℃. The samples were labeled with iTRAQ Reagent-8 plex Multiplex Kit (AB Sciex, USA) according to the manufacturer's instructions as follows: control 1 (tag 115), control 2 (tag 116), model 1 (tag 117), and model 2 (tag 118). Each group included two biological replicates, and each sample was pooled from ten individuals. Finally, all the labeled samples were mixed in equal amounts.

Protein fractionation and LC-MS/MS analysis

The labeled samples were fractionated using high-performance liquid chromatography (HPLC) system (Thermo Dinoex, USA) using a Durashell C18 column (5 be, 100 Å, 4.6 mm × 250 mm). Finally, 12 fractions were collected. LC-MS/MS analysis was performed using a Triple TOF 5600 plus system (AB Sciex, USA).

Data analysis

The original MS/MS file data were loaded into the Protein Pilot Software version 4.5 (AB Sciex, USA) for data analysis. For protein identification, the data was searched against the Uniprot database. Only unique peptides were considered for iTRAQ labeling quantification. In addition, only data with a false discovery rate (FDR) of < 1% were used for subsequent analyses. Proteins with fold change ratios ≥ 1.5 or ≤ 0.67 and P-values ≤ 0.05 were considered to be significantly differentially expressed. To determine the biological and functional properties of all the identified proteins, the identified protein sequences were mapped with Gene Ontology (GO) terms (http://geneontology.org/). The GO term matching was performed using blast2go v4.5 pipeline 5. The GO and Kyoto Encyclopedia of Genes and Genomes (KEGG) analyses were considered statistically significant at P < 0.05.

Results

Identification of differentially expressed proteins (DEPs) in the model and control groups

In this study, the mice in the model group showed obvious diarrhea, hematochezia, weight loss and so on, which indicated that the DSS administration had successfully induced acute UC. Using iTRAQ combined with LC-MS/MS proteomics technology, a total of 4019

proteins were identified, and 317 DEPs were identified in the model group, compared to the control group; of these, 156 proteins were upregulated and 161 were downregulated according to the criteria for defining DEPs (fold change ratios of ≥ 1.5 or ≤ 0.67, and $P \leq 0.05$). The top 10 upregulated proteins and top 10 downregulated proteins have been listed in Table 1.

GO analysis of the DEPs

GO analysis has been widely used to describe the molecular function of proteins [10]. In the GO analysis, all the DEPs were mapped to the terms in the GO database. The DEPs were classified into 48 functional categories, which contained biological process, cellular component, and molecular function. Biological processes accounted for 26 GO terms (such as cellular process, metabolic process, biological regulation, and response to stimulus), cellular components accounted for 10 GO terms (such as cell, cell part, organelle, and extracellular region), and molecular functions accounted for 12 GO terms (the most frequent were binding and catalytic activity), as shown in Fig. 1.

KEGG pathway analysis of the DEPs

KEGG pathways were constructed to better understand the biological pathways and elucidatethe molecular mechanisms involved in the progress of UC. Based on 317 differentially expressed proteins, the KEGG pathway analysis identified 160 vital pathways. We discovered that most of the DEPs were enriched in the metabolic pathways, microbial metabolism in diverse environments, and oxidative phosphorylation (Table 2 and Fig. 2).

Table 1 Top 10 upregulated and downregulated proteins (model vs. control, $P < 0.05$)

Accession	Protein name (Gene name)	Ratio (Model/control)	*P*-value
Upregulation			
Q53X15	S100 (S100a8)	26.2	0.001660956
Q3UBS3	Haptoglobin (Hp)	24.4	1.17489E-06
Q3TGR2	Fibrinogen (Fgb)	22.8	3.48954E-09
Q3UEM7	Fgg	18.6	9.71003E-06
Q3V2G1	Apoa1	18.4	4.85304E-06
O35744	Chil3	16.9	0.001728216
Q91VE7	Cramp	16.6	0.02424784
Q542I8	Itgb2	15.9	0.01233843
E9PV24	Fga	12.9	6.94809E-07
Q9DCE9	Igtp	11.8	0.001547599
Downregulation			
A0A0R4J077	Pentaxin (Mptx1)	0.05	0.000801551
Q9D7Z6	Clca1	0.19	2.86455E-10
Q8C7U7	Galnt6	0.21	0.007778632
Q53YP5	Fabp2	0.21	0.028193399
O88312	Agr2	0.22	6.66103E-05
E9QNL5	Sult1a1	0.22	0.000238775
Q3UER1	Aldob	0.26	0.000422554
A0A0R4J034	Pdxdc1	0.26	4.42615E-07
P05784	Keratin (Krt18)	0.26	1.57795E-06
Q545S0	Sulfurtransferase (Tst)	0.26	0.024794869

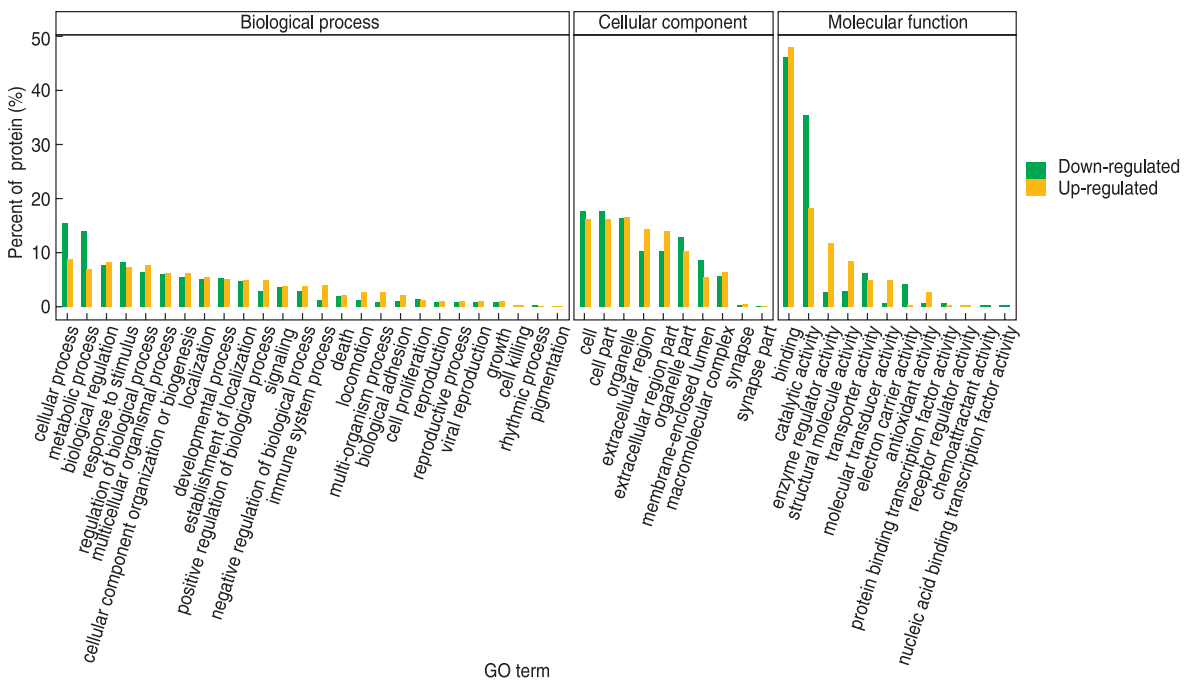

Fig. 1 GO classification. GO (Gene Ontology) analysis of all DEPs (model vs. control) according to the biological processes (left), cellular component (middle), and molecular function (right). Percent of proteins in each category are shown. The yellow color represents the upregulated proteins and the green color represents the downregulated proteinsk

Discussion

UC is a chronic condition in which the overreacting immune system may play an important role. Some studies have found that the incidence of UC has increased steadily in developed countries, while in developing countries, its incidence has rapidly been on the rise over the past few decades. This high incidence is manifested mainly in European and American countries; this could possibly be associated with the living environment and lifestyle of the West (such as drug use, environmental pollution, life stress) [11–12]. Therefore, there is an urgent need to understand the pathogenesis of UC and look for

Table 2 The top 10 pathways in the pathway enrichment analysis of DEPs in the model and control groups

Pathway ID	Pathway name	Proteins quantity
Ko00020	Citrate cycle (TCA cycle)	14
Ko01100	Metabolic pathways	89
Ko01120	Microbial metabolism in diverse environments	32
Ko04610	Complement and coagulation cascades	14
Ko00190	Oxidative phosphorylation	19
Ko05150	Staphylococcus aureus infection	12
Ko05012	Parkinson' disease	19
Ko00620	Pyruvate metabolism	11
Ko04972	Pancreatic secretion	13
Ko04512	ECM-receptor interaction	12

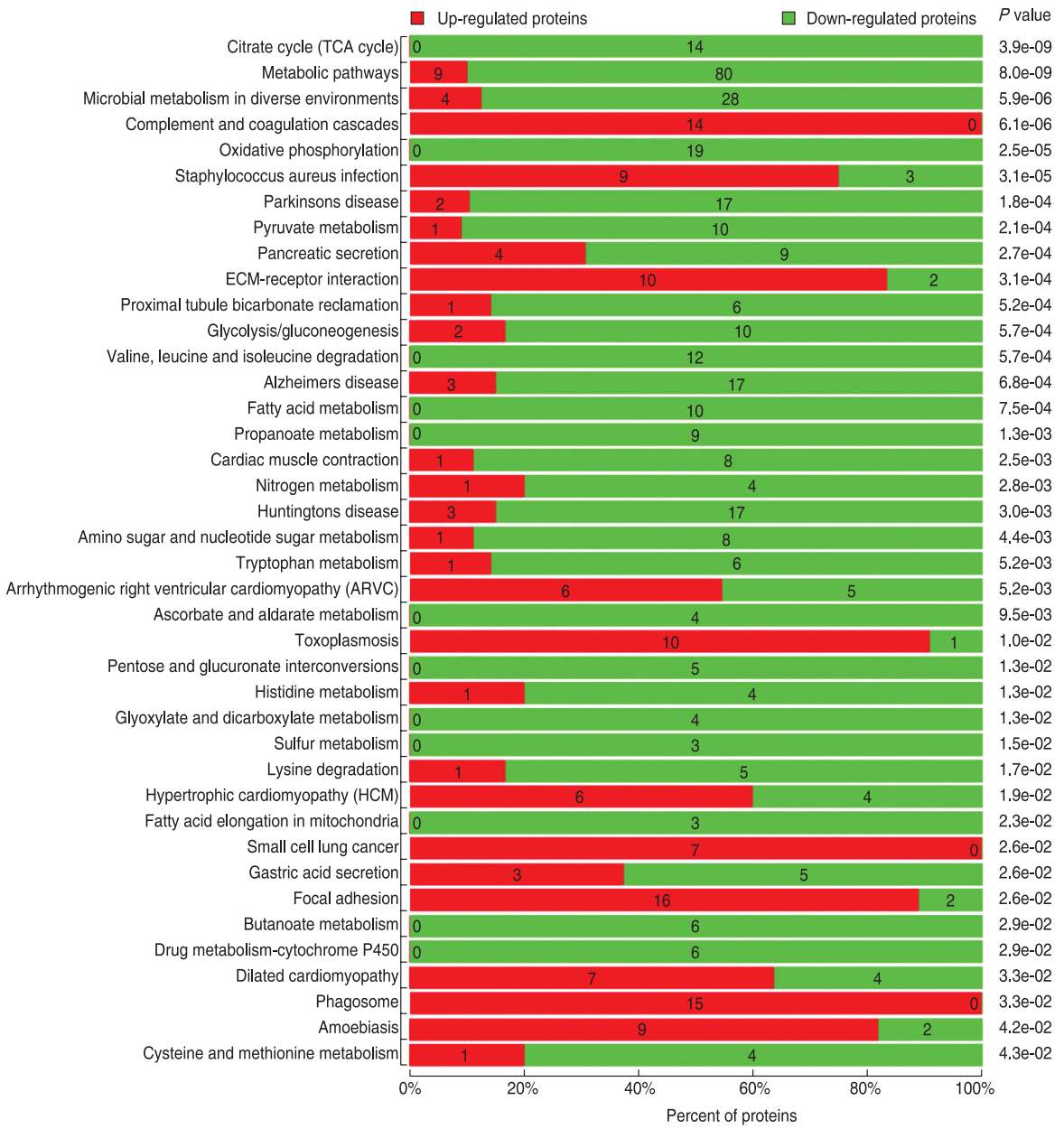

Fig. 2 Statistics of KEGG pathways (The red color represents the upregulated proteins and the green color represents the downregulated proteins)

effective biomarkers.

The present study is the first to report the proteomic profiling of mice with UC using iTRAQ combined with the LC-MS/MS technique; 4019 proteins were identified using the iTRAQ technique. Among the relative quantitative results, 317 significant DEPs were identified (proteins with fold change ratios ≥ 1.5 or ≤ 0.67 and $P \leq 0.05$), among which 156 proteins were found to be upregulated and 161 proteins were found to be downregulated.

Of these proteins, a significant increase of S100A8 expression was observed in the model group samples, when compared to the control group samples. As we all know, S100A8 is a low-molecular-weight (10.8-kDa) calcium-binding protein. In addition, it is also an important member of the S100 protein family. S100A8 and S100A9 form noncovalent homodimers and a heterodimer (S100A8/A9) in a calcium-dependent manner [13]. The S100 proteins participate in the onset of many inflammatory diseases such as rheumatoid arthritis (RA) [14], inflammatory bowel disease (IBD) [15], and so on. The bioinformatics analysis showed that S100A8 was mainly located in the cytoplasm, cell membrane, and cytoskeleton, mediating immune and biological functions. Some scholars believe that S100A8 can stimulate the migration and adhesion of human neutrophils to inflammatory sites and other pro-inflammatory activities [13]. At present, S100A8 has been used as a biomarker of inflammatory response to monitor the disease status and evaluate the therapeutic effects [15]. Its proinflammatory activity may be explained by the fact that the immune complex can stimulate the secretion of S100A8/A9 by neutrophils. By binding with RAGE and TLR4, it can induce the secretion of IL-6, IL-1β, TNF-α, and other cytokines via the intracellular MAPK and NF-kappa B signaling pathways, which can produce a series of inflammatory reactions [16]. In addition, S100A8/A9 also promotes the activation of the MAPK and NF-kB signaling pathways and the proliferation of cancer cells in colon-associated cancer [17]. The above studies suggest that S100A8 is an important biochemical marker that can be used in the clinical diagnosis and treatment of UC.

From Table 1, we found that the protein of Agr2 was downregulated markedly in the model group samples, compared to the case for the control group samples. The bioinformatics analysis showed that Agr2 was mainly located in the extracellular region, organelle, and cell part that participated in the regulation of biological processes. Previous researches have reported Agr2 mutationsin mice associated with diarrhea and goblet cell dysfunction; similar changes have been observed in patients with UC. Agr2 was expressed in tissues or organs that possess mucous-secreting cells or functions. Thus, Agr2 may be involved in the epithelial barrier function [18]. It is well known that UC is related to the destruction of colonic epithelial barriers that sustain the inflammation of the colon mucosa caused by the recruitment of lymphocytes and neutrophils into the lamina propria [19]. Some researchers have found that the expression level of Agr2 in UC patients was significantly lower than that in healthy people, and that Agr2 may be involved in the maintenance of epithelial integrity inmouse models [18]. In addition, Park has found that Agr2 is notably required for MUC2 mucin production, which is essential for immune regulation. Moreover, the expression of pro-inflammatory cytokines would increase in the absence of Agr2 [20]. Importantly, previous studies have shown that $Agr2^{-/-}$ mice spontaneously develop severe colitis [21]. The observations of all the above studies are consistent with our findings. Thus, we can select Agr2 as an effective and potential candidate biomarker for in-depth future investigations. However, the mechanism underlying this observation has not yet been fully explored.

In summary, this study used iTRAQ-based quantitative proteomics to analyze the DEPs in UC to unravel the unknown molecular mechanisms of UC. In addition, the present study demonstrates that S100A8 and Agr2 maybe potential biomarkers for UC. However, this study is only a preliminary study, and the specific functions and mechanisms of a series of DEPs need to be further verified.

Conflicts of interest

The authors indicate no potential conflicts of interest.

References

1. Mirza AH, Berthelsen CH, Seemann SE, *et al*. Transcriptomic landscape of lncRNAs in inflammatory bowel disease. Genome Med, 2015, 7: 39.
2. Adams SM, Bornemann PH. Ulcerative colitis. Am Fam Physician, 2013, 87: 699–705.
3. Pekow J, Meckel K, Dougherty U, *et al*. miR-193a-3p is a key tumor suppressor in ulcerative colitis-associated colon cancer and promotes carcinogenesis through upregulation of IL17RD. Clin Cancer Res, 2017, 23: 5281–5291.
4. Eaden JA, Abrams KR, Mayberry JF. The risk of colorectal cancer in ulcerative colitis: a meta-analysis. Gut, 2001, 48: 526–535.
5. Zhang YZ, Li YY. Inflammatory bowel disease: pathogenesis. World J Gastroenterol, 2014, 20: 91–99.
6. Wang WS, Liu XH, Liu LX, *et al*. iTRAQ-based quantitative proteomics reveals myoferlin as a novel prognostic predictor in pancreatic adenocarcinoma. J Proteomics, 2013, 91: 453–465.
7. Ross PL, Huang YN, Marchese JN, *et al*. Multiplexed protein quantitation in Saccharomyces cerevisiae using amine-reactive isobaric tagging reagents. Mol Cell Proteomics, 2004, 3: 1154–1169.
8. Karp NA, Huber W, Sadowski PG, *et al*. Addressing accuracy and precision issues in iTRAQ quantitation. Mol Cell Proteomics, 2010, 9: 1885–1897.
9. Bradford MM. A rapid and sensitive method for the quantitation of microgram quantities of protein utilizing the principle of protein-dye

binding. Anal Biochem, 1976, 72: 248–254.
10. Munk S, Refsgaard JC, Olsen JV. Systems analysis for interpretation of phosphoproteomics data. Methods Mol Biol, 2016, 1355: 341–360.
11. Kaplan GG, Ng SC. Understanding and preventing the global increase of inflammatory bowel disease. Gastroenterology, 2017, 152: 313–321.
12. Shouval DS, Rufo PA. The role of environmental factors in the pathogenesis of inflammatory bowel diseases: A review. JAMA Pediatr, 2017, 171: 999–1005.
13. Ryckman C, Vandal K, Rouleau P, *et al*. Proinflammatory activities of S100: proteins S100A8, S100A9, and S100A8/A9 induce neutrophil chemotaxis and adhesion. J Immunol, 2003, 170: 3233–3242.
14. Hammer HB, Odegard S, Fagerhol MK, *et al*. Calprotectin (a major leucocyte protein) is strongly and independently correlated with joint inflammation and damage in rheumatoid arthritis. Ann Rheum Dis, 2007, 66: 1093–1097.
15. Foell D, Wittkowski H, Ren Z, *et al*. Phagocyte-specific S100 proteins are released from affected mucosa and promote immune responses during inflammatory bowel disease. J Pathol, 2008, 216: 183–192.
16. Tydén H, Lood C, Gullstrand B, *et al*. Increased serum levels of S100A8/A9 and S100A12 are associated with cardiovascular disease in patients with inactive systemic lupus erythematosus. Rheumatology (Oxford), 2013, 52: 2048–2055.
17. Ichikawa M, Williams R, Wang L, *et al*. S100A8/A9 activate key genes and pathways in colon tumor progression. Mol Cancer Res, 2011, 9: 133–148.
18. Zheng W, Rosenstiel P, Huse K, *et al*. Evaluation of AGR2 and AGR3 as candidate genes for inflammatory bowel disease. Genes Immun, 2006, 7: 11–18.
19. Thomas S, Hoxha K, Alexander W, *et al*. Intestinal barrier tightening by a cell-penetrating antibody to Bin1, a candidate target for immunotherapy of ulcerative colitis. J Cell Biochem, 2019, 120: 4225–4237.
20. Park SW, Zhen G, Verhaeghe C, *et al*. The protein disulfide isomerase AGR2 is essential for production of intestinal mucus. Proc Natl Acad Sci USA, 2009, 106: 6950–6955.
21. Zhao F, Edwards R, Dizon D, *et al*. Disruption of Paneth and goblet cell homeostasis and increased endoplasmic reticulum stress in Agr2-/- mice. Dev Biol, 2010, 338: 270–279.

DOI 10.1007/s10330-018-0317-7
Cite this article as: Chen N, Zhou ZY. Analyzing proteins in colonic tissues from mice with ulcerative colitis using the iTRAQ technology. Oncol Transl Med, 2019, 5: 6–11.

Oncology and Translational Medicine
DOI 10.1007/s10330-018-0326-6

February 2019, Vol. 5, No. 1, P12–P18

ORIGINAL ARTICLE

Predictive value of tumor volume reduction rates before and after induction chemotherapy in determining the radiosensitivity and prognosis of locally advanced nasopharyngeal carcinomas

Yang Song, Ge Wang, Chuan Chen, Yun Liu, Bin Wang (✉)

Cancer Center, Institute of Surgery Research, Third Affiliated Hospital, Army Medical University (Third Military Medical University), Chongqing 400042, China

Abstract

Objective This study investigated the predictive value of tumor volume reduction rates (TVRRs) before and after induction chemotherapy in determining the radiosensitivity and prognosis of patients with locally advanced nasopharyngeal carcinomas (NPCs).

Methods The clinical data of 172 patients with locally advanced primary NPCs who were treated from January 2009 to December 2012 were collected. Tumor regression was evaluated based on the results of the computed tomography scan or magnetic resonance imaging studies. Data about the tumor diameters before and after induction chemotherapy and after radiotherapy as well as the survival times of the patients were obtained.

Results All 172 patients had NPCs. After radiotherapy, the TVRR in patients without residual tumor cells was higher than that in patients with residual tumor cells after induction chemotherapy (median values: 47.7% and 15.1%, respectively), and the 5-year survival rates were 80.3% and 45.6%, respectively. Neck lymph node metastasis was observed in 161 of 172 patients, and the TVRRs were similar (median values: 46.8% in 161 patients without residual tumor cells and 11.1% in 161 patients with residual tumor cells). The 5-year survival rate of the 161 patients without residual tumor cells was 84.5%, and that of patients with residual tumor cells was 37.3%. As shown by the receiver operating characteristic (ROC) curve, the area under the curve (AUC) of the ROC curve for TVRRs in patients with primary NPCs but without residual tumors was 0.851, whereas that for TVRRs in patients with neck lymph node metastasis but without residual tumors was 0.784. This result indicates that TVRR has a high diagnostic performance. The univariate Cox regression analysis showed that clinical stage, TVRR in primary NPCs, neck lymph node metastatic lesions before and after induction chemotherapy, presence or absence of residual tumor cells in primary NPCs, and neck lymph node metastatic lesions after radiotherapy were significantly correlated to overall survival (OS). Results of the multivariate Cox regression analysis showed that clinical stage and presence or absence of residual tumor cells in the lymph nodes after radiotherapy were the independent prognostic factors of OS.

Conclusion The TVRR after induction chemotherapy may be an effective predictive indicator of the treatment efficacy of radiotherapy in patients with NPC.

Key words: nasopharyngeal carcinomas; induction chemotherapy; radiosensitivity; prognosis

Received: 18 December 2018
Revised: 23 January 2019
Accepted: 27 January 2019

✉ Correspondence to: Bin Wang. Email: coco7520@163.com

The prevalence rate of nasopharyngeal carcinomas (NPCs) is extremely high in southern China. Considering the anatomical position of the nasopharynx and the different clinical symptoms of NPCs, these carcinomas are usually not diagnosed until they are at a locally advanced stage. Radiotherapy is the first choice in the treatment of NPCs. Although the efficacy of radiotherapy is high, local recurrence and distant metastasis commonly occur [1]. The prognosis of patients with NPC recurrence or distant metastasis after radiotherapy is poor, and the 5-year survival rate of patients with local recurrence is only 33% [2]. The average survival time of patients with distant metastasis is 22 months [3]. Therefore, to improve the prognosis of patients with NPC, the radiosensitivity of NPCs must be predicted, and a reliable predictive indicator should be established to guide clinical treatment.

Induction chemotherapy can reduce tumor burden, which results in local control, helps improve blood supply and radiosensitivity, and reduces the risk of subclinical metastasis. However, an ineffective induction chemotherapy delays radiotherapy, causes accelerated re-proliferation of tumor cells, and reduces local control rates. Furthermore, it causes tumor cells to be insensitive to radiotherapy transfer. Therefore, the efficacy of induction chemotherapy determines the efficacy of radiotherapy. Research about the potential ability of induction chemotherapy in predicting the efficacy of radiotherapy is limited. In our previous study, we found that changes in plasma Epstein–Barr virus (EBV) DNA levels before and after induction chemotherapy helped predict tumor volume regression after radiotherapy, although the predictive value of plasma EBV DNA levels was lower than that of imaging data [4]. Therefore, this study aimed to validate the potential ability of TVRRs before and after induction chemotherapy in predicting tumor regression and survival rates after radiotherapy.

Materials and methods

Inclusion and exclusion criteria

The inclusion criteria were as follows: (1) patients with a pathologically confirmed NPC; (2) those with locally advanced stage III/IVA NPC without distant metastasis according to the Chinese 2008 staging system; (3) those who underwent examination of the nasopharynx via computed tomography (CT) scan or magnetic resonance imaging (MRI) before treatment, after induction chemotherapy, and after radiotherapy, electronic nasopharyngoscopy, chest CT scan, or chest radiography in addition to upper abdominal CT scan or abdominal B ultrasonography and whole-body bone scan examinations; (4) those treated with radiotherapy for the first time; (5) those with KPS ≥ 80; and (6) those with contraindications for radiotherapy treatment, which include infections, severe anemia, pulmonary tuberculosis, heart disease, kidney disease, and other comorbidities. Meanwhile, the exclusion criterion included patients who did not undergo radical radiotherapy treatment.

Clinical data of the participants

A total of 172 patients with primary NPCs who were treated in the Department of Oncology, Third Affiliated Hospital of the Third Military Medical University from January 2009 to December 2012 were included. All the patients had a pathological diagnosis of NPCs prior to treatment and underwent physical examination, complete blood count examination, liver and kidney function examination, chest radiography, abdominal B ultrasonography, head and neck CT/MRI, and whole-body bone scan. Table 1 shows the summary of the baseline information of the patients.

Treatment

Induction chemotherapy

The patients received docetaxel plus paclitaxel (TP)-or docetaxel, paclitaxel, fluorouracil (TPF)-based induction chemotherapy. The TP regimen consisted of 75 mg/m^2 of docetaxel or 135 mg/m^2 of paclitaxel on day 1 plus 80 mg/m^2 of nedaplatin on day 1. The TPF regimen involved 120 h of continuous intravenous infusion of 60 mg/m^2 of docetaxel or 135 mg/m^2 of paclitaxel on day 1 plus 80 mg/m^2 of nedaplatin on day 1 plus fluorouracil 450–550 mg/m^2 on days 1–5. Each cycle was completed within 3 weeks, and each patient received chemotherapy treatment in two cycles.

Concurrent chemotherapy during radiotherapy

The patients received 2–3 cycles of 80 mg/m^2 of nedaplatin every 3 weeks or a total of 6 cycles of 40 mg/m^2 of nedaplatin weekly.

Radiotherapy

All patients received intensity-modulated radiation therapy using a 6-MV linear accelerator (Elekta, Stockholm, Sweden) after 3–4 weeks after the completion of induction chemotherapy. A large-aperture 16-row spiral CT scanning was used after fixation with low-temperature thermoplastic film covering the head, neck, and shoulders. The treatment target was outlined based on pretreatment MRI results and the International Commission on Radiation Units and Measurements (ICRU) guidelines (reports 50 and 62). The high-risk clinical target volume (CTV1) comprised GTVnx and GTVnd with a margin of 5–10 mm, which include the whole nasopharynx, inferior two-thirds of the sphenoid sinus, the anterior third of the clivus, pterygoid fossae, posterior third of nasal cavity and maxillary sinuses, retropharyngeal nodes, parapharyngeal space, and the drainage of the upper neck. The total dose delivered to CTV1 was 60 Gy. CTV2 comprised of CTV1 with

a margin of 3–5 mm as well as the lower neck and the supraclavicular lymphatic drainage region. PTV included CTV with a margin of 3–5 mm. The prescription dose was set as follows: GTVnx PTV: 70–72.6 Gy, GTVnd PTV: 66 Gy, CTV1 PTV: 60 Gy, and CTV2 PTV: 54 Gy. The total dose of GTVnx PTV, GTVnd PTV, CTV1 PTV, and CTV2 PTV was delivered within 33 fractions. The dose for critical organs, including the brain stem, spinal cord, optic nerve, optic chiasm, temporal lobe, eyeball, lens, mandible, temporomandibular joint, parotid gland, submandibular gland, and thyroid, was in accordance with the RTOG-0615 protocol. The maximum dose of each organ at risk was below its tolerance limit. Based on the gross target volume of the primary tumor (GTVnx), a single dose of 2.12–2.2 Gy was administered, resulting in a total dose of 70–72.6 Gy. Based on the gross target volume of the metastatic lymph nodes (GTVnd), a single dose of 2.00 Gy was administered, and the total dose was 66 Gy. The maximum dose for critical organs was determined according to the RTOG-0615 protocol.

Measurement of tumor volume

Once the delineation of the rational target volume was finished, the GTVnx and GTVnd and gross tumor volume (GTV) were automatically calculated using the Elekta TPS treatment planning system (TPS). Residual lymph nodes after treatment were defined as follows: enhanced MRI results showing that the smallest diameter of the lymph nodes was > 1 cm on the maximum cross-sectional image, and enhanced scan showing obvious enhancement of lymph nodes or extracapsular invasion of lymph nodes.

Evaluation of short-term efficacy

The treatment efficacy was evaluated according to the 2009 RECIST (version l.1) 3–4 weeks after induction chemotherapy and 1 month after radiotherapy. Efficacy was defined as follows: a complete response, defined as disappearance of all target lesions; a partial response (PR), defined as at least a 30% decrease in the sum of the longest diameter (LD) of target lesions; progressive disease, defined as at least a 20% increase in the sum of the LD of the target lesions or the appearance of one or more new lesions; and stable disease, defined as neither enough shrinkage of the lesion to qualify for PR nor enough increase in the size of the lesion to qualify for progressive disease.

Follow-up

After 5 years post-treatment, the patients were re-examined every 3 months. After 1-year post-treatment, they were re-examined every 6 months. In the re-examination, chest radiography, abdominal color ultrasonography, nasopharyngeal MRI, and nasopharyngoscopy were performed. Brain MRI and whole-body bone ECT scan were performed in patients with clinical symptoms. The follow-up was conducted via telephone for a maximum of 102 months. For patients who were lost to follow-up, the results of the last department visits for outpatients were used. The follow-up for all patients lasted at least 5 years. The median follow-up was 61 (range: 6–101) months.

Statistical analysis

The Kruskal–Wallis test was performed to compare the TVRRs of the patient groups with and without residual tumor cells before and after induction chemotherapy. The Cox regression model was used to analyze different clinical pathological characteristics, relationships between TVRRs and presence or absence of residual tumor cells after radiotherapy as well as OS, and independent prognostic factors of OS. All statistical analyses were performed using the Statistical Package for the Social Sciences software version 20.0 (IBM, New York), and a P value < 0.05 was considered statistically significant.

Results

Correlation between TVRRs before and after induction chemotherapy and residual tumor cells after radiotherapy

Nasopharyngeal lesions were noted in 172 patients. Neck lymph node metastasis was observed in 161 cases (Table 1). The values of the primary tumor volume (GTV) before and after induction chemotherapy were 2.8 (interquartile range [IQR]: 2.0–3.6) and 2.0 (IQR: 1.0–3.0), respectively. The values of the neck lymph node metastatic lesions (GTV) before and after induction chemotherapy were 4.0 (IQR: 2.5–6.0) and 2.8 (IQR: 1.2–4.0), respectively. In the patient group with primary NPCs without residual tumor cells after radiotherapy, the median TVRR after induction chemotherapy was 47.7% (range: 0.0%–100%), which was significantly higher than that of the patient group with residual tumor cells (median: 15.1%; range: –15.4%–87.0%, P < 0.001). The results for neck lymph node metastatic lesions were similar. The TVRRs (median: 46.8%; range: 0.0%–100%) of the patient group without residual tumor cells were significantly higher than those of the patient group with residual tumor cells (median: 11.1%; range: –20.0%–70.0%, P < 0.001) (Fig. 1).

ROC curve analyses validated the value of TVRRs after induction chemotherapy in predicting a complete response in patients with residual tumors after radiotherapy

As patients sensitive to induction chemotherapy were also sensitive to radiotherapy, the ability of TVRRs postinduction chemotherapy in predicting the absence of residual tumor cells after radiotherapy was identified via

Table 1 Baseline characteristic of the whole population

Characteristics	*n*	%
Sex		
Female	52	30.4
Male	119	69.6
T		
T1	11	6.4
T2	47	27.3
T3	62	36.0
T4	52	30.2
N		
N0	11	6.4
N1	37	21.5
N2	108	62.8
N3	16	9.3
Stage		
III	108	62.8
IV	64	37.2
Residual tumor of primary lesion		
Residual	44	25.6
Non-Residual	128	74.4
Residual tumor of node lesion		
Residual	47	27.3
Non-Residual	125	72.7
Response of primary lesion		
CR	24	14.1
PR	83	48.8
SD	63	37.1
PD	0	0.0
Response of node lesion		
CR	10	6.2
PR	94	58.4
SD	56	34.8
PD	1	0.6
ORR of primary lesion		
SD + PD	63	37.1
CR + PR	107	62.9
ORR of node lesion		
SD + PD	57	35.4
CR + PR	104	64.6
TVRR of primary lesions (median,range)		
0.410 (–0.154–1.000)		
TVRR of node lesions (median,range)		
0.396 (–0.200–1.000)		

TVRR: tumor volume reduction rates; ORR: objective response; CR: complete response; PR: partial response; SD: stable disease; PD: progression disease

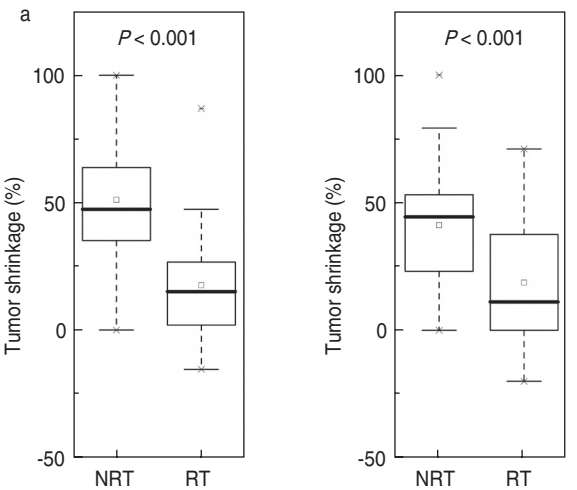

Fig. 1 Boxplot showing that patients without residual tumor had a significantly higher tumor shrinkage than those with residual tumor. (a) Nasopharyngeal primary lesion; (b) Nodal metastatic lesion. NRT: non-residual tumor; RT: residual tumor

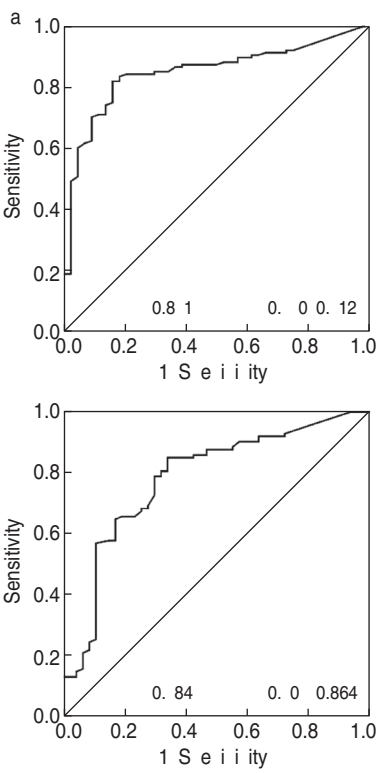

Fig. 2 Receiver operating characteristic curves illustrating the efficacy of tumor shrinkage to identify patients without tumor residual after radiation from other patients. (a) Nasopharyngeal primary lesion; (b) Nodal metastatic lesion

analysis of the ROC curve. As shown in Fig. 2, the AUC of the ROC curve for TVRRs in patients with primary NPCs but without residual tumors was 0.851 (95% confidence interval [CI]: 0.790–0.912). Moreover, the AUC of the ROC curve for TVRRs in patients with neck lymph node metastasis but without residual tumors was 0.784 (95% CI: 0.703–0.864). These results indicate that TVRRs have a high diagnostic performance. A cut-off value of 0.297 for TVRR was selected according to the maximum of Youden's statistic, which showed a specificity of 84.1%

and sensitivity of 82.0% for predicting the absence of residual primary tumors. Meanwhile, with a cut-off value of 0.1833 based on the Jorden's statistic, the specificity and sensitivity for predicting the absence of residual neck lymph node tumors was 66.0% and 85.1%, respectively.

Influence of TVRRs before and after induction chemotherapy and residual tumor cells after radiotherapy on OS

In the univariate Cox regression analysis, clinical stages, TVRRs of primary NPCs, neck lymph node metastatic lesions before and after induction chemotherapy, presence or absence of residual tumor cells in primary nasopharyngeal lesions, and neck lymph node metastatic lesions after radiotherapy were correlated to OS. The median OS of the patient group with residual tumor cells detected in primary NPCs after radiotherapy was 50.67 months (95% CI: 19.03–82.30), and the 5-year survival rate was 45.6%. The patient group without residual tumor cells did not reach the median OS due to an outstanding prognosis, and the 5-year survival rate was 80.3% (log-rank test, $P < 0.001$) (Fig. 3a). The median OS of the patient group with residual tumor cells and neck lymph node metastatic lesions was 39.6 months (95% CI: 25.72–53.48), and the 5-year survival rate was 37.3%. The patient group without residual tumor cells did not reach the median OS, and the 5-year survival rate was 84.5% (log-rank test, $P < 0.001$) (Fig. 3b). Sex, age, and TN staging were used in the multivariate Cox regression analysis. Results showed that the clinical stage and presence or absence of residual tumor cells in the lymph nodes after radiotherapy were the independent prognostic factors of OS. The risk of mortality in patients with stage IV disease increased by 97.5% compared with that of patients with stage III disease. After radiotherapy, the risk of mortality in patients without residual tumor cells and neck lymph node metastasis decreased by 67% compared with that of patients with residual tumor cells (Table 2).

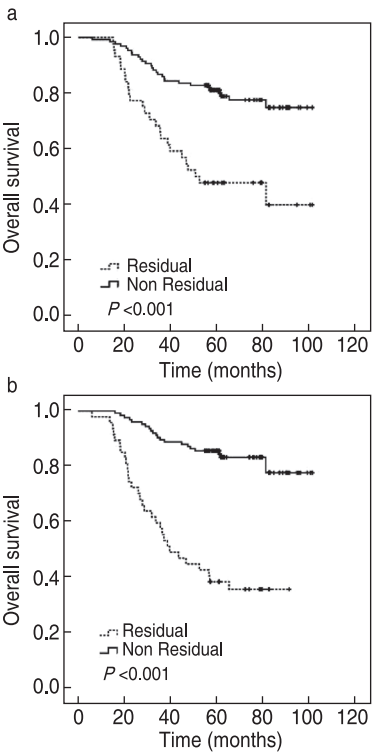

Fig. 3 Kaplan–Meier estimates of overall survival. Patients without any tumor residuals after radiotherapy exhibited a significantly longer overall survival than those with tumor residuals. (a) Nasopharyngeal primary lesion; (b) Nodal metastatic lesion

Subgroups analysis for evaluating the potential influence of T and N stage on the prognostic value of TVRRs in identifying OS

Except for the presence or absence of residual tumor cells in the lymph nodes, all other important prognostic factors observed in the whole population did not show a significant association with OS in the T1–T2 subset. In contrast, in the T3-T4 subgroup, the TVRRs of primary NPCs, neck lymph node metastatic lesions, presence or

Table 2 Results of Cox regression analysis

Factors	Univariable Cox		Multivatiable Cox	
	HR (95% CI)	*P*	HR (95% CI)	*P*
Sex (Male vs. Female)	1.036 (0.269–1.888)	0.908	1.047 (0.553–1.982)	0.888
Age†	0.993 (0.968–1.018)	0.572	0.978 (0.949–1.007)	0.137
T (T3–T4 vs T1–T2)	1.856 (0.973–3.540)	0.060	1.231 (0.582–2.604)	0.587
N (N1–N3 vs. N0)	22.75 (0.252–2051)	0.174	a	a
Stage (IV vs. III)	2.307 (1.337–3.983)	0.003	1.975 (1.091–3.574)	0.025
Shrinkage of primary lesion†	0.145 (0.051–0.413)	<0.001	0.618 (0.185–2.066)	0.434
Shrinkage of nodal lesion†	0.098 (0.031–0.315)	<0.001	0.480 (0.131–1.757)	0.268
Residual of primary lesion (No vs. Yes)	0.312 (0.181–0.540)	<0.001	0.577 (0.302–1.104)	0.097
Residual of nodal lesion (No vs. Yes)	0.186 (0.107–0.323)	<0.001	0.326 (0.171–0.621)	0.001

†as continuous covariates entered into equations
a: Degree of freedom reduced because of constant or linearly dependent covariates

Table 3 Univariate Cox regression in subgroup

	T1–T2		T3–T4		$P_{interaction}$
	HR (95% CI)	*P*	HR (95% CI)	*P*	
Shrinkage of primary lesion†	0.595 (0.093–3.802)	0.584	1.047 (0.553–1.982)	0.888	0.100
Shrinkage of nodal lesion†	0.111 (0.007–1.696)	0.114	0.978 (0.949–1.007)	0.137	0.895
Residual of primary lesion (No vs Yes)	1.024 (0.132–7.959)	0.982	1.231 (0.582–2.604)	0.587	0.227
Residual of nodal lesion (No vs Yes)	0.309 (0.100–0.961)	0.043	a	a	0.336
	N0–N1		N2–N3		$P_{interaction}$
	HR (95% CI)	*P*	HR (95% CI)	*P*	
Shrinkage of primary lesion†	0.022 (0.002–0.329)	0.006	0.178 (0.056–0.564)	0.003	0.171
Shrinkage of nodal lesion†	0.087 (0.007–1.070)	0.056	0.081 (0.020–0.324)	0.000	0.923
Residual of primary lesion (No vs Yes)	0.181 (0.048–0.684)	0.012	0.298 (0.159–0.561)	0.000	0.531
Residual of nodal lesion (No vs Yes)	0.132 (0.040–0.438)	0.001	0.214 (0.115–0.400)	0.000	0.503

†as continuous covariates entered into equations

absence of residual tumor cells in primary nasopharyngeal lesions, and neck lymph node metastatic lesions were significantly associated with OS in the whole population. However, in the multivariate Cox regression analysis, which used each of these four factors were, T stage binary variable (T3–T4 and T1–T2) and the interaction of these two variables were included as covariates. However, the interactions were not significant. Moreover, these four factors were consistently associated with OS in both the N0-N1 and N2-N3 subgroups. However, the interactions were not significant (Table 3). These results showed that at least N stage may not be influenced by the prognostic value of TVRRs.

Discussion

At present, clinical staging is the most important tool for predicting the prognosis of NPC. However, clinical staging is based only on the parts and regions invaded by tumors and does not consider tumoral heterogeneity. Moreover, it is essential in building a diverse prediction model.

Induction chemotherapy plays an important role in the treatment of locally advanced NPCs. A prospective, multicentered, randomized controlled clinical study has shown that induction chemotherapy did not only reduce the metastatic rate of locally advanced NPCs but also improve the OS rate of patients [5]. According to the literature, other than reducing tumor burden, induction chemotherapy has the following benefits: It helps protect organs around the tumor that are at risk during radiotherapy treatment, improves radiation dose, reduces the incidence rates of radiotherapy infections, increases local control rates, improves blood supply and radiosensitivity, and reduces the risk of subclinical metastasis. An increasing number of scholars believe that radiotherapy must be tailored for each individual patient with NPC, and radiation doses should be adjusted based on specific patient-related factors. Grade III–IV toxic reactions due to the use of high doses of radiotherapy for short or long periods of time have been a topic of interest. A method that can predict the short- and long-term efficacy of radiotherapy is used for the development of tailored treatment plans for NPC.

Several factors influence the efficacy of radiotherapy. Of these, multiple drug resistance and radiotherapy resistance are particularly important. Chorna *et al* [6] have irradiated cells sensitive to radiation and resistant to doxorubicin using an X-ray machine and have detected the expression of Bax, Bad, and Bcl-2 proteins before and after radiation. Moreover, they have found a significant difference in the expression of the proapoptotic proteins Bax and Bad and antiapoptotic protein Bcl-2 in cells sensitive to radiation, with the expression of Bax and Bad increasing and that of Bcl-2 decreasing. In contrast, the expression of these proteins in irradiated cells resistant to doxorubicin did not change significantly. The same study has reported increased DNA repair capacity and decreased DNA damage in X-ray irradiated cells resistant to doxorubicin and has concluded that this may explain the resistance of these cells to X-ray radiation treatment. Leng *et al*.[7] have applied radiation treatment to a tongue squamous cell carcinoma cell line (Tca 8113) and Tca 8113/CBDEA cell line resistant to drugs and used an MTT (3-(4,5-dimethylthiazol-2-yl)-2,5-diphenyltetrazolium bromide) assay to detect survival curves for both cell lines. Their results showed that the ID50 of the Tca 8113/CBDEA cell line was 1.24 times than that of the Tca 8113 cell line. They have concluded that the tongue squamous cell carcinoma cell line resistant to drugs was also resistant to radiotherapy. Several other studies have showed that drug resistance by mutations in circulating tumoral DNA may be correlated to radiotherapy resistance. [8-10] The findings of the aforementioned studies have suggested that some head and neck tumor cells resistant to drugs are not sensitive to radiation, whereas cells sensitive to chemotherapy are also sensitive to radiotherapy. However, the conclusions obtained in these studies are

based on fundamental research. Similar findings have not been reported in the clinical observations of NPCs.

The results of the present clinical study of locally advanced NPCs are in accordance with those in the literature. We found that higher TVRRs before induction chemotherapy were associated with lower residual tumor rates. Furthermore, NPCs insensitive to chemotherapy were also insensitive to radiotherapy, and the presence of residual tumor cells after radiotherapy was positively correlated to the OS rate.

In conclusion, this retrospective study showed that the tumor regression status of NPCs after induction chemotherapy may be positively correlated to residual tumor cells after radiotherapy and that residual tumor cells influenced survival rates. The findings indicated that the TVRR after the induction chemotherapy of NPCs may be an effective predictive indicator of postradiotherapy efficacy. A prospective study must be conducted to validate the findings of the present study. Patient-specific treatment plans for NPC must be used to reduce the adverse reactions of radiotherapy.

Conflicts of interest

The authors declare no potential conflicts of interest.

References

1. Yeh SA, Tang Y, Lui CC, *et al*. Treatment outcomes and late complications of 849 patients with nasopharyngeal carcinoma treated with radiotherapy alone. Int J Radiat Oncol Biol Phys, 2005, 62: 672–679.
2. Smee RI, Meagher NS, Broadley K,*et al*. Recurrent nasopharyngeal carcinoma: current management approaches. Am J Clin Oncol, 2010, 33: 469–473.
3. Leong SS, Wee J, Rajan S, *et al*. Triplet combination of gemcitabine. paelitaxel, and carboplatin followed by maintenance 5fluorouracil and folinic acid in patients with metastatic nasopharyngeal carcinoma. Cancer, 2008, 113: 1332–1337.
4. Song Y, Xiao H, Yang Z, *et al*. The predictive value of pre-and post-induction chemotherapy plasma EBV DNA level and tumor volume for the radiosensitivity of locally advanced nasopharyngeal carcinoma. EXCLI J, 2017, 16: 1268–1275.
5. Sun Y , Li WF, Chen NY, *et al*. Induction chemotherapy plus concurrent chemoradiotherapy versus concurrent chemoradiotherapy alone in locoregionally advanced nasopharyngeal carcinoma: a phase 3, multicentre, randomised controlled trial. Lancet Oncol, 2016, 17: 1509–1520.
6. Chorna IV, Datsyuk LO, Stoika RS. Expression of Bax, Bad and Bcl-2 proteins under X-radiation effect towards human breast cracinoma MCF-7 cells and their doxorubiein-resistant derivatives. Exp Oncol, 2005, 27: 196–201.
7. Leng WD, Wang DZ, Feng G, *et al*. Effect of radiation on multidrug resistance of tongue squamous cell carcinoma cell line Tca 8113. Hua Xi Kou Qiang Yi Xue Za Zhi (Chinese), 2006, 22: 615–619.
8. Weichselbaum RR, Ishwaran H, Yoon T, *et al*. An interferon-related gene signature for DNA damage resistance is a predictive marker for chemotherapy and radiation for breast cancer. PNAS, 2008, 105: 18490–18495.
9. Pavlopoulou A, Oktay Y, Vougas K, *et al*. Determinants of resistance to chemotherapy and ionizing radiation in breast cancer stem cells. Cancer Lett, 2016, 380: 485–493.
10. Goldstein M, Kastan MB. The DNA damage response: implications for tumor responses to radiation and chemotherapy. Annu Rev Med, 2015, 66: 129–143.

DOI 10.1007/s10330-018-0326-6
Cite this article as: Song Y, Wang G, Chen C, *et al*. Predictive value of tumor volume reduction rates before and after induction chemotherapy in determining the radiosensitivity and prognosis of locally advanced nasopharyngeal carcinomas. Oncol Transl Med, 2019, 5: 12–18.

Oncology and Translational Medicine
DOI 10.1007/s10330-018-0328-8
February 2019, Vol. 5, No. 1, P19–P24

ORIGINAL ARTICLE

Clinical value of serum pepsinogen levels for the diagnosis of esophageal squamous cell carcinoma

D.J. Rivadeneira, Hesheng Luo, Jingyuan Tian (✉)

Department of Gastroenterology, Renmin Hospital of Wuhan University, Wuhan 430060, China

Abstract

Objective Pepsinogens have been previously studied as markers of gastric atrophy. The objective of this study was to investigate the clinical significance of the serum levels of pepsinogen (PG) I and II, as well as the pepsinogen I/II ratio (PGR) in the diagnosis of esophageal squamous cell carcinoma.

Methods A retrospective data analysis of patients who underwent gastroscopy and PG examination in Renmin Hospital was performed. The subjects were grouped into cancer and healthy control groups, and the differences in the serum levels of PGI and PGII, as well as the PGRs were compared. The receiver operating curve and the area under the curve (AUC) were also compared between the groups.

Results A total of 351 Chinese patients were enrolled in the study, 209 with esophageal squamous cell carcinoma and 142 healthy controls. Overall, the levels of PGI ($P < 0.0001$) and PGII ($P = 0.0007$), as well as the PGR ($P = 0.007$) of the cancer group were lower than those of the control group. Male subjects in the cancer group had lower PGI ($P < 0.0001$), PGII ($P < 0.0001$), and ($P = 0.0138$). The subjects < 65 years old in the cancer group showed lower PGI ($P < 0.0001$), PGII ($P = 0.001$), and PGR ($P = 0.0087$).Overall, these results show that the levels of PGI (AUC 0.64) and PGII (AUC 0.60) have a predictive ability for discriminating esophageal carcinoma. Moreover, in males < 65 years old, PGI (AUC 0.73) and PGII (AUC 0.69) also showed to have a predictive ability for discriminating esophageal carcinoma.

Conclusion Serum PG levels in patients with esophageal squamous cell carcinoma, especially in males aged < 65 years old, are lower than those in healthy people. PGI and PGII are useful for screening esophageal squamous cell carcinoma.

Received: 29 December 2018
Revised: 10 January 2019
Accepted: 20 January 2019

Key words: pepsinogen; esophageal squamous cell carcinoma; screening

Pepsinogens (PG) are a class of endopeptidases that are secreted by the gastric epithelium and released into the circulation [1]. PGI is secreted by oxyntic glands located in the gastric fundus and body, whereas PGII is secreted by all gastric and duodenal glands. Serum PG has been used as a biomarker of gastric inflammation and mucosal status [2].

A low serum PGI concentration and a low serum pepsinogen I/II ratio (PGR) are suggestive of the presence of extensive intestinal metaplasia and atrophic gastritis, which are recognized as a risk factor for gastric cancer. Serum PG testing has, therefore, been proposed to identify individuals with higher risk for gastric cancer who could benefit from gastric cancer screening using upper endoscopy [3–4].

Esophageal cancer is the eighth most common cancer and the sixth most common cause of cancer death worldwide; it has a poor prognosis and survival rate due to its late clinical presentation with advanced disease, with less than 15% patients surviving more than 5 years [5–6]. The esophageal squamous cell carcinoma (ESCC) rates are the highest in the so-called "esophageal cancer belt," which includes Iran, Central Asia, and North-Central China. Within China, the rates in the Hebi and Hunyuan counties have been reported to range from 1.4 to 140 per 100,000 people [7].

Previous studies have found an association between chronic atrophic gastritis and ESCC [8–11]. One meta-analysis reports a two to threefold increased risk for developing ESCC in patients with chronic atrophic gastritis, while another concludes that PGI serum level could aid in the early detection of ESCC [12–13]. However, other studies have concluded that there is little or no evidence for an association of PG values with ESCC risk [14–15].

This study analyzes the clinical significance of the

✉ Correspondence to: Hesheng Luo. Email: xhnk@163.com

differences between the serum levels of PGI and PGII, as well as the PGR in ESCC patients versus healthy controls in Wuhan, China.

Materials and methods

Study participants, questionnaire and biological sample collection

A retrospective analysis was performed using the data collected from July 2015 to December 2016 in Renmin Hospital, Wuhan, China. A total of 351 Chinese patients who underwent gastroscopic examination for suspected esophageal diseases were enrolled into the study and their serum samples were subsequently collected. Among the 351 patients, 226 were males and 125 were females, and the ages of the patients ranged from 32 to 89 years old. According to endoscopic and pathological findings, 209 patients had ESCC, whereas 142 patients were free of any esophageal disease (control group).

All subjects did not receive antibiotics, acid suppressants, or mucosal protective agents within a month prior to examination. The exclusion criteria for the patients included moderate to severe gastric diseases, other esophageal diseases or findings, gastrointestinal or non-gastrointestinal cancer, and previous gastrointestinal surgeries. The design and conduct of the study were approved by the hospital ethics committee, the endoscopic center, and the gastroenterology department. All subjects provided written informed consent.

Serum pepsinogen assays

Fasting venous blood (5 mL) was collected from all subjects in the morning, and the serum was obtained for centrifugation. The serum PGI and PGII levels were detected by Siemens Advia 2400 automatic biochemical analyzer and supporting reagents; the PGR was subsequently calculated. The operation was carried out in strict accordance with the instructions by an experienced laboratory scientist. Gastroscopy was performed by a trained gastroenterologist with more than 5 years of experience. The biopsies were fixed in 80% ethanol, embedded in paraffin, cut in 5-μm sections, and stained with hematoxylin and eosin; they were subsequently observed and read independently by 2 pathologists with no previous knowledge of the patients' situations. If there was discrepancy in the diagnosis, a joint review would take place.

Statistical analysis

Statistical analyses were conducted using the GraphPad Prism 6.0 and SPSS 20.0 statistical softwares. The data conforming to the normal distribution were represented as the mean with the standard deviation [x(_) ± s], whereas the data exhibiting skewed distribution were expressed as the median with the inter-quartile range (IQR).

The data of the two groups with normal distribution and variance were compared using the independent sample *t* test, whereas, the two groups with skewed distribution and variance were compared using the Mann-Whitney U rank sum test. The chi-square test was used to compare the ratio or composition ratio of the count data. A *P*-value < 0.05 was considered statistically significant.

The clinical value of PG in the diagnosis of ESCC was analyzed, and the sensitivity and specificity across cut-offs generated the receiver operating characteristic (ROC) curve with the area under the curve (AUC) to determine the inherent ability of the PG test to discriminate between the ESCC and control groups. AUC = 1 means the diagnostic test is perfect in differentiating between the two groups, while AUC = 0.5 means the chance of discrimination of the curve is located on the diagonal line in the ROC space.

Results

Table 1 showed the demographic characteristics of the ESCC and control subjects: the pepsinogen serum medium values in each group, the male-to-female ratio, and the subjects younger and older than 65 years in the ESCC and control groups.

Table 2 compared and analyzes the serum levels of PGI and PGII, as well as the PGR between the ESCC and control groups with respect to all of the patients. The serum levels of PGI (P <0.0001) and PGII (P = 0.0007), as well as the PGR (P = 0.007) in the ESCC subjects were significantly lower than those in the controls.

Table 3 compared the PG serum levels between the male and female groups. It shows that the levels of PGI

Table 1 Demographic characteristics of the esophageal squamous cell carcinoma and control groups

	n	PG I (ng/mL)[1]	PG II (ng/mL)	PGR	Female	Male	< 65[2]	≥ 65[3]
ESCC	209	46.0	11.8	4.1	66	143	125	84
Control group	142	67.0	15.4	4.6	59	83	97	45
Total	351				125	226	222	129

[1] Pepsinogen I, II medium values are expressed in ng/mL

[2] < 65 younger than 65 years old

[3] ≥ 65 equal or older than 65 years old

Proportions of female and male subjects in the ESCC and control groups

Table 2 Serum levels of pepsinogen I and II, as well as pepsinogen I/II ratio in the esophageal squamous cell carcinoma and control groups

	n	PG I (ng/mL)	PG II (ng/mL)	PGR
ESCC	209	46.0 (30.5,89.0)	11.8 (8.1,19.5)	4.1 (3.0,5.4)
Control group	142	67.0 (50.0,91.5)	15.4 (10.5,21.5)	4.6 (3.7,5.4)
Total	351	*P* < 0.0001	0.0007	0.007

ESCC = esophageal squamous cell carcinoma

Pepsinogen I, II, ratio median values are expressed in ng/ml with their inter-quartile range

P value < 0.05 is statistically significant

($P < 0.0001$) and PGII ($P = 0.0001$), as well as the PGR ($P = 0.0138$) in the male ESCC group were significantly lower than those in the control group. Within the female subjects, no statistically significant differences were observed.

Table 4 compared PG serum levels between different ages in the ESCC and control groups.

Subjects were divided into an elderly group (≥ 65 years old) and a young–middle-aged group (< 65 years old). Upon analyzing the elderly group, the serum levels of PGI ($P < 0001$) and PGII ($P = 0.001$) and the PGR ($P = 0.0087$) in the ESCC group were found to be significantly lower than those in the control group. Within the elderly group, no statistically significant differences were observed.

Fig. 1 analyzed the clinical value of the levels of PGI and PGII, as well as the PGR in the diagnosis of ESCC in the totality of the subjects. Table 5 showedthe corresponding cut-off values for the sensitivity, specificity, and the AUC.

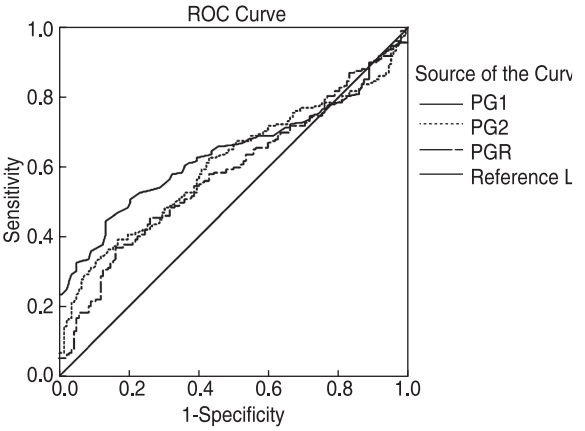

In this ROC curve the sensitivity (true positive rate) is plotted in function of the 1-specificity (false positive rate) for different cut-off points. Each point of the pepsinogen I, II, ratio values from the overall group on the ROC curve represent a sensitivity/specificity pair corresponding to a particular decision threshold.

Fig. 1 Receiver operating characteristic curve of pepsinogen I, II, ratio levels in the diagnosis of esophageal squamous cell carcinoma in the overall subject

The best cut-off value for PGI was 42.7 ng/mL (sensitivity 44.5%, specificity 86.6%) with the AUC = 0.64 (95% CI: 0.58–0.69, $P = 0.000$). For PGII, the best cut-off value was 8.9 ng/mL (sensitivity 31.1%, specificity 90.8%) with the AUC=0.60 (95% CI: 0.55–0.65, $P = 0.000$). Whereas, the best cut-off value for PGR was 3.5 ng/mL (sensitivity 37.8%, specificity 81.6%) with the AUC = 0.5 (95% CI:

Table 3 Serum levels of pepsinogen I and II, as well as pepsinogen I/II ratio in the esophageal squamous cell carcinoma and control groups classified by gender

	Male				Female			
	n	PG I (ng/mL)[1]	PG II (ng/mL)	PGR	*n*	PG I (ng/mL)[1]	PG II (ng/mL)	PGR
ESCC	143	43.0 (26.0, 86.0)	11.5 (7.7, 18.6)	4.2 ± 1.8	66	52.0 (38.0, 113.3)	13.0 (9.7, 20.4)	4.5 ± 2.1
Control group	83	73.0 (55.0, 101.0)	16.7 (11.9, 21.7)	4.4 (3.6,5.8)	59	59.0 (43.0, 81.0)	12.1 (9.4, 21.4)	4.6 ± 1.4
	226	*P* < 0.0001	*P* < 0.0001	*P* < 0.0138	125	*P 0.3582*	0.6961	0.604

In the male and female groups pepsinogen I and II in ESCC and control group are represented by the median with inter-quartile range.

PGR in the ESCC male and female ESCC and control group are represented by the mean with standard deviation

P value < 0.05 is statistically significant

Table 4 Serum levels of pepsinogen I and II, as well as pepsinogen I/II ratio in the esophageal squamous cell carcinoma and control groups classified by age

	< 65 years				≥ 65 years			
	n	PG I (ng/mL)[1]	PG II (ng/mL)	PGR	*n*	PG I (ng/mL)[1]	PG II (ng/mL)	PGR
ESCC	125	42.0 (27.0, 72.5)	10.6 (7.5, 16.4)	4.2 ± 1.6[2]	84	58.5 (38.0, 119.0)	13.4 (9.4, 30.4)[1]	4.0 (3.0, 6.1)[1]
Control group	97	65.0 (48.5, 84.0)	13.7 (10.2, 19.5)	4.5(3.7, 5.4)[1]	45	75.0 (54.0, 113.0)	20.8 ± 9.0[2]	4.6 ± 1.8[2]
	222	*P* < 0.0001	0.001	0.0087	129	*P* 0.101	0.063	0.383

[1] Data with non-symmetric distribution represented by the median with inter-quartile range

[2] Data with symmetric distribution represented by the mean with standard deviation

P value < 0.05 is statistically significant

Table 5 Cut-off values, sensitivity, specificity, and area under the curve of levels of pepsinogen I and II, as well as pepsinogen I/II ratio in the diagnosis of esophageal squamous cell carcinoma in the overall group

	Cut-off[1]	Sensitivity	95%CI	Specificity	95%CI	AUC[2]
PGI	42.7	44.5	37.6–51.5	86.6	79.9–91.75	0.64
PGII	8.9	31.1	24.8–37.8	90.8	84.8–95.0	0.60
PGR	3.5	*37.8*	31.2–44.7	81.6	74.3–87.6	0.58

[1] Pepsinogen I, II, ratio cut-off values for sensitivity and specificity calculated with the Jordan Index

[2] Area under the curve generated after the receiver operating characteristic curve

0.53–0.63, P = 0.001), indicating that its capacity to discriminate between ESCC and normal subjects is no better than the chance level. The ROC and the AUC demonstrate that PGI and PGII serum levels have a predictive ability in discriminating ESCC from normal subjects, and PGI has a greater discrimination capacity than PGII. To assess the difference between the two AUC values, the z test was performed (z = 0.83, two tailed P = 0.40) and it found that the difference was not statistically significant.

Fig. 2 showed the analysis of the clinical values of PGI and PGII serum levels and the PGR in the young–middle-aged male group. Table 6 showed the corresponding cut-off values for the sensitivity and specificity and the AUC. The best cut-off value for PGI was 50.5 ng/mL (sensitivity 60.6%, specificity 84.4%) with the AUC = 0.73 (95% CI: 0.65–0.80, P = 0.000). For PGII, the best cut-off value was 10.1 ng/mL (sensitivity 50.5%, specificity 93.1%) with

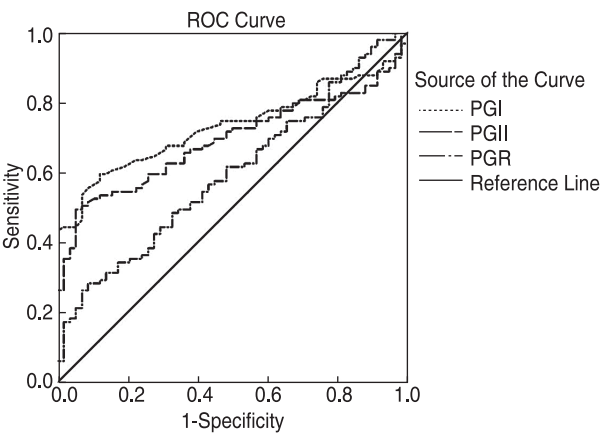

In this ROC curve the sensitivity (true positive rate) is plotted in function of the 1-specificity (false positive rate) for different cut-off points. Each point of the pepsinogen **I**, **II**, ratio values from the young-middle aged male group on the ROC curve represent a sensitivity/specificity pair corresponding to a particular decision threshold.

Fig. 2 Receiver operating characteristic curve of pepsinogen I, II, ratio levels in the diagnosis of esophageal squamous cell carcinoma in the young-middle aged male group

Table 6 Cut-off values, sensitivity, specificity, and area under the curve of levels of pepsinogen I and II, as well as pepsinogen I/II ratio in the diagnosis of esophageal squamous cell carcinoma in the young–middle-aged male group

	Cut-off[1]	Sensitivity	95%CI	Specificity	95%CI	AUC[2]
PGI	50.5	60.6	50.2–70.2	84.4	72.5–92.6	0.73
PGII	10.1	50.5	40.2–60.7	93.1	81.0–97.1	0.69
PGR	3.5	*34.3*	25.0–44.5	81.0	68.5–90.1	0.59

[1] Pepsinogen I, II, ratio cut-off values for sensitivity and specificity calculated with the Jordan Index

[2] Area under the curve generated after the receiver operating characteristic curve

the AUC=0.69 (95% CI: 0.61–0.76, P = 0.000). The best cut-off value for PGR was 3.5 ng/mL (sensitivity 34.3%, specificity 81%) with the AUC=0.59 (95% CI: 0.53–0.63, P = 0.001), indicating that its capacity to discriminate between ESCC and normal young–middle-aged male subjects is no better than the chance level. The ROC and AUC values demonstrate that among the young–middle-aged male subjects, PGI and PGII have a predictive ability for discriminating patients with ESCC from normal subjects and that PGI has a greater discrimination capacity than PGII. To assess the difference between these two AUC values, the z test was performed (z = 1.04, two tailed P = 0.29) and it showed that the difference was not statistically significant.

Discussion

Several studies have demonstrated that low PGI serum levels and low PGR are sensitive and specific markers for gastric atrophy [16–17]; later, a consistent association was found between pepsinogen serum levels and the risk of gastric cancer [18]. However, it was not until a Swedish study found an association between chronic gastric atrophy and ESCC that demonstrated patients with pernicious anemia had a relative risk of 3.2 to present ESCC [8]. Many hypotheses have suggested the potential causes of this association, such as that the atrophic mucosa produces less acid, thus allowing more bacteria to proliferate, and that there might be an increased production of acetaldehyde and N-nitroso compounds that may act like risk factors for ESCC [19]. Further studies have demonstrated a two to threefold increased risk of gastric atrophy, ESCC, and gastric adenocarcinoma [10].

Although the incidence of ESCC is not high compared to other carcinomas, the survival rate is low because of late clinical presentation. In China, ESCC has high incidence and mortality rates with a multi-causal association, such as family aggregation [20], poor nutritional status, smoking, low intake of fruits and vegetables, high temperatures, and drinking beverages [21].

Because of the high impact of ESCC on mortality and survival rates, there is a need to find an early detection method for this disease. With the controversial findings of previous studies, we aimed to investigate the clinical association and significance of pepsinogen serum values with the detection of ESCC.

Our results demonstrate that, in general, the serum levels of PGI and PGII, as well as PGR are decreased in ESCC patients compared to non-ESCC patients; however, the difference was only statistically significant within the young–middle-aged male group, and not in the female and ≥ 65 years old groups. A Chinese study demonstrated the associations of the differences in PG serum levels with gender, age, Helicobacter pylori infection, and consumption of alcohol and tobacco [22]. Our study sample is too small and may be susceptible to bias; thus, further studies need to be conducted to validate the causality of these differences in larger sample sizes.

The ROC analysis in this study showed that PGI (AUC = 0.64) has the highest predictive ability for screening ESCC in the totality of the patients. With the optimal cut-off value of 42.7 ng/mL, the sensitivity was 44.5% and the specificity was 86.6%. However, this predictive value is poor in general, especially considering the low sensitivity; thus, there is a large risk for misdiagnosis. The results in this study corroborate those found in previous studies, wherein serum PGI levels patients with severe atrophic gastritis were found to be reduced but PGII levels remained normal or even increased [23], and that there is a correlation between severe gastric mucosal atrophy and a higher risk of ESCC [24].

Based on our analysis, the PGI serum levels in the young–middle-aged male group were found to have a high sensitivity (60.6%) and the highest predictive ability in discriminating ESCC from normal subjects (AUC = 0.73). Even though the AUC from PGI and PGII levels in the overall dataset and the young–middle-aged male groups were different, this difference was not statistically significant.

Some reports have shown that PGR alone is a superior marker of atrophy, but other reports have also shown that serum PGI level is more strongly associated with atrophy [25–26]. In our study, PGR did not present a higher capacity than chance to discriminate patients with ESCC from normal subjects (AUC = 0.58), and this may be due to unknown mechanisms that are unrelated to atrophy. Large-sample multicenter studies are needed to further explore the differences in serum PG levels.

The strengths of this study include the asymptomatic subjects at the time of enrollment in the study, the endoscopy gastroenterologist and the laboratory scientist who performed the assays unaware of the patients' clinical diagnoses, and the calibrated laboratory materials; the measurement of PG serum levels and the accurate classification of the ESCC patients permitted the analysis using cut-off points to generate the ROC and AUC data.

The limitations include the small sample size, the measurement of the biomarkers at only one point during the study, the imperfect correlation between the level of PGI and the PGR, the lack of gastric atrophy diagnosis, and the presence of an unknown confounder that cannot be totally ruled out.

In conclusion, this study suggests that gastric mucosal atrophy with low PG serum levels are closely related to the occurrence of ESCC and that the relationship between gastric mucosal atrophy and esophageal cancer needs further exploration through trials with a larger patient cohort, which also consider factors, such as age, gender, Helicobacter pylori infection, lifestyle habits, and optimal timepoint biomarker measurement.

A serum PG test alone is valuable for the diagnosis of ESCC, but its sensitivity as a marker is low; thus, it is necessary to combine the detection of PG and other tumor markers to come up with a new, fast, and convenient serological detection method for predicting the development of ESCC.

Further investigations should, therefore, be conducted to come up with a method for effectively screening individuals at risk of developing ESCC at an early stage of cancer.

Acknowledgment

We thank the gastroenterology, endoscopy, laboratory and histopathology department that collaborated in this study. We thank Doctor Xiangyu Meng for reviewing this paper.

Ethical Statement

Authors declare that all procedures followed were in accordance with the ethical standards of the responsible committee on human experimentation (institutional and national) and with the Helsinki Declaration of 1964 and later versions. Informed consent or substitute for it was obtained from all patients for being included in the study.

Conflicts of interest

The authors declare no potential conflicts of interest.

References

1. Gritti G, Banfi D, Roi S. Pepsinogens: physiology, pharmacology pathophysiology and exercise. Pharmacol Res, 2000, 41: 265–281.
2. Miki K, Urita YJ. Using serum pepsinogens wisely in a clinical practice. J Dig Dis, 2007, 8: 8–14.
3. Loong TH, Soon NC, Nik Mahmud NRK, *et al*. Serum pepsinogen and gastrin-17 as potential biomarkers for pre-malignant lesions in the gastric corpus. Biomed Rep, 2017, 7: 460–468.
4. Miki K, Fujishiro M, Kodashima S, *et al*. Long-term results of gastric cancer screening using the serum pepsinogen test method among an

asymptomatic middle-aged Japanese population. Dig Endosc, 2009, 21: 78–81.
5. Cancer research UK. Oesophageal cancer incidence statistics. Cancer Research UK; 2016. Available at: http://www.cancerresearchuk.org/ health-professional/cancer-statistics/statistics-by-cancer-type/oesopha geal-cancer/incidence#heading-Three. [Accessed 5 October 2018].
6. Cancer Research UK. Oesophageal cancer survival statistics; 2016. Available at: http://www.cancerresearchuk.org/health-professional/can cer-statistics/statistics-by-cancer-type/oesophageal-cancer/survival#heading-Zero. [Accessed 5 October 2018].
7. Yang CS. Research on Esophageal Cancer in China: a Review. Cancer Res, 1980, 40: 2633–2644.
8. Hsing AW, Hansson LE, McLaughlin JK, *et al*. Pernicious anemia and subsequent cancer, a population-based cohort study. Cancer, 1993, 71: 745–750.
9. Ye W, Nyrén O. Risk of cancers of the oesophagus and stomach by histology or subsite in patients hospitalised for pernicious anaemia. Gut, 2003, 52: 938–941.
10. Islami FP, Sheikhattari JS, Ren F, *et al*. Gastric atrophy and risk of oesophageal cancer and gastric cardia adenocarcinoma—a systematic review and meta-analysis. Ann Oncol, 2011, 22: 754–760.
11. Iijima K, Koike T, Abe Y, *et al*. Extensive gastric atrophy: an increased risk factor for superficial esophageal squamous cell carcinoma in Japan. Am J Gastroenterol, 2007, 102: 1603–1609.
12. Almodova Ede C, de Oliveira WK, Machado LF, *et al*. Atrophic gastritis: risk factor for esophageal squamous cell carcinoma in a Latin-American population. World J Gastroenterol, 2013, 19: 2060–2064.
13. Kunzmann A, Úna T, McMenamin C, *et al*. Blood biomarkers for early diagnosis of oesophageal cancer: a systematic review. European J Gastroenterol Hepatol, 2017, 30: 263–273.
14. Ren JS, Kamangar F, Qiao YL, *et al*. Serum pepsinogens and risk of gastric and oesophageal cancers in the General Population Nutrition Intervention Trial cohort. Gut, 2009, 58: 636–642.
15. Xue L, Xing L, Wang J, *et al*. Serum pepsinogens and Helicobacter pylori are not associated with esophageal squamous cell carcinoma in a high-risk area in China. Tumori, 2013, 99: 134–138.
16. Correa P. Serum pepsinogens in gastric cancer screening. Dig Dis Sci, 2010, 55: 2123–2125.
17. Kim N, Jung HC. The role of serum pepsinogen in the detection of gastric cancer. Gut Liver, 2010, 4: 307–319.
18. Kamangar F, Diaw L, Qiang WW, *et al*. Serum pepsinogens and risk of esophageal squamous dysplasia. Int J Cancer, 2009,124: 456–460.
19. Kamangar F, Chow WH, Abnet CC, *et al*. Environmental causes of esophageal cancer. Gastroenterol Clin North Am, 2009, 38: 27–57.
20. Chang-Claude J, Becher H, Blettner M, *et al*. Familial aggregation of oesophageal cancer in a high incidence area in China. Int J Epidemiol, 1997, 26: 1159.
21. Tran GD, Sun XD, Abnet CC, *et al*. Prospective study of risk factors for esophageal and gastric cancers in the Linxian general population trial cohort in China. Int J Cancer, 2005, 113: 456.
22. Li Y. Influence factors on serum pepsinogen. Labeled Immunoassays & Clin Med (Chinese), 2016, 23: 312–315.
23. Samloff IM, Varis K, Ihamaki T, *et al*. Relationship among serum pepsinogen I, serum pepsinogen II, and gastric mucosal histology. A study in relatives of patients with pernicious anemia. Gastroenterology. 1982, 83: 204–209.
24. Iijima K, Koike T, Abe Y, *et al*. Gastric hyposecretion in esophageal squamous-cell carcinomas. Dig Dis Sci, 2010, 55: 1349–1355.
25. Samloff IM, Taggart RT. Pepsinogens, pepsins, and peptic ulcer. Clin Invest Med, 1987, 10: 215–221.
26. Derakhshan MH, El-Omar E, Oien K, *et al*. Gastric histology, serological markers and age as predictors of gastric acid secretion in patients infected with Helicobacter pylori. J Clin Pathol, 2006, 59: 1293–1299.

DOI 10.1007/s10330-018-0328-8
Cite this article as: Rivadeneira DJ, Luo HS, Tian JY. Clinical value of serum pepsinogen levels for the diagnosis of esophageal squamous cell carcinoma. Oncol Transl Med, 2019, 5: 19–24.

Oncology and Translational Medicine
DOI 10.1007/s10330-019-0338-8

February 2019, Vol. 5, No. 1, P25–P29

ORIGINAL ARTICLE

Comparison of efficacy and safety between late-course and simultaneous integrated dose-increasing intensity-modulated radiation therapy for cervical cancer complicated with pelvic lymph node metastasis

Yi Cheng[1], Nan Huang[2], Jing Zhao[1], Jianhua Wang[1], Chen Gong[1], Kai Qin[1] (✉)

[1] Department of Oncology, Tongji Hospital, Tongji Medical College, Huazhong University of Science and Technology, Wuhan 430030, China
[2] Allergy Department, Tongji Hospital, Tongji Medical College, Huazhong University of Science and Technology, Wuhan 430030, China

Abstract

Objective This study aimed to compare and analyze the clinical efficacy and safety of late-course and simultaneous integrated dose-increasing intensity-modulated radiation therapy (IMRT) for cervical cancer complicated with pelvic lymph node metastasis.

Methods Sixty patients with cervical cancer complicated with pelvic lymph node metastasis who were admitted to our hospital from January 2013 to January 2015 were enrolled. The patients were randomly divided into the late-course dose-increasing IMRT group and the simultaneous integrated dose-increasing IMRT group, with 30 cases included in each group, respectively. All patients were concurrently treated with cisplatin. After treatment, the clinical outcomes of the two groups were compared.

Results The remission rate of symptoms in the simultaneous integrated dose-increasing IMRT group was significantly higher than that in the late-course dose-increasing IMRT group ($P < 0.05$). The follow-up results showed that the overall survival time, progression-free survival time, and distant metastasis time of patients in the simultaneous integrated dose-increasing IMRT group were significantly longer than those in the late-course dose-increasing IMRT group ($P < 0.05$). The recurrent rate of lymph nodes in the radiation field in the simultaneous integrated dose-increasing IMRT group was significantly lower ($P < 0.05$) than in the late-course dose-increasing IMRT group. There was no significant difference in the incidence of cervical and vaginal recurrence and distant metastasis between the two groups ($P > 0.05$). The radiation doses of Dmax in the small intestine, D1cc (the minimum dose to the 1 cc receiving the highest dose) in the bladder, and Dmax in the rectum in the simultaneous integrated dose-increasing IMRT group were significantly lower ($P < 0.05$) than in the late-course dose-increasing IMRT group. There was no significant difference in intestinal D2cc (the minimum dose to the 2 cc receiving the highest dose) between the two groups ($P > 0.05$). The incidence of bone marrow suppression in the simultaneous integrated dose-increasing IMRT group was significantly lower ($P < 0.05$) than in the late-course dose-increasing IMRT group.

Conclusion The application of simultaneous integrated dose-increasing IMRT in the treatment of cervical cancer patients complicated with pelvic lymph node metastasis can significantly control tumor progression, improve the long-term survival time, and postpone distant metastasis time with high safety.

Received: 26 December 2018
Revised: 10 January 2019
Accepted: 23 February 2018

Key words: simultaneous integrated dose-increasing intensity-modulated radiation therapy; late-course dose-increasing intensity-modulated radiation therapy; cervical cancer complicated with pelvic lymph node metastasis; clinical efficacy; safety

✉ Correspondence to: Kai Qin. Email: qinkaitj@126.com

Cervical cancer is one of the most common malignant tumors for Chinese women. The incidence of cervical cancer is increasing annually. A high proportion of young patients are affected by this disease; therefore, its Cervical Cervical cancer is one of the most common malignant tumors for Chinese women. The incidence of cervical diagnosis cancer is increasing annually. A high proportion of young patients are affected by this disease; therefore, its diagnosis and treatment has become increasingly important for doctors and researchers [1–2].Currently, most clinical guidelines recommend concurrent chemoradiotherapy as the preferred treatment for advanced patients. With thedevelopment of intensity-modulated radiation therapy (IMRT), precision radiotherapy has become the widely used treatment. However, there is no standard option [3–4]. This study aimed to compare the clinical efficacy and safety of late-course and simultaneous integrated dose-increasing IMRT for cervical cancer complicated with pelvic lymph node metastasis.

Materials and methods

Baseline

Sixty patients who were admitted to our hospital from January 2013 to January 2015 were enrolled this study, all of whom were diagnosed with cervical cancer complicated with pelvic lymph node metastasis. The patients were randomly divided into the following two groups: the late-course dose-increasing IMRT group and the simultaneous integrated dose-increasing IMRT group, 30 cases each, respectively. The patients in the late-course dose-increasing IMRT group were 34–61 years old, with an average of 54.6 (±5.8) years. According to the International Federation of Gynecology and Obstetrics (FIGO) staging system, 20 cases were categorized as having stage IIB; 7 cases, stage III A; and 3 cases, stage III B. The pathological classification of the patients included the following: 7 cases of adenocarcinoma, 22 cases of squamous cell carcinoma, and 1 case of adenosquamous cell carcinoma. The patients in the simultaneous integrated dose-increasing IMRT group were 34–63 years old, with an average of 54.2 (±5.9) years. According to the FIGO staging system, 22 cases were categorized as having stage II b; 6 cases, stage III A; and 2 cases, stage III B. The pathological classification of the patients included the following: 6 cases of adenocarcinoma, 23 cases of squamous cell carcinoma, and 1 case of adenosquamous cell carcinoma. There was no significant difference in the baseline between the two groups.

Inclusion and exclusion criteria

Inclusion criteria

All the patients who were diagnosed with cervical cancer by pathological biopsy, who had stage IIB–IIIB according to the FIGO staging system [5], and who were newly diagnosed without history of surgery or radiotherapy.

Exclusion criteria

Patients with history of pelvic and abdominal surgery, with organ dysfunction such as in the liver and kidney, and with cognitive impairment and patients who are pregnant or lactating.

Method

The IMRT conformed to standards of the Radiation Therapy Oncology Group (RTOG). GTV-n (Gross Target Volume for lymph nodes) included positive lymph nodes. CTV-n (Clinical Target Volume for lymph nodes) included the bilateral obturator, extrailiac, intrailiac, common iliac, and presacral lymph nodes. GTV-t (Gross Target Volume for tumor) included the primary tumor of cervical cancer. GTV-t (Clinical Target Volume for tumor) included the parametrium, cervix, uterine body, and vagina 3 cm below the lesion. Ondansetron was administered before chemotherapy to prevent nausea and vomiting. A total of 300 μg of recombinant human granulocyte colony-stimulating factor was injected subcutaneously per day when the white blood cell (WBC) count was detected to be $< 3.0 \times 10 \times 10^9$/L during chemotherapy, and it will be discontinued when the WBC count is within the normal range. In the late-course dose-increasing IMRT group, the prescription dose was 1.8 Gy/f × 25f firstly, followed by 2.2 Gy × 7f for GTV-n. The total dose was 60 Gy. In the simultaneous integrated dose-increasing IMRT group, the prescription dose for GTV-n was 2.4 GY/f × 25f, while the prescription doses for GTV-t, CTV-t, and CTV-n were 1.8Gy/f × 25f. The total dose was 60 Gy. Brachytherapy was performed after the patients were done with the external radiation for 15 times. The radiation dose at A point was 600 cGy/time (1 time/w for 5 times). Cisplatin 40 mg/m^2 was administered intravenously once a week for 6 times.

Endpoints

All patients were followed up for 30 months, and the clinical efficacy was recorded. Referring to the Response Evaluation Criteria in Solid Tumors criteria, the patients were divided into the following four grades: complete remission (CR), partial remission (PR), stabilization (SD), and progression (PD). The overall survival time, progression-free survival time, and distant metastasis time of the two groups were compared. Lymph node recurrence and distant metastasis were compared. The dosages of Dmax in the small intestine, D2cc in the small intestine, D1cc in the bladder, and Dmax in the rectum were recorded. The toxicity and side effects between the two groups were compared according to the RTOG/

European Organisation for Research and Treatment of Cancer standards of acute radiation injury.

Statistical analysis

Statistical Package for the Social Sciences version 16.0 was used to analyze the data. The numerical data were described as the mean (± standard deviation), and *t*-value test was used; the categorical data were described as percentage, and χ^2 test was used; $P < 0.05$ was considered to be statistically significant.

Results

Comparison of clinical efficacy between the two groups

A total of 20 CR, 9 PR patients, 1 SD patient, and 0 PD patients were enrolled in the simultaneous integrated dose-increasing IMRT group, while a total of 13 CR patients, 10 PR patients, 7 SD patients, and 0 PD patients were enrolled in the late-course dose-increasing IMRT group; the symptom relief rate of the simultaneous integrated dose-increasing IMRT group was significantly higher ($P < 0.05$) than in the late-course dose-increasing IMRT group, as shown in Table 1.

Comparison of follow-up between the two groups

The follow-up results showed that the overall survival time, progression-free survival time, and distant metastasis time of the patients in the simultaneous integrated dose-increasing IMRT group were significantly longer than those patients in the late-course dose-increasing IMRT group ($P < 0.05$). In the simultaneous integrated dose-increasing IMRT group ,there was 1 case of lymph node recurrence in the radiation field, 3 cases of cervical and vaginal recurrence, and 2 cases of distant metastasis . In the late-course dose-increasing IMRT group, there were 10 case of lymph node recurrence in the radiation field, 4 cases of cervical and vaginal recurrence, and 2 cases of distant metastasis. The recurrence rate of lymph nodes in the simultaneous integrated dose-increasing IMRT group was significantly lower ($P < 0.05$) than in the late-course dose-increasing IMRT group. There was no significant difference in the incidence of cervical and vaginal recurrence and distant metastasis between the two groups ($P > 0.05$). Data were shown in Table 2.

Comparison of radiation dose between the two groups

The Dmax dose in the small intestine, D1cc in the bladder, and Dmax in the rectum in the simultaneous integrated dose-increasing IMRT group were significantly lower than that in the late-course dose-increasing IMRT group ($P < 0.05$). There was no significant difference in D2cc in the small intestine between the two groups ($P > 0.05$), as shown in Table 3.

Comparisons of toxicity and side effects between the two groups after treatment

The incidence of bone marrow suppression was significantly lower in the simultaneous integrated dose-increasing IMRT group than that in the late-course dose-increasing IMRT group ($P < 0.05$); there was no significant difference in the incidence of gastrointestinal reaction, liver injury, radiation-induced rectitis, and radiation-induced cystitis between the two groups ($P > 0.05$). Data were shown in Table 4.

Table 1 Comparison of clinical efficacy between the two groups

Group	Cases	CR	PR	SD	PD	Symptom relief rate
Late-course dose-increasing IMRT	30	13	10	7	0	76.67%
Simultaneous integrated dose-increasing IMRT	30	20	9	1	0	96.67%
χ^2	–	–	–	–	–	5.192
P	–	–	–	–	–	< 0.05

Table 2 Comparisons of follow-up between the two groups

Group	Cases	Overall survival time (months)	Progression-free survival time (months)	Distant metastasis time (months)	Lymph node recurrence in the radiation field (*n*)	Cervical and vaginal recurrence (*n*)	Distant metastasis (*n*)
Late-course dose-increasing IMRT	30	18.6 ± 2.7	13.1 ± 1.2	15.7 ± 2.3	10	4	2
Simultaneous integrated dose-increasing IMRT	30	22.7 ± 2.4	17.2 ± 1.5	19.4 ± 1.7	1	3	2
χ^2/t	–	6.216	11.690	7.086	9.017	0.162	0.000
P	–	< 0.05	< 0.05	< 0.05	< 0.05	> 0.05	> 0.05

Table 3 Comparison of radiation dose between the two groups (Gy)

Group	Cases	Dmax dose in the mall intestine	D2cc in the small intestine	D1cc in the bladder	Dmax in the rectum
Late-course dose-increasing IMRT	30	62.75 ± 6.20	53.51 ± 5.65	67.43 ± 5.89	66.14 ± 7.02
Simultaneous integrated dose-increasing IMRT	30	53.22 ± 5.84	54.26 ± 5.73	54.20 ± 6.17	54.21 ± 5.08
t	–	6.128	0.510	8.495	7.541
P	–	< 0.05	> 0.05	< 0.05	< 0.05

Table 4 Comparisons of toxicity and side effects between the two groups after treatment

Group	Cases	Bone marrow suppression	Liver injury	Gastrointestinal reaction	Radiation-induced rectitis	Radiation-induced cystitis
Late-course dose-increasing IMRT	30	25	3	20	14	10
Simultaneous integrated dose-increasing IMRT	30	11	3	17	13	8
χ^2	–	13.611	0.000	0.635	0.067	0.317
P	–	< 0.05	> 0.05	> 0.05	> 0.05	> 0.05

Discussion

Cervical cancer is the most common cancer in the female reproductive system, and lymph node metastasis is a major risk factor for poor prognosis. In the past, the prescription dose of 45 Gy in the areas of the tumor and lymph nodes can only control the progression of the subclinical lesions, and the long-term recurrence risk of lymph node metastasis was still high [6–7]. Additional irradiation of positive lymph nodes was often used to prolong the overall survival time of patients and improve their quality of life. Increasing the dose of the traditional two-dimensional radiotherapy may lead to the aggravation of radiation-induced toxicity and side effects. Some patients chose to discontinue their treatment because of intolerance. In contrast, IMRT is the symbol of "precision radiotherapy," which can reduce the dose of organs at risk (OAR) and decrease the incidence and severity of radiation-induced toxicity and side effects. It is the preferred treatment for the positive lymph node area as a supplementary radiotherapy [8–9]. The results of long-term follow-up study showed that late-course dose-increasing IMRT may affect the long-term survival rate and quality of life of patients with cervical cancer, and the main reason was that the prolonged time of chemotherapy may induce more toxicity and side effects. In contrast, simultaneous integrated dose-increasing IMRT can give different doses to areas with different risks in the same region; therefore, it effectively increases the dose of target areas and reduces toxicity and side effects [6–9].

In this study, patients with cervical cancer complicated with pelvic lymph node metastasis were treated with late-course or simultaneous dose-increasing IMRT concurrently with cisplatin. The results of treatment and follow-up showed that the objective remission rate of the patients treated with simultaneous dose-increasing IMRT in the near future was higher than that of patients treated with late-course dose-increasing IMRT; the overall survival time, progression-free survival time, and distant metastasis time of the patients treated with simultaneous dose-increasing IMRT were higher than in the late-course dose-increasing IMRT. The recurrence rate of lymph nodes in the simultaneous integrated dose-increasing IMRT group was significantly lower than in the late-course dose-increasing IMRT group. There was no significant difference in the incidence of cervical and vaginal recurrence and distant metastasis between the two groups. The results suggest that [5, 10] simultaneous dose-increasing IMRT has more obvious advantages in controlling tumor proliferation, prolonging the long-term survival time, and reducing the metastasis and recurrence than late-course dose-increasing IMRT. At the same time, the overall radiation dose of simultaneous dose-increasing IMRT was significantly lower than in the late-course dose-increasing IMRT, suggesting that it has the advantage of reducing the radiation dose of pelvic and abdominal organs and reducing the damage to OAR; the Dmax dose in the small intestine, D1cc in the bladder, and Dmax in the rectum in the simultaneous integrated dose-increasing IMRT group were significantly lower than in the late-course dose-increasing IMRT group. There was no significant difference in D2cc in the small intestine between the two groups, which may be related to factors such as relatively longer peristalsis time, faster peristalsis rate, and the absence of the maximum dose point in the fixed part of the small intestine area [10]. Analysis of toxicity and side effects showed that the incidence of bone marrow suppression was significantly lower in the simultaneous integrated dose-increasing IMRT group than that in the late-course dose-increasing IMRT group. There was no significant difference in the incidence of gastrointestinal reaction, liver injury, radiation-induced rectitis, and radiation-induced cystitis between the

two groups. The study suggests that the simultaneous integrated dose-increasing IMRT can reduce the incidence of bone marrow suppression and improved the patients' compliance and tolerance. This can be attributed to the fact that only the high-risk areas and lymph node metastasis areas are supplemented in the treatment, and the pelvic radiation dose is reduced; thus, the incidence and severity of bone marrow suppression decrease [11–12].

In conclusion, compared with the late-course dose-increasing IMRT, the simultaneous integrated dose-increasing IMRT in the treatment of cervical cancer patients complicated with pelvic lymph node metastasis can significantly control tumor progression, improve patients' long-term survival time, and postpone distant metastasis time with higher safety.

Conflicts of interest

The authors declare no potential conflicts of interest.

References

1. Zhu FP, REN QL. The new progress of cervical cancer and precancerous lesions in early screening. Mod Oncol (Chinese), 2016: 149–152.
2. Liu HQ. Epidemiological characteristics and risk factors of cervical cancer in China. Matern Child Health Care Chin (Chinese), 2016, 31: 1258–1260.
3. Jie L, Lin JB, Sun FJ, *et al*. Safety and efficacy of semiextended field intensity-modulated radiation therapy and concurrent cisplatin in locally advanced cervical cancer patients: An observational study of 10-year experience. Medicine, 2017, 96: e6158.
4. Liu Y, Yu J, Qian L, *et al*. Extended field intensity-modulated radiotherapy plus concurrent nedaplatin treatment in cervical cancer. Oncol Lett, 2016, 11: 3421–3427.
5. Wang W, Meng Q, Hou X, *et al*. Efficacy and toxicity of image-guided intensity-modulated radiation therapy combined with dose-escalated brachytherapy for stage IIB cervical cancer. Oncotarget, 2017, 8: 102965–102973.
6. Guo M, Huang E, Liu X, *et al*. Volumetric modulated Arc therapy versus fixed-field intensity-Modulated radiotherapy in radical irradiation for cervical cancer without lymphadenectasis: dosimetric and clinical results. Oncol Res Treat, 2018, 41: 105–109.
7. Du XX, Yang H, Zhang HJ, *et al*. Clinical study of intensity modulated radiotherapy and three-dimensional conformal radiotherapy with three-dimensional brachytherapy and concurrent chemotherapy for patients with advanced cervical cancer. Zhonghua Fu Chan Ke Za Zhi (Chinese), 2017, 52: 679.
8. Abe A, Furumoto H, Nishimura M, *et al*. Adjuvant chemotherapy following concurrent chemoradiotherapy for uterine cervical cancer with lymphadenopathy. Oncol Lett, 2012, 3: 571–576.
9. Wei LC, Wang N, Shi M, *et al*. Clinical outcome observation of preoperative concurrent chemoradiotherapy/radiotherapy alone in 174 Chinese patients with local advanced cervical carcinoma. Oncol Targets Ther, 2013, 33: 67–74.
10. Renard-oldrini S, Guinement L, Salleron J, *et al*. Dosimetric comparaison between VMAT and tomotherapy with paraaortic irradiation for cervix carcinoma. Cancer Radiother, 2015, 19: 733–738.
11. Sharfo AW, Voet PW, Breedveld S, *et al*. Comparison of VMAT and IMRT strategies for cervical cancer patients using automated planning. Radiother Oncol, 2015, 114: 395–401.
12. Wu MM, Wei K, Li ZQ. Comparative observation of different radiotherapy regimens in the treatment of advanced cervical cancer with pelvic lymph node metastasis. Lab Med Clin, 2018, 15: 705–707.

DOI 10.1007/s10330-019-0338-8
Cite this article as: Cheng Y, Huang N, Zhao J, *et al*. Comparison of efficacy and safety between late-course and simultaneous integrated dose-increasing intensity-modulated radiation therapy for cervical cancer complicated with pelvic lymph node metastasis. Oncol Transl Med, 2019, 5: 25–29.

Oncology and Translational Medicine
DOI 10.1007/s10330-018-0318-8

February 2019, Vol. 5, No. 1, P30–P32

ORIGINAL ARTICLE

Gene mutations in a patient with chronic myelomonocytic leukemia and changes upon progression to acute myeloid leukemia and during treatment*

Jiaming Li, Sujiang Zhang (✉)

Department of Hematology, Ruijin Hospital North Affiliated with Shanghai Jiao Tong University School of Medicine, Shanghai 201800, China

Abstract

Objective Chronic myelomonocytic leukemia (CMML) has been categorized as an uncommon hematological malignancy with overlapping features of myelodysplastic syndromes (MDS) and myeloproliferative neoplasms that have an inherent risk of progressing to acute myeloid leukemia (AML).

Methods This study presents a case of confirmed CMML combined with M protein, in which the molecular changes upon progression to AML and under decitabine (DAC) plus bortezomib therapy were reported by tracking variant allele frequency (VAF) of mutations in a series of bone marrow samples.

Results First, variable sensitivity of clones was observed during DAC treatment, and incomplete mutation clearance may be associated with low overall response rate and unsustained response. Secondly, DAC cannot prevent the new genetic alterations and accumulation of genetic progression on treatment, leading to acute transformation. Finally, autoimmunity was found to have acted as an important pathogenetic factor, increasing the additive mutations that further drive the clonal evolution in CMML.

Conclusion Overall, changes in mutations and clonal architecture during CMML progression or treatment are predictive of an early evaluation of therapeutic strategies in CMML.

Received: 10 October 2018
Revised: 25 October 2018
Accepted: 5 December 2018

Key words: chronic myelomonocytic leukemia; acute myeloid leukemia; mutation; decitabine; bortezomib; platelets; SETD2; LILRB4

Chronic myelomonocytic leukemia (CMML) is a clonal hematopoietic neoplasm that shares clinical and morphologic features with myelodysplastic syndromes (MDS) and myeloproliferative neoplasms. A number of molecular abnormalities are most frequently exhibited in patients with CMML, including TET2 (60%), SRSF2 (50%), ASXL1 (40%), and RAS (30%) mutations [1], which are variably distributed, yielding an enormous number of combinations that might be important during tumorigenesis and for the outcomes. CMML has been currently postulated to arise as a result of the acquisition of an initial driver mutation, and subclones emerge from an ancestral clone due to the sequential gain of mutations, leading to a proliferative oligoclonality and disease progression. Hypomethylating agents (HMAs), including decitabine (DAC), are approved for the treatment of CMML. However, only approximately 50% of patients show hematological improvement and short response duration. Mutations in genes, including TET2 or DNMT3A, have been previously reported as predictors of responses to HMAs, and the specific molecular signatures predict primary DAC resistance in CMML [2–3].

We described a clinical case of CMML, associated with presence of IgG-κ type M proteins that progressed to AML in a short period of time. The patient received DAC (20 mg/m^2, d1-3) every 2 months, and achieved marrow complete response after one cycle of therapy. However, the patient became more thrombocytopenic and required

✉ Correspondence to: Sujiang Zhang. Email: zhangsjb1181@126.com
* Supported by a grant from the Foundation of Ruijin Hospital North Affiliated with Shanghai Jiao Tong University School of Medicine (No. 2018ZY03).

Table 1 Changes of baseline characteristics during the whole duration of illness

Therapy	Plasma cell (%)	Blasts (%)	MK	PLT 10^9/L	κ	Serum Ig (mg/dl)			CD56 (%)
						IgG	IgA	IgM	
Pre		9.5	603	119	(+)	3060	304	806	5.5
D1-Pre	1.0	2	587	67	NA	2590	280	985	NA
D2-Pre	1.0	1.5	351	23	NA	2470	268	1030	4
D3-Pre	1.0	4	35	28	NA	2090	241	933	NA
B-Pre	1.0	0.5	624	60	(+)	1920	220	1060	3
D4-Pre	1.5	9.5	519	53	(–)	1840	200	1000	2
R-Pre	0.5	45	NA	195	(–)	1870	296	572	2

D-Pre: before DAC treatment; B-Pre: before bortezomib treatment; R-Pre: before ruxolitinib treatment; PLT: Platelet, MK: megakaryocytopoiesis, κ: Kappa light chain, NA: No test results

more platelet transfusions after 3 cycles of therapy. As a result, he was administered bortezomib (1.6 mg/m^2, d1/d8) and dexamethasone (20 mg/d, d1–4/8) regimen, and the platelet counts increased above 60 × 10^9/L without follow-up transfusions. Unfortunately, the CMML progressed to AML 11 months after. Shortly thereafter, he developed hyperleukocytosis and died. Table 1 illustrates the baseline characteristics of the patient's illness history.

To better understand the cytogenetic changes, a whole-exome (WES) approach was used to screen for mutations. Before DAC therapy, somatic variants in TET2, SRSF2, and ASXL1 genes had been identified. After three cycles of DAC therapy, WES analysis showed that TET2 p.P29R and SRSF2 p.P95H mutation VAFs were decreased, while TET2 p.I1873T and TET2 p.F1309fs remained unchanged. At the time of progression, FLT3 p.T2727M and ASXL1 p.G642fs VAFs increased to 62% and 40%, respectively (Fig. 1). This observation further suggested that the falling clones were susceptible to DAC, whereas stable or ascending clones were not, even a relative growth advantage [4–5]. Collectively, a large degree of variability in the response to DAC in patients with CMML was presented due to variable sensitivity of clones and incomplete mutation clearance.

DAC did not reduce the mutated allele burden. During DAC treatment, somatic mutations were successively acquired, and these mutations in each chromosome were listed in Fig. 2a. New gene mutations encoding a signaling protein (CSF3R, KRAS, SPEN, and MECOM) were identified. Additionally, these additional mutations were accompanied by expansion of the existing mutations involved in signaling pathway (FLT3 p.T227M, SETD2 p.M761I, KIAA1429 p.I826T, and MAP3K14 p.R99C) (Fig. 2b). Whether the acquisition of mutations was induced by DAC during the course of treatment or was part of the natural disease course remains unclear.

The patient in this study exhibited immune thrombocytopenia, reduced NK cell levels, and elevated

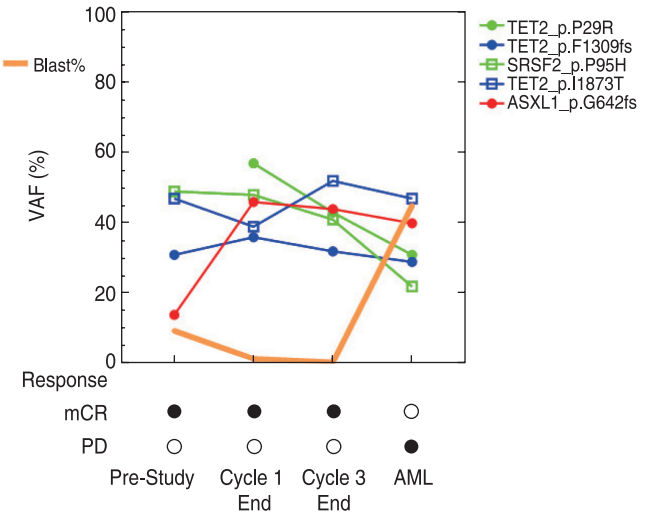

Fig. 1 Dynamic changes in mutation VAFs and incomplete mutation clearance during treatment. The blast % was indicated as a dark yellow line. The decreased, stable, and increased mutation VAF were shown as green, blue, and red lines, respectively

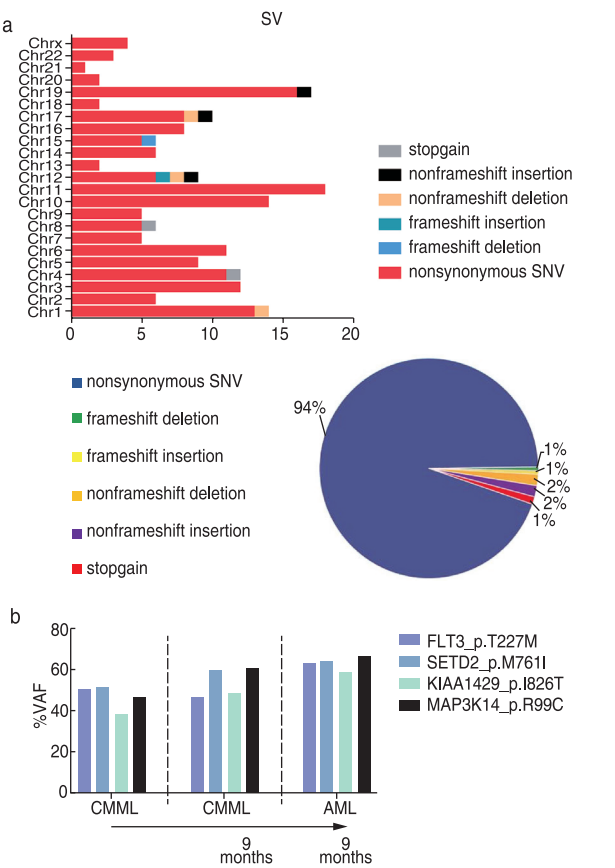

Fig. 2 Somatic variants in coding regions identified using the whole-exome sequencing. (a) The number and type of somatic mutations identified in each chromosome, showing a majority of nonsynonymous variants. Colors indicate the type of mutation; (b) Dynamic changes in mutation VAFs affecting signal transduction genes. Mutation VAF was sequenced before DAC therapy, after three cycles of DAC treatment, and during disease progression

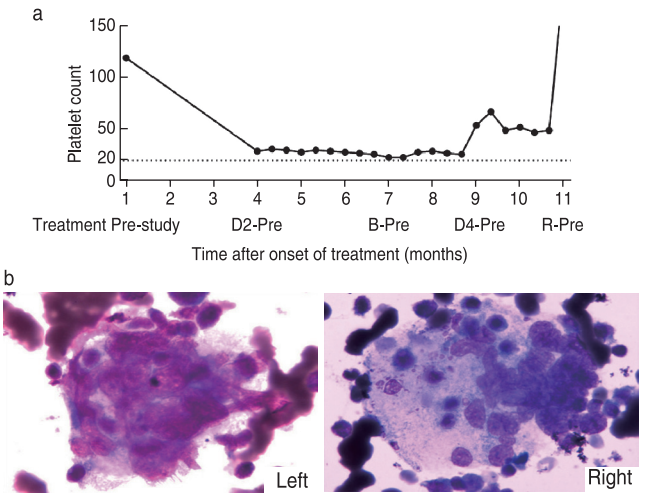

Fig. 3 Platelet response to decitabine/bortezomib therapy. (a) Time courses of platelet count during treatment; (b) Changes in megakaryocyte morphology before (left) and after (right) bortezomib treatment

M protein levels after three cycles of DAC therapy. At that time, new gene mutations involving immune conditions (LILRB4, MYBBP1A, NOTCH2, TNFAIP2, and MAGEC1) were detected. Autoimmune disease was suggested to be associated with increased risk of CMML progression, which is a threat to genomic stability.

These may be due to immune deregulation with aberrant immune responses and impaired tumor immune surveillance. Following the first cycle of bortezomib plus dexamethasone therapy, the patient achieved an excellent platelet response (Fig. 3). To our knowledge, this was the first reported case of CMML- and treatment-related thrombocytopenia s.fy.ated with bortezomib plus dexamethasone.

In conclusion, the findings in this study have clinical implications that may allow better evaluation of agents at earlier stages and guide strategies for subsequent treatment.

Ethics approval and consent to participate

Patient data were used after obtaining approval from the ethical committee of Ruijin Hospital.

Conflicts of interest

The authors declare no potential conflicts of interest.

References

1. Patnaik MM, Tefferi A. Chronic myelomonocytic leukemia: 2018 update on diagnosis, risk stratification and management. Am J Hematol, 2018, 93: 824–840.
2. Patel BJ, Przychodzen B, Thota S , *et al*. Genomic determinants of chronic myelomonocytic leukemia. Leukemia. 2017; 31: 2815–2823.
3. Meldi K, Qin T, Buchi F, *et al*. Specific molecular signatures predict decitabine response in chronic myelomonocytic leukemia. J Clin Invest, 2015, 125: 1857–1872.
4. Stosch JM, Heumüller A, Niemöller C, *et al*. Gene mutations and clonal architecture in myelodysplastic syndromes and changes upon progression to acute myeloid leukaemia and under treatment. Br J Haematol, 2018, 182: 830–842.
5. Uy GL, Duncavage EJ, Chang GS, *et al*. Fulton RS. Dynamic changes in the clonal structure of MDS and AML in response to epigenetic therapy. Leukemia, 2017, 31: 872–881.

DOI 10.1007/s10330-018-0318-8
Cite this article as: Li JM, Zhang SJ. Gene mutations in a patient with chronic myelomonocytic leukemia and changes upon progression to acute myeloid leukemia and during treatment. Oncol Transl Med, 2019, 5: 30–32.

Oncology and Translational Medicine
DOI 10.1007/s10330-018-0324-4

February 2019, Vol. 5, No. 1, P33–P42

REVIEW ARTICLE

Progress in the diagnosis and treatment of extensive-stage small cell lung cancer

Fei Xu[1, 2], Xiaoli Ren[1], Yuan Chen[1], Qianxia Li[1], Ruichao Li[1], Yu Chen[1], Shu Xia[1] (✉)

[1] Department of Oncology, Tongji Hospital, Tongji Medical College of Huazhong University of Science and Technology, Wuhan 430030, China
[2] Department of Oncology, Affiliated Hospital of Hebei University of Engineering, Handan 056000, China

Abstract

Lung cancer, being the most common cancer type, accounts for 13% of all newly diagnosed malignant tumors globally each year. Small cell lung cancer (SCLC) accounts for approximately 15% of newly diagnosed lung cancers each year, but its annual death toll accounts for 25% of that of lung cancer. We summarized relevant clinical studies to elaborate the epidemiology, pathological and clinical characteristics and the treatment status of small cell lung cancer. This paper first described the epidemiology and the pathological and clinical characteristics of SCLC and the systematic treatment of extensive-stage SCLC and then introduced the current targeted therapy and immunotherapy for SCLC to provide clinicians and patients with a more systematic, comprehensive, and beneficial treatment regimen. We expect that these studies can provide clinicians with a clear direction in molecularly targeted therapy or immunotherapy, so that a treatment approach with better antitumor effects and longer-lasting clinical benefits can be provided to the patients.

Received: 11 December 2018
Revised: 2 February 2019
Accepted: 14 February 2019

Key words: small cell lung cancer (SCLC); extensive-stage; targeted therapy; immunotherapy

Epidemiology of small cell lung cancer (SCLC)

As the leading cause of death in cancer diseases worldwide, lung cancer has a continuously increasing incidence. According to the World Health Organization's statistics of tumor morbidity and mortality, in 2012, there were 18 million newly diagnosed lung cancer cases worldwide. Lung cancer ranks first in the morbidity and mortality of solid tumors in male, while in female, its incidence ranks fourth, following breast cancer, colorectal cancer, and cervical cancer. The overall mortality rate of lung cancer, on the other hand, is at the top of well-diagnosed neoplastic causes. Taking China as an example, in 2015, there were 7.2 million newly diagnosed lung cancer cases and 6.1 million related deaths in China. Lung cancer has become the malignant tumor with the highest mortality in male and female in China [1].

SCLC is a highly malignant tumor with the following characteristics: short doubling time, high invasiveness, and early metastasis [2–3]. The incidence of SCLC accounts for 15%–17% that of lung cancer. Its risk is mostly related to smoking time and intensity, and we have also found that smoking cessation is associated with the significant drop in its morbidity and mortality rates [3]. In the past two decades, the incidence of SCLC has been declining, which is likely related to recently implemented tobacco production control measures and changes in smoking behaviors [4].

Because SCLC grows fast and is highly invasive, most patients demonstrate no surgical indications at the time of diagnosis. Therefore, chemotherapy or concurrent chemoradiotherapy is the main treatment method for SCLC. Although SCLC is sensitive to chemoradiotherapy, it still progresses rapidly in most patients after they receive first-line treatment. The substantial development in the tumor genomics and molecularly targeted therapy for non-SCLC in recent years cannot be fully applied to SCLC though, causing poor prognosis in patients with SCLC. For patients with limited-stage SCLC who received treatment, the median overall survival (OS) rate was 15–20 months, and the 5-year survival rate was 10%–13%,

✉ Correspondence to: Shu Xia. Email: xiashutj@hotmail.com

while for patients with extensive-stage SCLC, the median OS rate was 8–13 months, and the 5-year survival rate was merely 1%–2% [5–6]. Therefore, there is an urgent need to find an effective method to completely cure or control the progress of SCLC.

Histopathological characteristics of SCLC

SCLC originates from the K cells with neuroendocrine functions located in the bronchial epithelial mucous gland. The K cell is an undifferentiated neuroendocrine tumor composed of small cells with either no or unclear nucleoli, whose nuclear chromosomes have little cytoplasm, unclear cell boundaries, and fine grains. Its cancer cells are relatively small and often have an oval or spindle shape, or sometimes are like lymphocytes. The nuclei are deeply stained, often with mitoses. According to their morphological characteristics, the cancer cells can be divided into three subtypes: oat cell type, intermediate cell type, and mixed cell type. SCLC is a poorly differentiated malignant tumor that belongs to high-grade neuroendocrine tumors. This type of tumors shares the same distinctive pathological and molecular characteristics, but at the same time demonstrates different biological behaviors and prognosis. For example, poorly differentiated SCLC and large cell lung cancer have similar pathological characteristics with the less invasive carcinoid [7]. Therefore, in clinical practice, immunohistochemistry is often used to detect the expressions of related proteins to distinguish between SCLC and similar tumors. SCLC immunohistochemistry reveals related neuroendocrine markers, such as neural cell adhesion molecule (CD56), neuron-specific enolase, chromogranin A, and synaptophysin. Additionally, most SCLC exhibits a positive thyroid transcription factor-1 expression [8–9].

Clinical characteristics of SCLC

Because SCLC grows fast and is highly invasive, it may develop into distant metastasis in an earlier stage. According to the staging of SCLC defined by the expert group from the US Veterans Association, approximately one-third of newly diagnosed SCLC patients are still at the limited stage, when the lesion is located on one side of the chest only, or can be covered by one radiotherapy field; the rest of the patients are defined to have extensive-stage SCLC [10]. Patients with SCLC often have nonspecific cough and dyspnea as the initial presenting symptoms, which are mostly caused by the enlarged pulmonary hilar mass and mediastinal lymph nodes. However, because some patients with SCLC already had hematogenous metastasis at the first visit, their clinical manifestations are mainly symptoms caused by the primary lesions and metastatic lesions, such as significant weight loss, bone pain, headache, and vomiting. Furthermore, it is well known that SCLC has a certain neuroendocrine origin, which leads to the occurrence of corresponding paraneoplastic syndromes [11–13], including Lambert-Eaton myasthenic syndrome, encephalomyelitis, and other sensory neuropathies. Meanwhile, the cancer secretes some peptide hormones, such as antidiuretic hormone and adrenocorticotropic hormone, causing hyponatremia and Cushing's syndrome [14–15]. Additionally, some studies have confirmed that SCLC secretes insulin growth factor in an autocrine manner [16], which can act as a stimulator of tumors and their secretions and consequently result in related symptoms.

SCLC is very sensitive to initial chemoradiotherapy, but patients eventually die due to disease progression or lack of sensitivity to further treatment [17]. In the past three decades, there has been no breakthrough in the standard treatment of SCLC. For patients with limited-stage SCLC, chemoradiotherapy is used as the major treatment method to cure the disease, while for patients with extensive-stage SCLC, systemic chemotherapy can relieve symptoms and prolong life to a certain extent. Very few patients (2%–5%) have an operative chance at the time of diagnosis, and surgery is limited to stage I SCLC patients and some stage II SCLC patients.

Systematic treatment of extensive-stage SCLC

In the past three decades, the systematic treatment of extensive-stage SCLC has not changed significantly. For patients in this stage, systemic chemotherapy is the recommended treatment option, and additional local radiation therapy can be performed in selected patients to relieve symptoms.

The standard first-line treatment option for extensive SCLC in Europe and America is the administration of etoposide combined with cisplatin or carboplatin [18–22], while in Asia, it is the administration of etoposide or irinotecan combined with cisplatin or carboplatin [23–24]. Despite the fact that around 80% of the patients are sensitive to first-line chemotherapy, 80% of patients with limited-stage SCLC and almost all patients with extensive-stage SCLC suffered from disease recurrence approximately 1 year after the treatment with the following possible reason: residual tumor cells that are insensitive to the initial chemotherapy developed drug resistance [25]. The outcome of the first-line treatment is predictive of the effectiveness of second-line treatment. Most second-line treatments have limited options and are inefficient. In the United States, among all second-line treatment options, only topotecan has been approved by

the FDA [26], while in Japan, besides topotecan, amrubicin can also be administered [27]. Treatments subsequent to second-line treatment do not have a standard treatment regimen due to the low efficiency of chemotherapy, which is possibly a result of cross-resistance when multiple drugs are administered [25, 27]. The mechanisms of drug resistance in SCLC are complex. The currently identified ones include the following: abnormalities in the intracellular enzyme system, abnormal enhancement in the anti-apoptosis and repair functions of the cells, and overexpression of some membrane proteins, such as the lung resistance protein [28–29]. At present, effective drugs for successive treatment include lacquers, topotecan, irinotecan, and gemcitabine.

More than 50% of patients with SCLC will also develop intracranial metastasis. Therefore, prophylactic cranial irradiation (PCI) is recommended for patients with limited-stage SCLC who demonstrated good disease control after the initial induction chemotherapy [30]. Alternatively, for extensive-stage SCLC, early clinical trials have found that PCI can increase the 1-year survival rate (27.1% vs. 13.3%) of patients who are relatively sensitive to initial chemotherapy and additionally reduce the associated symptoms caused by brain metastasis (14.6% vs. 40.4%) [31]. However, a study reported at the 2014 American Society of Clinical Oncology (ASCO) annual conference had an almost totally opposite conclusion. This clinical study admitted 224 patients with extensive-stage SCLC who did not have brain metastasis and combined the platinum-based chemotherapy regimen and the PCI regimen (25 Gy/10 F) [32]. The results of the study revealed that for patients who received PCI, the median progression-free survival (PFS) and OS rates were 2.3 months and 11.6 months, respectively, while for patients in the control group, the PFS and OS rates were 2.4 months and 13.7 months, respectively. PCI did not reveal any advantages in improving patient survival, although it significantly reduced the incidence of brain metastases (the 1-year brain metastasis incidence decreased from 59% to 32.9%). These two opposite authoritative findings have led to controversy over whether PCI is required for patients with extensive-stage SCLC.

Targeted therapy for SCLC

In recent years, a few clinical studies have been conducted on the administration of molecularly targeted drugs as single agents or in conjunction with other antitumor drugs in the treatment of SCLC, but most clinical trials did not achieve an effective clinical benefit. Since SCLC is a type of tumor that is sensitive to chemotherapy, the overall response rate (ORR) of platinum-based chemotherapy is already quite high (75%–95%). Therefore, in the absence of a large number of patients with SCLC, the targeted therapy clinical trials could not provide a convincing increase in the response rate [33]. However, although SCLC demonstrates a high response rate to initial chemotherapy, tumor recurrence in a short period of time is inevitable. Therefore, an effective approach is to investigate the administration of molecularly targeted drugs in maintenance treatment.

Antiangiogenesis targeted drugs

In the field of molecularly targeted therapy for SCLC, antiangiogenesis drugs are the most widely studied. However, in general, clinical trials on antiangiogenesis targeted drugs have presented disappointing results. As is known, angiogenesis makes up a big part in tumor growth, invasion, and metastasis [34]. A study has indicated that the vascular endothelial growth factor (VEGF) plays an important role in tumor cell migration and infiltration, vascular permeability increase, and angiogenesis promotion and has been shown to inhibit tumor growth and angiogenesis in some preclinical models [34]. Moreover, elevated VEGF-A levels and high blood vessel counts are believed to be closely associated with poor prognosis in SCLC [35]. All these preclinical studies have suggested that treatment for angiogenesis may be a viable option. However, to our disappointment, this type of research has barely achieved any clinical benefit.

Monoclonal antibodies

In the 2016 ASCO annual conference, the result of an Italian study was reported. The study was a stage III clinical trial (GOIRC-AIFA FARM6PMFJM) that compared the efficacy of the etoposide and cisplatin (EP) chemotherapy regimen with the bevacizumab combined with EP chemotherapy regimen as the first-line treatments of patients with SCLC [36]. The results suggested that bevacizumab combined with EP chemotherapy regimen was able to improve the patients' median PFS rate significantly, and the difference when compared to that of the chemotherapy alone group was statistically significant. The median PFS rates were 6.7 months and 5.7 months for the combined treatment group and the chemotherapy alone group (HR = 0.72, P = 0.03), respectively; the median OS rates were 9.8 months and 8.9 months for the combined treatment group and the chemotherapy alone group, respectively; and the one-year survival rates were 37% and 25%, whose difference was not statistically significant (HR = 0.78, P = 0.112), for the combined treatment group and the chemotherapy alone group, respectively. In terms of side effects, except that the combined treatment group demonstrated a higher incidence of hypertension, with the difference between the groups being statistically significant, for the rest of the toxic side effects, the two groups did not show any obvious difference. A wide view of all studies on the use of bevacizumab to treat extensive-stage SCLC showed

that the SALUTE trial also obtained positive PFS rates (5.5 months vs. 4.4 months; HR = 0.53; 95% CI, 0.32–0.86) [37], while the IFCT-0802 [38] trial only obtained negative results and was consequently terminated in advance.

Casamino acid kinase inhibitors

As a small-molecule, multitargeted drug for casamino acid kinase inhibitor, sunitinib has exhibited a certain antitumor activity in multiple clinical trials. The CALGB 30504 study assessed the efficacy of using sunitinib as the maintenance treatment regimen after the administration of EP chemotherapy. The result revealed that the OS and PFS rates for the group that received sunitinib as the maintenance treatment and the group that received placebo as the maintenance treatment were 9.0 months and 6.9 months and 3.7 months and 2.1 months, respectively, among which the advantage of sunitinib in the PFS rate was statistically significant (P = 0.02) [39]. A few studies were conducted to report the use of sunitinib as a single agent for the second-line treatment of patients with recurrent SCLC. In a phase II trial that administered sunitinib as a follow-up treatment of patients with recurrent or progressing SCLC after chemotherapy, it was found that the patients' tolerance to sunitinib was extremely poor, as 63% patients developed grade III–IV thrombocytopenia and 25% patients developed grade III–IV leukopenia [40]. Alternatively, the EORTC-08061 trial reported a patient whose partial response (PR) lasted for 10 months and another patient whose stable disease (SD) lasted for 20 months after undergoing sunitinib single-agent treatment [41]. Future research should explore the predictive factors for the effectiveness of sunitinib treatment to guide its clinical use.

DNA repair pathway-targeted therapy

The initiation and development of SCLC involves abnormalities in transcriptional regulation and DNA repair pathway. Sequencing of postoperative pathology in SCLC patients also confirmed the inactivation mutations of tumor protein 53 (TP53) and the retinoblastoma protein 1 (RB1), the amplification of Myc family members, and the mutation of histone modification [42].

Poly (ADP-ribose) polymerase (PARP) has a high level of expression in SCLC than in other types of cancers [43]. PARP repairs damaged DNAs via base excision. Additionally, in some preclinical studies, it was found that the loss of PARP1 activity resulted in DNA strand breaks, which in turn enhanced chemoradiotherapy sensitization [44]. It is known that platinum-based chemotherapy presents a higher response rate in patients with SCLC, and at the same time PARP inhibitors prevent tumor cells from repairing DNA damage. Therefore, it is suspected that by inhibiting DNA repairs, PARP inhibitors may achieve some clinical benefits when used in the maintenance treatment of patients who are sensitive to platinum. Consequently, cytotoxic drugs combined with PARP inhibitors may be a promising treatment approach. In a phase I clinical trial (E2511) that assessed the use of veliparib, a PARP inhibitor, together with EP chemotherapy as the first-line treatment of patients with extensive-stage SCLC, its antitumor effect has been preliminarily demonstrated [45]. Other clinical studies on the use of PARP inhibitors as the second-line treatment or the maintenance treatment following first-line chemotherapy of patients with SCLC have also been launched. In the future, we expect various studies to confirm the antitumor effect of PARP and will continue to explore its relevant biological predictors.

Notch signaling pathway-targeted therapy

The Notch signaling pathway is important for the growth and development of the embryo through the regulation of cell proliferation, differentiation, and apoptosis. Additionally, it also affects the developments of the hematopoietic system and the mammary gland, the maturation of the gastrointestinal epithelial cells, and the immune regulation, angiogenesis, and growth and development of neural stem cells [46]. Some clinical trials and preclinical model studies have demonstrated the role of Notch signaling pathway in maintaining the cancer stem cells (CSCs) [47–48], while these CSCs play a fundamental role in promoting tumor growth and progression and inducing drug resistance [49]. There is increasing evidence that abnormalities in the Notch signaling pathway are related to tumors in the blood system, solid tumors, and tumor angiogenesis [50–51]. Complete genome sequencing has revealed that abnormalities in the Notch family gene are detected in 25% of patients with SCLC. Additionally, the high invasiveness, easy drug resistance, and heterogeneity of SCLC all indicate that it may contain a larger number of CSCs. Based on the above mechanisms, the Notch signaling pathway is considered a potential target for the treatment of SCLC.

Treatments targeting the Notch signaling pathway mainly involve small-molecule inhibitors or monoclonal antibodies of macromolecules. These treatments have now all started clinical trials, such as a phase Ib study on the use of a Notch 2/Notch 3 humanized IgG2 antibody, tarextumab, in conjunction with EP chemotherapy as the first-line treatment of patients with extensive-stage SCLC. We look forward to the outcomes of this study and its subsequent studies.

However, a mouse model study showed that Notch pathway inhibitors could rapidly transform the intestinal proliferative cells into goblet cells, which in turn led to secretory diarrhea [52]. Therefore, the most critical and serious toxic side effect of the administration of Notch inhibitors is intractable diarrhea, which is more likely to happen when the drug is administered continuously

[53]. Therefore, the development of this type of clinical research is facing certain challenges due to the limitations of intestinal adverse reactions. In some studies, attempts were made to intermittently administer Notch inhibitors together with a certain dose of steroid hormones, which not only ensured the efficacy of the clinical treatment to a certain extent but also effectively relieved the treatment-related diarrhea [54].

Immunotherapy for SCLC

At present, immunotherapy has achieved several breakthroughs in the treatment of malignant tumors, such as melanoma, lung cancer, and kidney cancer. Recent research data have revealed that lung cancer types with a high mutational load are more sensitive to immunotherapy [such as blocking the programmed cell death-1 (PD-1) pathway] because of the formation of substantial tumor antigens, which are then presented to T cells and eventually trigger the immune responses. SCLC is the type of cancer with a high mutational load [55]; therefore, inhibiting the PD-1 pathway may be an effective treatment. Although, in principle, it is feasible to perform immunotherapy to SCLC, in practice, very few studies are available. To date, clinical trials on the immunosuppressive agents (ipilimumab, nivolumab, and pembrolizumab), interferon (IFN), and tumor vaccines have been gradually launched, with the results of immunosuppressive agent research showing the most promising clinical benefits.

Cytotoxic T-lymphocyte antigen 4 (CTLA-4) inhibitor is the first immunosuppressive agent administered to patients with SCLC. In a randomized, double-blind phase II study (NCT00527735), the safety and efficacy of ipilimumab combined with carboplatin and paclitaxel in treating newly diagnosed NSCLC or SCLC patients were observed and were compared to those patients performing chemotherapy alone. The result indicated that ipilimumab combined with chemotherapy could significantly extend the immune-related PFS rates in patients with SCLC (6.4 months vs. 5.3 months, HR = 0.64, P = 0.03) [56]. Despite the encouraging effects demonstrated in this phase II clinical trial, another phase III multicenter, double-blind clinical trial (NCT01450761) was performed using ipilimumab combined with EP chemotherapy to treat patients with extensive-stage SCLC, and the result instead prompted people to question this treatment option. In this study, when compared to the chemotherapy alone group, the combined treatment group did not successfully extend the patients' OS rates (10.97 months vs. 10.94 months, HR = 0.936, P = 0.3775). Some ongoing clinical studies are investigating the use of ipilimumab in conjunction with other treatment regimens. A phase II open study (NCT01331525) that uses ipilimumab combined with etoposide and carboplatin to treat patients with limited-stage SCLC is currently underway, and another clinical study (NCT02239900) that combines ipilimumab with stereotactic radiotherapy has also been launched.

Research on PD-1 receptors is another important direction in immunotherapy [57]. The KEYNOTE-028 (NCT02054806) study [58] revealed that pembrolizumab, as a PD-1 monoclonal antibody, exhibited a strong and prolonged antitumor effect when used on SCLC patients whose programmed death ligand-1 (PD-L1) expressions were positive (defined as the expression of the tumor cell membrane, PD-L1, larger than or equal to 1%). Of the patients whose efficacy was evaluated, 4 cases (25%) reached PR, 1 case (7%) reached SD, disease control rate (DCR) reached 31%, and no serious toxic side effects were developed. Relevant basic research has shown that CTLA-4 inhibitor upregulates the expression of PD-1 on the surface of tumor-infiltrating cells, while PD-1 inhibitor upregulates the expression of CTLA-4 on the surface of tumor-infiltrating cells [59]. These studies have provided us with a new treatment approach, that is, that blocking CTLA-4 and PD-1 simultaneously may produce synergistic antitumor effects. The CheckMate 032 (NCT01928394) study was launched on the above theoretical basis. It is an ongoing, randomized, open phase I/II study that compares nivolumab combined with ipilimumab to nivolumab alone in treating five different malignant cancers, including SCLC [60]. The primary end point of the study was objective response rate, and the secondary end point was safety. The analysis of PD-L1 as a biomarker was also included in the study. The study admitted 183 patients whose SCLC progressed after first-line or multiline treatments. The effectiveness data of the midterm analysis of the study were obtained from 55 patients who received nivolumab alone and 45 patients who received nivolumab combined with ipilimumab. The ORR were 13% and 31% and the corresponding disease control rates were 29% and 53% for patients who received nivolumab alone and for patients who received nivolumab combined with ipilimumab, respectively. The average effect onset time were 1.6 months and 2.2 months, respectively; the median OS rates were 3.6 months and 7.8 months, respectively; and the median PFS rates were 1.4 months and 3.4 months, respectively, for patients who received nivolumab alone and for patients who received nivolumab combined with ipilimumab, respectively. Interestingly, antitumor responses occurred in all patients whether they were platinum-sensitive, drug-resistant, or refractory and were irrelevant with the expression of PD-L1 (tumor cell PD-L1 expression less than 1% vs. that larger than or equal to 1%). The safety assessment revealed that the adverse reactions were under control in each treatment group, although grade III–IV treatment-related adverse reactions were more common in the combined treatment group (11%

vs. 32%). In general, in terms of response rate and tumor regression, the combined treatment was potentially more advantageous; especially in recurrent SCLC patients who demonstrated drug resistance, it exhibited a long-lasting antitumor activity. Although the combined treatment presented a higher incidence of adverse reactions, these reactions were basically controllable. Despite difficulties in comparing survival benefits across various studies, the interim result of the CheckMate 032 study appeared to be better than that of studies on other drugs used for the second-line treatment of SCLC (such as topotecan or amrubicin) [61]. More mature data are expected to further guide the use of nivolumab as a single agent or combined with ipilimumab in the treatment of SCLC patients. Furthermore, more clinical studies comparing the use of PD-1 monoclonal antibodies in the first-line, second-line, and maintenance treatments of SCLC to chemotherapy are being launched (NCT02481830, NCT02046733, and NCT02538666).

IFN, as an immunotherapy method, was first administered to patients with SCLC in the 1980s as a combined treatment. Unfortunately, some recent studies did not find a sufficient antitumor activity [62–63]. Among these, a phase II study (NCT00062010) evaluated the efficacy and safety of combined IFN-α with chemotherapy in treating patients with recurrent SCLC [62]. In the final 34 patients enrolled, 3 cases (9%) reached PR and 5 cases (15%) reached SD. The median PFS rate was 2 months (95% CI, 1.8–3.9), and the median OS rate was 6.2 months (95% CI, 4.7–9.8). Obviously, the proposed treatment regimen did not significantly improve the survival outcomes. Another phase II study combined IFN-α or IFN-γ with chemotherapy to treat limited-stage or extensive-stage SCLC patients (n = 164) [63]. Patients included in the study were randomly divided into the chemotherapy alone group (carboplatin, etoposide, or ifosfamide), the chemotherapy combined with IFN-α group, the chemotherapy combined with IFN-γ group, and the chemotherapy combined with both IFN-α and IFN-γ group (in this group, each IFN was administered in half of the dose given to the other groups). Although the OS rate of each group was not significantly different, subgroup analysis revealed that the patients with limited-stage SCLC who received IFN-α treatment demonstrated a significant increase in the median OS rate (34 months vs. 13.6–19.0 months, P = 0.039). Toxic effects were present in all treatments, especially in the group that received chemotherapy combined with both IFN-α and IFN-γ, but all effects were basically controllable. Therefore, the optimal treatment approach of applying IFN to extensive-stage SCLC and the potential benefit groups need further investigation.

Tumor vaccine, being another rare and novel immunotherapy method, has started to demonstrate certain antitumor effects in some clinical studies on SCLC, but the clinical benefits so far are limited. Binding polysialic acid to the neural cell adhesion molecules highly expressed on the surface of SCLC cells can act as a tumor vaccine; as in a SCLC phase I clinical study, it was found that this type of vaccine can produce a strong antigen-antibody reaction [64]. A common adverse reaction is the reaction at the injection site. Although in one case the patient developed peripheral neuropathy and ataxia, the adverse reaction was immediately relieved after the treatment was discontinued. Another approach exploring tumor vaccines was to utilize the P53 gene, which is known as a common mutant gene in SCLC. Transducing the adenoviruses expressing P53 to the dendritic cells induced the T cell response in 57% of patients with limited-stage SCLC, which in turn increased the clinical objective response rate to a higher level (61.9%) in the subsequent chemotherapy [65]. Another vaccine treatment approach is related to Bec2, which is an anti-idiotypic antibody highly expressed in the neuroectodermal-derived gangliosides on the SCLC cell surface. In a phase II study, a vaccine with Bec2 was used in patients with limited-stage SCLC after undergoing standard chemoradiotherapy, but it did not improve the patients' OS rates [66]. Recently, research on tumor vaccines is still in the early stages, and the vaccines have not been specifically administered to SCLC patients.

From the development of immunotherapy and the progress of multiple clinical trials, it is concluded that the exploration of effective biological predictors is important to find patients who will benefit from the immunotherapy. The expression of PD-L1 is the closest indicator we can use to somehow predict the immunotherapy's efficacy, but it still has some disadvantages [67]. Variations in lab conditions, tumor types, and previous treatments can all cause differences in PD-L1 expression. The design of a treatment plan based on the PD-L1 expression requires careful consideration, as we have also found cases whose PD-L1 expression was negative, but the treatment was effective. Therefore, when selecting an effective biological predictor to predict the treatment effect of PD-L1/PD-1 inhibitors, additional factors may need to be considered, such as the tumor antigen load. Future clinical trials should further investigate relevant content to guide individualized clinical treatment.

Antibody-drug conjugate (ADC) therapy for SCLC

In recent years, because of their high specificity and affinity, monoclonal antibodies have been used together with cytotoxic drugs for the treatment of malignant tumors and have gradually attracted people's attention since then. The antibody-drug conjugates (ADCs) can

specifically recognize antigens on the tumor cell surface and at the same time use the cytotoxic drugs they carry for tumor treatment. Therefore, this mode of drug delivery can reduce the killing and damaging effects of cytotoxic drugs on normal cells. At present, two ADCs, Adcetris and Kadcyla, have been approved by the FDA and are used for the treatment of Hodgkin's lymphoma and Her-2-positive breast cancer, respectively. However, most of the ADCs currently under investigation have a narrow therapeutic window, and future developments should focus on enhancing the therapeutic potential of ADCs.

Lorvotuzumab mertansine (LM) is an ADC formed by conjugating a humanized CD56 antibody with the tubulin-damaging factor DM-1, and it is known that approximately 76% of SCLC cells express CD56 on the surface [68]. In some preclinical model studies, LM has demonstrated some antitumor activity whether used as a single agent or in combination with chemotherapy [68]. In a phase I study of patients who developed solid tumors with a positive CD56 expression, the clinical effective rate of LM in treating 113 SCLC patients was 25% [69]. Although these initial studies have achieved encouraging results, LM has not been further developed into a drug that can be widely used to treat SCLC.

Immunohistochemistry of SCLC revealed that 72% to 85% of cells expressed delta-like 3 (DLL3), while in adenocarcinoma, this value was 3.7%; in squamous cell carcinoma, it was 0%; and in normal tissue cells, it was also 0%. Therefore, compared with normal tissues, DLL3 was overexpressed in SCLC and its transplanted tumor [70]. Rovalpituzumab tesirine is an ADC containing a humanized DLL3 monoclonal antibody that currently exhibits a certain antitumor activity in the treatment of SCLC [70]. In a study of transplanted tumor model originated from SCLC patients, it was found that treatment using rovalpituzumab tesirine could induce long-lasting antitumor responses and eliminate tumor-initiating cells, while it is well known that tumor-initiating cells did not respond well to treatment and were considered the cause of rapid recurrence or progression of SCLC [70]. A recent phase I clinical trial assessed the efficacy and safety of rovalpituzumab tesirine in treating 22 patients with recurrent SCLC. The total response rate was 22%, where 7 cases reached PR, and the disease control rate was 53%. Of the 16 patients whose DLL-3 expressions were positive, 7 cases reached PR, and 8 cases reached SD. The common grade III–IV adverse reactions were capillary leak syndrome (14%) and thrombocytopenia (6%) [71]. Consequently, the use of rovalpituzumab tesirine in treating SCLC patients whose DLL3 expression is positive may become a promising treatment approach.

Thoughts on targeted therapy and immunotherapy for SCLC

Over the past decade or so, the emergence of molecularly targeted therapies has changed the treatment management and approach of multiple malignant tumors and has consequently benefited many patients who have been screened by relevant biological predictors. Although the advantages of molecularly targeted therapy and immunotherapy have been confirmed in many solid tumors, satisfactory results have not been achieved in the exploration of SCLC. The possible reasons behind this include the following: first, most of the targeted drugs whose use in SCLC are being explored have already achieved promising effects in other malignant tumors, which indicates that these drugs are not developed on the biological characteristics of SCLC, and second, although the molecular and biological characteristics of SCLC have been further understood, the development of its targeted therapy is still in phase II studies, and most of the patients included in the study are unselected SCLC patients. Therefore, it is difficult to acquire meaningful results from these studies, and, consequently, it is challenging to proceed to phase III clinical trials.

Based on the analysis of whole exome sequencing, it is realized that translational studies on the identification of molecular and signaling pathway abnormalities that are critical for the initiation and development of SCLC are urgently needed. Combining these results with clinical outcomes is important to finding the predictors and consequently the patients who are most likely to benefit from immunotherapy and molecularly targeted therapy. During this process, the biggest challenge we face is the acquisition of the pathological tissues of SCLC, and due to insufficient pathological tissues, it is difficult to conduct related molecular studies. As a result, the development of circulating tumor cells (CTCs) or circulating plasma DNA (cpDNA) results in the deficiency of pathological tissue sources to a certain extent and can therefore be used as a method for translational research. Additionally, translational studies can explore the mechanisms of patients who develop drug resistance after undergoing targeted therapy or immunotherapy, which is another key factor in the future development of combined treatment. These approaches can potentially overcome the treatment resistance, thereby providing SCLC patients with further clinical benefits.

Consequently, in the future, there may be a novel treatment example of SCLC that includes the molecular analysis of all pathological tissues or cells before and during the entire course of the treatment, as this can help in establishing a more optimized treatment course management and in selecting the most suitable individualized treatment option based on the patient's

situation. Therefore, for patients with SCLC, pathological tissues should be obtained and examined in the early stage of diagnosis to be used for molecular analysis, and during the course of treatment, blood samples should be collected at different stages for CTCs of cpDNA analysis. Such a translational study can then predict the patient's response to treatment via the discovery of gene and molecular signaling abnormalities. Furthermore, clinical studies on cancer patients or derived from transplanted tumor CTC can to some extent be used to guide individualized treatment approaches. As a result, the acquisition of patient pathological tissues, CTCs, and cpDNA and the establishment of a transplanted tumor model during the course of treatment will play an important role in the timely monitoring of patient's disease and the continuous molecular analysis of tumor tissues. These study models have demonstrated some prospect in the treatment of SCLC patients. One of the limitations is that in SCLC patients, the establishment of the translational tumor model is time consuming, but when the disease is progressing rapidly, treatment must proceed without any delay. However, with the advancement and refinement in science and technology, time spent in the modeling process is shortening; therefore, this transplanted tumor technique may become the key to guiding treatment approaches and overcoming drug resistances and solving other problems.

In conclusion, we expect that the aforementioned translational studies can provide clinicians with a clear direction in molecularly targeted therapy or immunotherapy, so that a treatment approach with better antitumor effects and longer-lasting clinical benefits can be provided to the patients.

Conflicts of interest

The authors indicate no potential conflicts of interest.

References

1. Chen W, Zheng R, Baade PD, *et al*. Cancer statistics in China, 2015. CA Cancer J Clin, 2016, 66: 115–132.
2. Elias AD. Small cell lung cancer: state-of-the-art therapy in 1996. Chest, 1997, 112 (4 Suppl): 251S–258S.
3. Zhang GZ, Liu ZZ, Han T, *et al*. Treatment of etoposide capsule combined with cisplatin or carboplatin in elderly patients with small cell lung cancer. Chinese-German J Clin Oncol, 2014, 13: 528–531.
4. Torre LA, Bray F, Siegel RL, *et al*. Global cancer statistics, 2012. CA Cancer J Clin, 2015, 65: 87–108.
5. Govindan R, Page N, Morgensztern D, *et al*. Changing epidemiology of small-cell lung cancer in the United States over the last 30 years: analysis of the surveillance, epidemiologic, and end results database. J Clin Oncol, 2006, 24: 4539–4544.
6. Rosti G, Carminati O, Monti M, *et al*. Chemotherapy advances in small cell lung cancer. Ann Oncol, 2006, 17 (Suppl 5): v99–v102.
7. Lally BE, Urbanic JJ, Blackstock AW, *et al*. Small cell lung cancer: have we made any progress over the last 25 years? Oncologist, 2007, 12: 1096–1104.
8. Travis WD, Brambilla E, Nicholson AG, *et al*. The 2015 World Health Organization classification of lung tumors: impact of genetic, clinical and radiologic advances since the 2004 classification. J Thorac Oncol, 2015, 10: 1243–1260.
9. Rekhtman N. Neuroendocrine tumors of lung: an update. Arch Pathol Lab Med, 2010, 134: 1628–1638.
10. Micke P, Faldum A, Metz T, *et al*. Staging small cell lung cancer: Veterans Administration Lung Study Group versus International Association for the Study of Lung Cancer – what limits limited disease? Lung cancer, 2002, 37: 271–276.
11. Gandhi L, Johnson BE. Paraneoplastic syndromes associated with small cell lung cancer. J Natl Compr Canc Netw, 2006, 4: 631–638.
12. Kazarian M, Laird-Offringa IA. Small-cell lung cancer-associated autoantibodies: potential applications to cancer diagnosis, early detection, and therapy. Mol Cancer, 2011, 10: 33.
13. Marchioli CC, Graziano SL. Paraneoplastic syndromes associated with small cell lung cancer. Chest Surg Clin N Am, 1997, 7: 65–80.
14. Johnson BE, Chute JP, Rushin J, *et al*. A prospective study of patients with lung cancer and hyponatremia of malignancy. Am J Respir Crit Care Med, 1997, 156: 1669–1678.
15. Delisle L, Boyer MJ, Warr D, *et al*. Ectopic corticotropin syndrome and small-cell carcinoma of the lung. Clinical features, outcome, and complications. Arch Intern Med, 1993, 153: 746–752.
16. Macaulay VM, Everard MJ, Teale JD, *et al*. Autocrine function for insulin-like growth factor I in human small cell lung cancer cell lines and fresh tumor cells. Cancer Res, 1990, 50: 2511–2517.
17. Alvarado-Luna G, Morales-Espinosa D. Treatment for small cell lung cancer, where are we now? – a review. Transl Lung Cancer Res, 2016, 5: 26–38.
18. Lara PN Jr, Natale R, Crowley J, *et al*. Phase III trial of irinotecan/cisplatin compared with etoposide/cisplatin in extensive-stage small-cell lung cancer: clinical and pharmacogenomic results from SWOG S0124. J Clin Oncol, 2009, 27: 2530–2535.
19. Hanna N, Bunn PA Jr, Langer C, *et al*. Randomized phase III trial comparing irinotecan/cisplatin with etoposide/cisplatin in patients with previously untreated extensive-stage disease small-cell lung cancer. J Clin Oncol, 2006, 24: 2038–2043.
20. Rudin CM, Ismaila N, Hann CL, *et al*. Treatment of small-cell lung cancer: American Society of Clinical Oncology Endorsement of the American College of Chest Physicians Guideline. J Clin Oncol, 2015, 33: 4106–4111.
21. Früh M, De Ruysscher D, Popat S, *et al*. Small-cell lung cancer (SCLC): ESMO Clinical Practice Guidelines for diagnosis, treatment and follow-up. Ann Oncol, 2013, 24 (Suppl 6): vi99–vi105.
22. Sundstrøm S, Bremnes RM, Kaasa S, *et al*. Cisplatin and etoposide regimen is superior to cyclophosphamide, epirubicin, and vincristine regimen in small-cell lung cancer: results from a randomized phase III trial with 5 years' follow-up. J Clin Oncol, 2002, 20: 4665–4672.
23. Zhi XY, Wu YL, Bu H, *et al*. Chinese guidelines on the diagnosis and treatment of primary lung cancer (2011). J Thorac Dis, 2012, 4: 88–101.
24. Shi Y, Xing P, Fan Y, *et al*. Current small cell lung cancer treatment in China. Thorac Cancer, 2015, 6: 233–238.
25. Demedts IK, Vermaelen KY, van Meerbeeck JP. Treatment of extensive-stage small cell lung carcinoma: current status and future prospects. Eur Respir J, 2010, 35: 202–215.
26. von Pawel J, Schiller JH, Shepherd FA, *et al*. Topotecan versus cyclophosphamide, doxorubicin, and vincristine for the treatment of recurrent small-cell lung cancer. J Clin Oncol, 1999, 17: 658–667.

27. Onoda S, Masuda N, Seto T, *et al*. Phase II trial of amrubicin for treatment of refractory or relapsed small-cell lung cancer: Thoracic Oncology Research Group Study 0301. J Clin Oncol, 2006, 24: 5448–5453.
28. Asai N, Ohkuni Y, Kaneko N, *et al*. Relapsed small cell lung cancer: treatment options and latest developments. Ther Adv Med Oncol, 2014, 6: 69–82.
29. Roberti A, La Sala D, Cinti C. Multiple genetic and epigenetic interacting mechanisms contribute to clonally selection of drug-resistant tumors: current views and new therapeutic prospective. J Cell Physiol, 2006, 207: 571–581.
30. Rossi A, Martelli O, Di Maio M. Treatment of patients with small-cell lung cancer: from meta-analyses to clinical practice. Cancer Treat Rev, 2013, 39: 498–506.
31. Slotman B, Faivre-Finn C, Kramer G, *et al*. Prophylactic cranial irradiation in extensive small-cell lung cancer. N Engl J Med, 2007, 357: 664–672.
32. Takahashi T, Yamanaka T, Seto T, *et al*. Prophylactic cranial irradiation versus observation in patients with extensive-disease small-cell lung cancer: a multicentre, randomised, open-label, phase 3 trial. Lancet Oncol, 2017, 18: 663–671.
33. Abidin AZ, Garassino MC, Califano R, *et al*. Targeted therapies in small cell lung cancer: a review. Ther Adv Med Oncol, 2010, 2: 25–37.
34. Salven P, Ruotsalainen T, Mattson K, *et al*. High pre-treatment serum level of vascular endothelial growth factor (VEGF) is associated with poor outcome in small-cell lung cancer. Int J Cancer, 1998, 79: 144–146.
35. Fontanini G, Faviana P, Lucchi M, *et al*. A high vascular count and overexpression of vascular endothelial growth factor are associated with unfavourable prognosis in operated small cell lung carcinoma. Br J Cancer, 2002, 86: 558–563.
36. Tiseo M, Boni L, Ambrosio F, *et al*. Italian, multicenter, phase III, randomized study of cisplatin plus etoposide with or without bevacizumab as first-line treatment in extensive-disease small-cell lung cancer: the GOIRC-AIFA FARM6PMFJM trial. J Clin Oncol, 2017, 35: 1281–1287.
37. Spigel DR, Townley PM, Waterhouse DM, *et al*. Randomized phase II study of bevacizumab in combination with chemotherapy in previously untreated extensive-stage small-cell lung cancer: results from the SALUTE trial. J Clin Oncol, 2011, 29: 2215–2222.
38. Pujol JL, Lavole A, Quoix E, *et al*. Randomized phase II–III study of bevacizumab in combination with chemotherapy in previously untreated extensive small-cell lung cancer: results from the IFCT-0802 trial. Ann Oncol, 2015, 26: 908–914.
39. Ready NE, Pang HH, Gu L, *et al*. Chemotherapy with or without maintenance sunitinib for untreated extensive-stage small-cell lung cancer: a randomized, double-blind, placebo-controlled phase II study-CALGB 30504 (Alliance). J Clin Oncol, 2015, 33: 1660–1665.
40. Han JY, Kim HY, Lim KY, *et al*. A phase II study of sunitinib in patients with relapsed or refractory small cell lung cancer. Lung Cancer, 2013, 79: 137–142.
41. Abdelraouf F, Smit E, Hasan B, *et al*. Sunitinib (SU11248) in patients with chemo naive extensive small cell lung cancer or who have a 'chemosensitive' relapse: A single-arm phase II study (EORTC-08061). Eur J Cancer, 2016, 54: 35–39.
42. Ross JS, Wang K, Elkadi OR, *et al*. Next-generation sequencing reveals frequent consistent genomic alterations in small cell undifferentiated lung cancer. J Clin Pathol, 2014, 67: 772–776.
43. Byers LA, Wang J, Nilsson MB, *et al*. Proteomic profiling identifies dysregulated pathways in small cell lung cancer and novel therapeutic targets including PARP1. Cancer Discov, 2012, 2: 798–811.
44. Rouleau M, Patel A, Hendzel MJ, *et al*. PARP inhibition: PARP1 and beyond. Nat Rev Cancer, 2010, 10: 293–301.
45. Owonikoko TK, Dahlberg SE, Khan SA, *et al*. A phase 1 study of veliparib, a poly (ADP-ribose) polymerase (PARP) inhibitor, in combination with cisplatin and etoposide in extensive-stage small cell lung cancer (SCLC) patients: An Eastern Cooperative Oncology Group study (E2511). 2014 Annual Meeting of the American Society of Clinical Oncology, ASCO. Chicago, IL United States. 2014, 32 (15 Suppl 1).
46. Dontu G, Jackson KW, McNicholas E, *et al*. Role of Notch signaling in cell-fate determination of human mammary stem/progenitor cells. Breast Cancer Res, 2004, 6: R605–R615.
47. Pannuti A, Foreman K, Rizzo P, *et al*. Targeting Notch to target cancer stem cells. Clin Cancer Res, 2010, 16: 3141–3152.
48. Takebe N, Harris PJ, Warren RQ, *et al*. Targeting cancer stem cells by inhibiting Wnt, Notch, and Hedgehog pathways. Nat Rev Clin Oncol, 2011, 8: 97–106.
49. Malik B, Nie D. Cancer stem cells and resistance to chemo and radio therapy. Front Biosci (Elite Ed), 2012, 4: 2142–2149.
50. Aster JC, Blacklow SC. Targeting the Notch pathway: twists and turns on the road to rational therapeutics. J Clin Oncol, 2012, 30: 2418–2420.
51. Li JL, Harris AL. Notch signaling from tumor cells: a new mechanism of angiogenesis. Cancer cell, 2005, 8: 1–3.
52. Nakamura T, Tsuchiya K, Watanabe M. Crosstalk between Wnt and Notch signaling in intestinal epithelial cell fate decision. J Gastroenterol, 2007, 42: 705–710.
53. van Es JH, van Gijn ME, Riccio O, *et al*. Notch/gamma-secretase inhibition turns proliferative cells in intestinal crypts and adenomas into goblet cells. Nature, 2005, 435: 959–963.
54. Wei P, Walls M, Qiu M, *et al*. Evaluation of selective gamma-secretase inhibitor PF-03084014 for its antitumor efficacy and gastrointestinal safety to guide optimal clinical trial design. Mol Cancer Ther, 2010, 9: 1618–1628.
55. Peifer M, Fernández-Cuesta L, Sos ML, *et al*. Integrative genome analyses identify key somatic driver mutations of small-cell lung cancer. Nat Genet, 2012, 44: 1104–1110.
56. Reck M, Bondarenko I, Luft A, *et al*. Ipilimumab in combination with paclitaxel and carboplatin as first-line therapy in extensive-disease-small-cell lung cancer: results from a randomized, double-blind, multicenter phase 2 trial. Ann Oncol, 2013, 24: 75–83.
57. Pardoll DM. The blockade of immune checkpoints in cancer immunotherapy. Nat Rev Cancer, 2012, 12: 252–264.
58. Ott PA, Elez E, Hiret S, *et al*. Pembrolizumab for ED SCLC: Efficacy and relationship with PD-L1 expression. The 16th World Conference on Lung Cancer. Denver, CO United States. 2015, 10 (9 Suppl 2): S193.
59. Ott PA, Hodi FS, Robert C. CTLA-4 and PD-1/PD-L1 blockade: new immunotherapeutic modalities with durable clinical benefit in melanoma patients. Clin Cancer Res, 2013, 19: 5300–5309.
60. Antonia SJ, López-Martin JA, Bendell J, *et al*. Nivolumab alone and nivolumab plus ipilimumab in recurrent small-cell lung cancer (CheckMate 032): a multicentre, open-label, phase 1/2 trial. Lancet Oncol, 2016, 17: 883–895.
61. von Pawel J, Jotte R, Spigel DR, *et al*. Randomized phase III trial of amrubicin versus topotecan as second-line treatment for patients with small-cell lung cancer. J Clin Oncol, 2014, 32: 4012–4019.
62. Pillai RN, Aisner J, Dahlberg SE, *et al*. Interferon alpha plus 13-cis-retinoic acid modulation of BCL-2 plus paclitaxel for recurrent small-

cell lung cancer (SCLC): an Eastern Cooperative Oncology Group study (E6501). Cancer Chemother Pharmacol, 2014, 74: 177–183.
63. Zarogoulidis K, Ziogas E, Boutsikou E, *et al*. Immunomodifiers in combination with conventional chemotherapy in small cell lung cancer: a phase II, randomized study. Drug Des Devel Ther, 2013, 7: 611–617.
64. Krug LM, Ragupathi G, Hood C, *et al*. Immunization with N-propionyl polysialic acid-KLH conjugate in patients with small cell lung cancer is safe and induces IgM antibodies reactive with SCLC cells and bactericidal against group B meningococci. Cancer Immunol Immunother, 2012, 61: 9–18.
65. Antonia SJ, Mirza N, Fricke I, *et al*. Combination of p53 cancer vaccine with chemotherapy in patients with extensive stage small cell lung cancer. Clin Cancer Res, 2006, 12 (3 Pt 1): 878–887.
66. Giaccone G, Debruyne C, Felip E, *et al*. Phase III study of adjuvant vaccination with Bec2/bacille Calmette-Guerin in responding patients with limited-disease small-cell lung cancer (European Organisation for Research and Treatment of Cancer 08971-08971B; Silva Study). J Clin Oncol, 2005, 23: 6854–6864.
67. Naidoo J, Page DB, Wolchok JD. Immune modulation for cancer therapy. Br J Cancer, 2014, 111: 2214–2219.
68. Whiteman KR, Johnson HA, Mayo MF, *et al*. Lorvotuzumab mertansine, a CD56-targeting antibody-drug conjugate with potent antitumor activity against small cell lung cancer in human xenograft models. MAbs, 2014, 6: 556–566.
69. Beck A, Lambert J, Sun M, *et al*. Fourth World Antibody-Drug Conjugate Summit: February 29–March 1, 2012, Frankfurt, Germany. MAbs, 2012, 4: 637–647.
70. Saunders LR, Bankovich AJ, Anderson WC, *et al*. A DLL3-targeted antibody-drug conjugate eradicates high-grade pulmonary neuroendocrine tumor-initiating cells *in vivo*. Sci Transl Med, 2015, 7: 302ra136.
71. Rudin CM, Spigel DR, Bauer TM, *et al*. A DLL3-targeted ADC, rovalpituzumab tesirine, demonstrates substantial activity in a phase I study in relapsed and refractory SCLC. The 16th World Conference on Lung Cancer. Denver, CO United States. 2015, 10 (9 Suppl 2): S192–S193.

DOI 10.1007/s10330-018-0324-4
Cite this article as: Xu F, Ren XL, Chen Y, *et al*. Progress in the diagnosis and treatment of extensive-stage small cell lung cancer. Oncol Transl Med, 2019, 5: 33–42.

Oncology and Translational Medicine
DOI 10.1007/s10330-018-0315-5

February 2019, Vol. 5, No. 1, P43–P48

REVIEW ARTICLE

Aurora kinases: novel anti-breast cancer targets

Yiliyaer[1], Yusufu Maimaiti[2] (✉)

[1] Xinjiang Medical University, Graduate School, Urumqi 830054, China
[2] People's Hospital of Xinjiang Uygur Autonomous Region, Urumqi 830000, China

Abstract

Aurora kinases regulate multiple steps of mitotic cell division in eukaryotic cells. Overexpression of aurora kinases has been observed in some tumor cells, which suggests that abnormalities in aurora kinases are closely related to tumorigenesis. In additon, aurora kinases are often amplified or overexpressed in breast cancer cells, leading to chromosomal segregation abnormalities and genomic disorder, and thereby activating oncogenic pathways. Novel Aurora A kinase inhibitors are currently being studied in multiple phase I and II studies. In this review, we describe the biological functions and mechanisms of aurora kinases in breast cancer cells and summarize the preclinical findings related to aurora kinases in breast cancer.

Received: 15 December 2018
Revised: 26 December 2018
Accepted: 17 January 2019

Key words: aurora kinases; breast cancer; inhibitors

Breast cancer is one of the most common malignant tumors in women in both developed and developing countries. It accounts for approximately one in three cancer diagnoses in women in the United States, and it is the second leading cause of cancer death in women. According to the latest statistics, there are an estimated 234, 580 new cases of breast cancer and 40,030 deaths from breast cancer in the US each year [1]. The incidence of breast cancer in developed countries is increasing due to various factors, including urbanization and changes in women's lifestyles [2]. Although there are many factors that determine the occurrence of breast cancer, including malformative, infective, endocrine, autoimmune, and psychological factors [3], the differentiation and proliferation of breast epithelial cells, which is mediated by hormonal factors, is the main factor driving tumorigenesis [4–5]. Biological targeted therapies are a major treatment modality for breast cancer and have further improved prognosis [6]. However, drug resistance is still a big clinical challenge. Thus, new treatment strategies for breast cancer are greatly needed.

Human epidermal growth factor receptor 2 (HER2) overexpression drives 20% of breast cancers, and this receptor is now a standard therapeutic target [7]. HER2-targeted therapies significantly improve outcomes for HER2-positive patients with both early and metastatic breast cancer. However, there are likely other potential targets in breast cancer.

Aurora kinases, which are a family of mitotically regulated serine/threonine kinases, are increasingly being recognized as key regulators of chromosome segregation and cytokinesis [8]. The first aurora kinase was discovered in 1995 [9]. Yeast has a single aurora kinase, while mammals have multiple genes encoding three, Aurora A, B, and C [10]. These three mammalian aurora paralogues are very similar in sequence, particularly in the carboxy terminal domain, and human Aurora A and B share 71% identity [11].

Aurora kinases are important for cell cycle progression. Aurora kinases A and B are expressed in most normal cells, but expression of these kinases has also been observed in several tumor types, including breast, lung, colon, prostate, pancreas, liver, skin, stomach, rectum, esophagus, endometrium, cervix, bladder, ovary, and thyroid cancers, and these tumors show high expression compared to the corresponding normal tissues[12–13]. Aurora A and B are expressed in most cell types, whereas Aurora C is specifically expressed in the testicles. Both Aurora A and B play key roles in regulating the cell cycle, from G2 phase to cell division. Aurora C plays a unique physiological role in spermatogenesis and functions as a passenger protein on chromosomes, like Aurora B during mitosis [14]. A previous study by Ye [15] examined aurora kinase expression in acute myelocytic leukemia (AML) and showed that blasts overexpress Aurora A and B compared to the levels in control CD34+ cells. Compared

✉ Correspondence to: Yusufu Maimaiti. Email: docyusufu@163.com

to other tissues, Aurora B and C are highly expressed in testis. Aurora B seems to play an essential role in the regulation of chromosome segregation and cytokinesis, while aurora C appears to have unique functions in late spermiogenesis [16].

Overexpression of aurora kinases in cancer cells leads to aberrant chromosome segregation, genomic instability, and activation of oncogenic pathways [17–18]. Recent research results identified Aurora A and B as part of the gene expression profile predicting poor prognosis. Novel targeted agents that inhibit the activities of Aurora A and/or B have been developed and are being tested for their anti-tumor efficacy [19]. This review is focused on the deregulation of aurora kinases in human cancers, with an emphasis on breast cancer, the progress in targeting these important regulators in the treatment of cancers, and the aurora kinase inhibitors being tested in preclinical trials [20].

Aurora kinase A in breast cancer

Human Aurora A is encoded by a gene (*AURKA*) that is located on chromosome 20q13.2. It is composed of 403 amino acids and has a molecular weight of 46 kDa. Aurora A has crucial roles in every step of mitosis [21–22], and it is involved in mitotic entry, separation of centriole pairs, accurate bipolar spindle assembly, alignment of metaphase chromosomes, and completion of cytokinesis [23]. It functions as a key regulator of multiple mitotic events, including centrosome maturation and separation [24], which are commonly amplified in a broad range of tumor tissues [25]. Aurora A expression levels are high, and then rapidly decrease via degradation by the ubiquitin-proteasome pathway [26].

Transcription of *AUKA* is cell-cycle regulated. Aurora A is expressed in all phases of the cell cycle. Thus, the promoters of *AUKA* contain specific elements that are responsible for inducing its transcription at G2 phase of the cell cycle [26]. In additionthe levels of Aurora A are usually regulated during the cell cycle by two different processes, including ubiquitin-independent proteolysis [27]. Aurora A and its activator interact with Polo-like kinase 1 (Plk1) to initiate mitosis. However, in cells transformed with Aurora A, the mTOR pathway is activated [28]. Aurora A expression levels are high, and then rapidly decrease via degradation by the ubiquitin proteasome pathway [26].

Aurora A regulates the G2 to M phase transition. The commitment of cells to mitosis in late G2 phase involves the activation of both Aurora A and CDK1-cyclin B. This activation involves a feedback mechanism in which Aurora A activation requires CDK1-cyclin B activation. Aurora A has been shown to phosphorylate BRCA1 , and other studies have shown that BRCA1 is also localized to the centrosome and binds to γ-tubulin [30–31].

Several trials have revealed that in breast cancer cells, knockdown of Aurora A expression with a specific siRNA significantly attenuates tumor cell growth and increases apoptotic cell death. In addition, recent studies have added new insights into how Aurora A induces cell transformation. Under physiological conditions, Aurora A and its activator collaborate with Plk1 to initiate mitosis. In cells transformed with Aurora A, the mTOR pathway is activated [28]. The Aurora A protein has a variable amino terminal regulatory domain, with three putative aurora boxes (A boxes I, II, and III), and a conserved carboxyl terminal catalytic domain, with an activation motif and a destruction box [32].

Imen Ferchichi *et al* reported that 84.6% of non-tumoral tissues overexpress Aurora A. This observation supports the reasoning underlying malignant processing; although this tissue is morphologically healthy, it may have already begun to become cancerous. In addition, an association has been reported between high Aurora A expression in malignant tissue and positive nodal status [33]. Another retrospective analysis showed that high Aurora A expression is strongly associated with decreased survival (P = 0.0005), and in the multivariable analysis, Aurora A remained an independent prognostic marker [34–36].

Gene expression profiling has provided a large number of different signatures that are related to breast cancer prognosis. The results of a meta-analysis of publicly available breast cancer gene expression and clinical data by Wiripati P *et al* [37] underscored the important role of proliferation in breast cancer prognosis.

Aurora kinase B in breast cancer

Aurora B kinase belongs to the family of chromosome passenger proteins, which includes inner centrosome protein (INCENP), survivin, and borealin [38]. The *AURKB* gene is located at 17p13 [39]. The substrates of Aurora B include two mitotic checkpoint proteins BubR1 and Mad2. It is also widely expressed in normal proliferating cells, with maximum expression at G2/M phase of the cell cycle [40], and it is mostly activated by autophosphorylation after association with the passenger complex [41–42].

Aurora B is a chromosomal passenger protein that localizes to centromeres during prometaphase and subsequently relocates to midzone microtubules and midbodies during anaphase and telophase [43]. Aurora B has also been implicated in microtubule-kinetochore attachment by interacting with the kinetochore-specific histone H3 variant CENP-A [44]. Inhibition of Aurora B by RNA interference compromised the mitotic checkpoint, resulting in increased numbers of aneuploid cells [45]. In addition, inhibition of Aurora B by RNA interference showed that it is required for cytokinesis [46].

Some studies have shown that forced expression of Aurora B can enhance cellular transformation. For example, Aurora B expression in CHO cells was reported to promote aneuploidy and increase invasiveness in xenograft experiments [47]. Furthermore, Aurora B has been mapped to a chromosomal region that is known to contain tumor-associated amplicons [48].

Aurora B inhibitors, unlike classic antimitotics (e.g., kinesin inhibitors), do not induce mitotic arrest but instead result in a failure of cytokinesis, leading to cell death. Therefore, inhibitors of Aurora B would be expected to show clinical effects that are distinct from those of antitubulin compounds and other antimitotic drugs known to cause mitotic arrest. A pan-aurora kinase inhibitor, ZM447439, has been studied in breast cell lines, and the results showed cellular changes that most resemble a loss of Aurora B function [49]. Therefore, it is not difficult to infer that Aurora B is an effective drug target and predictor of survival.

Aurora kinase C in breast cancer

Aurora C, which is also known as Aurora 3, is the less well studied member of the family. It was initially thought to be restricted to testicular tissue, where it plays a role in meiosis and spermatogenesis [50]. However, it was also recently found that Aurora C also functions as a chromosomal passenger protein and might compensate for a loss of Aurora B function [51]. Although several studies have detected aberrant expression of Aurora C in colorectal, breast, and prostate cancers, knowledge regarding the relationship between Aurora C and cancer is limited [52].

Aurora kinases in different molecular subtypes of breast cancer

Breast cancer is not a homogeneous disease, thus it is necessary to differentiate among the different molecular subtypes. Estrogen receptor (ER), progesterone receptor (PR), and HER2 tyrosine kinase are major determinants of the molecular phenotype and dictate the course of treatment [53–54]. There are at least four subtypes of breast cancer: luminal A, luminal B, HER2-enriched, and basal-like, as well as a normal-like type, which show significant differences in terms of risk factors, incidence, baseline prognoses, and responses to systemic therapies [55]. To date, no consistent molecular predictor of response to aurora kinase inhibitors has been defined [56]. Thus, the subset of breast cancer patients that would most likely benefit from aurora kinase inhibitor treatment has yet to be identified. Therefore, new molecular biomarkers are greatly needed.

Xu J *et al* concluded that Aurora A is a potential therapeutic target for triple-negative breast cancer (TNBC), and inhibition of Aurora A kinase is a promising regimen for TNBC cancer therapy [57]. The results of a study by Diamond JR *et al* [58] also showed that Aurora kinase inhibitors exhibited robust anticancer activity in models of TNBC, and that aurora kinases are candidate predictive biomarkers. *In vitro*, the aurora kinase inhibitor AMG900 induced polyploidy and apoptosis and inhibited the growth of P-gp-expressing TNBC cells at nanomolar concentrations [59–60].

Aurora kinase A overexpression in ER+ cell lines showed that there is a strong relationship between aurora kinase and luminal a cell lines. Some researchers have suggested aurora kinases as standard clinical biomarker with molecular covariates that outperform other markers [61].

Table 1 Clinical trials of Aurora kinase inhibitors

Drug	Manufacturer	Targeted Aurora	Clinical trial	Main toxicities	Dose	Route	IC_{50}	Reference
AZD1152	Astra Zeneca	B	Phase II	Fibric neutrogena, stomatitis	50–1600 mg/d, 7 d	IV	1369 nma and 0.36 nmb	65
MLN-8237	Millennium	A, B	Phase II	Fibric neutrogena, fatigue, stomatitis, anemia	50 mg bid, 7 d	PO	61 nm	66
AT9283	Astex Therapeutics	A, B	Phase II	–	–	PO	3 nm	67
ENMD-2076	EntreMed	A, B	Phase II	Fatigue, lyphlitis, syncope	225–236 mg/d, 7 d	PO	25–700 μm	68
AMG900	Amgen	A, B, C	Phase I	–	3.75–15 mg/d	PO	0.6 nma and 18 nmb	69
VX-680	Pfizer	A, B	Phase I	–	–	PO		70
CYC116	Cyclacel	A, B	Phase I	–	–	PO	34–1370 nm	71
AS703569	Merck Sereno	A, B	Phase I	–	3–37 mg bid, 7 d	PO		72
MK5108	Merck	A	Phase I	–	–	PO	0.16–6.4 μm	73
MLN8237	Millennium Pharmaceuticals	A	Phase II	Neutrogena, asthenia, thrombocytopenia	50 mg bid, 7d	PO		74
SNS-314	——	A, B	Phase I		–		9 nma and 31 nmb	75

No reported in breast cancer inhibiters: XL228, kw-2249

Another study demonstrated the antineoplastic activity of the AZD1152-HQPA inhibitor in HER2-overexpressing cell lines. AZD1152-HQPA specifically inhibited Aurora B kinase activity in breast cancer cells, thereby causing mitotic catastrophe and polyploidy, which led to apoptosis [62]. Siggelkow *et al* showed an association between the ER+/HER2- molecular subtype and Aurora A. In contrast, Aurora A was not significantly associated with metastasis-free survival in ER-/HER2- and HER2+ carcinomas [63].

A study by Schmidt also revealed a strong correlation between Aurora A and proliferation metagenes. AURKA RNA levels were correlated with histological grade ($P < 0.001$) and tumor size ($P < 0.001$), and AURKA mRNA levels were higher in ER-/HER2- and HER2+ tumors, whereas expression was lower in ER+/HER2- carcinomas. AURKA, also the proliferation metagene was associated with MFI in ER+/HER2- but not in ER-/HER2- or HER2+ carcinomas [64].

Transcriptome-based analysis of primary breast cancers showed that increased expression of AURKA and AURKB is correlated with elevated proliferation, ER negativity, and primarily (but not exclusively) poorly differentiated non-luminal tumors.

Conclusion

Aurora kinases are emerging as potential therapeutic targets in breast cancer, and the combination of aurora kinase inhibitors with other drugs could enhance treatment effects. In addition, aurora kinase expression levels can predict tumor stage and prognosis.

Inhibition of aurora kinases greatly inhibits tumor cell growth in culture and xenograft studies. Therefore, inhibition of aurora kinases is an attractive novel therapeutic strategy for breast cancer. Aurora kinase inhibitors might delay the development of drug resistance and reverse resistance, and should allow for more effective treatment of patients with aurora kinase-overexpressing tumors who are at high risk for disease recurrence.

We discovered that aurora kinases are highly active in breast cancer cell lines and identified biomarkers that predict response to aurora kinase inhibitors *in vitro*. Specifically, TP53 loss of function cell lines. However, this observation requires clinical validation, by TP53 somatic mutation analysis and/or p21 expression, to identify the patients who are most likely to benefit from aurora kinase inhibitor treatment.

The roles of aurora kinases in the various molecular subtypes of breast cancer are still unclear, if we can determine the relationship between aurora kinases and different subtypes, we could predict the risk of recurrence and improve treatment.

Conflicts of interest

The authors indicated no potential conflicts of interest.

References

1. Rebecca Siegel, MPH, Deepa Naishadham, MA, MS, Ahmedin Jemal, DVM, PhD. Cancer Statistics, 2013. CA Cancer J CLIN 2013, 63:11–30
2. Desantis C, Ma J, Bryan L, *et al*. Breast Cancer Statistics, 2013. CA Cancer J Clin. 2013, Oct 1
3. Makar RS, Toth TL. The evaluation of infertility. Am J Clin Pathol,117: S95–S103.
4. Barron TI, Cahir C, Sharp L, *et al*. A nested case-control study of adjuvant hormonal therapy persistence and compliance, and early breast cancer recurrence in women with stage I-III breast cancer. Br J Cancer, 2013, 109: 1513–1521.
5. Sestak I, Dowsett M, Zabaglo L, *et al*. Factors predicting late recurrence for estrogen receptor-positive breast cancer. J Natl Cancer Inst, 2013,105: 1504–1511.
6. Zhang M, Zhang X, Zhao S, *et al*. Prognostic value of survivin and EGFR protein expression in triple-negative breast cancer (TNBC) patients. Target Oncol, 2014, 9: 349–357.
7. Jelovac D, Emens LA. HER2-directed therapy for metastatic breast cancer. Oncology, 2013, 27: 166–175.
8. Bischoff JR, Plowman GD. The Aurora/Ipl1p kinase family: regulators of chromosome segregation and cytokinesis. Trends Cell Biol, 1999, 9: 454–459.
9. Glover DM, Leibowitz MH, McLean DA, *et al*. Mutations in aurora prevent centrosome separation leading to the formation of monopolar spindles. Cell, 1995, 81: 95–105.
10. Carmena M, Earnshaw WC. The cellular geography of Aurora kinases. Nat Rev Mol Cell Biol, 2003, 4: 842–854.
11. Bischoff JR, Anderson L, Zhu Y, *et al*. A homologue of Drosophila aurora kinase is oncogenic and amplified in human colorectal cancers. EMBO J, 1998, 17: 3052–3065.
12. Fu J, Bian M, Jiang Q, Zhang C. Roles of Aurora kinases in mitosis and tumorigenesis. Mol Canc Res, 2007, 5: 1–10.
13. Wang X, Zhou YX, Qiao W, *et al*. Overexpression of Aurora kinase A in mouse mammary epithelium induces genetic instability preceding mammary tumor formation. Oncogene, 2006, 25: 7148–7158.
14. Marumoto T, Zhang D, Saya H. Aurora-A – A guardian of poles. Nat Rev Cancer, 2005, 5: 42–50.
15. Ye D, Garcia-Manero G, Kantarjian HM, *et al*. Analysis of Aurora kinase A expression in CD34(+) blast cells isolated from patients with myelodysplastic syndromes and acute myeloid leukemia. J Hematop, 2009, 2: 2–8.
16. Kimmins S, Crosio C, Kotaja N, *et al*. Differential functions of the Aurora-B and Aurora-C kinases in mammalian spermatogenesis. Mol Endocrinol, 2007, 21: 726–739.
17. Fukushige S, Waldman FM, Kimura M, *et al*. Frequent gain of copy number on the long arm of chromosome 20 in human pancreatic adenocarcinoma. Genes Chromosomes Cancer,1997, 19: 161–169.
18. Wang LH, Xiang J, Yan M. The mitotic kinase Aurora-A induces mammary cell migration and breast cancer metastasis by activating the Cofilin-F-actin pathway. Cancer Res, 2010, 70: 9118–9128.
19. Kollareddy M, Zheleva D, Dzubak P, *et al*. Aurora kinase inhibitors: progress towards the clinic. Invest New Drugs, 2012, 30: 2411–2432.
20. Kelly KR, Ecsedy J, Mahalingam D, *et al*. Targeting Aurora kinases in

cancer treatment. Curr Drug Targets, 2011, 12: 2067–2078.
21. T. Marumoto, D. Zhang, H. Saya, Aurora A-a guardian of poles. Nat Rev Cancer, 2005, 5: 42–50.
22. Sen S, Zhou H, White RA. A putative serine/threonine kinase encoding gene BTAK on chromosome 20q13 is amplified and overexpressed in human breast cancer cell lines. Oncogene, 1997, 14: 2195–2200.
23. Marumoto T, Honda S, Hara T, *et al*. Aurora-A kinase maintains the fidelity of late and early mitotic events in HeLa cells. J Bio Chem, 2004, 278: 51786–51795.
24. Saeki T, Ouchi M, Ouchi T. Physiological and oncogenic Aurora-A pathway. Int J Biol Sci, 2009, 5: 758–762.
25. Tanaka E, Hashimoto Y, Ito T, *et al*. The clinical significance of Aurora-A/STK15/BTAK expression in human esophageal squamous cell carcinoma. Clin Cancer Res, 2005, 1: 1827–1834.
26. Bischoff JR, Anderson L, Zhu Y, *et al*. A homologue of Drosophila aurora kinase is oncogenic and amplified in human colorectal cancers. EMBO J, 1998, 17: 3052–3065.
27. Littlepage LE, Ruderman JV. Identification of a new APC/C recognition domain, the A box, which is required for the Cdh1-dependent destruction of the kinase aurora-A during mitotic exit. Genes Dev 2002, 16: 2274–2285.
28. Taga M, Hirooka E, Ouchi T. Essential roles of mTOR/Akt pathway in Aurora-A cell transformation. Int J Biol Sci, 2009, 19: 444–450.
29. Taguchi Si, Honda K, Sugiura K, *et al*. Degradation of human Aurora-A protein kinase is mediated by hCdh1. FEBS Lett, 2002, 519: 59–65.
30. Xu X, Weaver Z, Linke SP, *et al*. Centrosome amplification and a defective G2-M cell cycle checkpoint induce genetic instability in BRCA1 exon 11 isoform-deficient cells. Mol Cell, 1999, 3: 389–395.
31. Anand S, Penrhyn-Lowe S, Venkitaraman AR, *et al*. Aurora-A amplification overrides the mitotic spindle assembly checkpoint, inducing resistance to Taxol. Cancer Cell, 2003. 3: 51–62.
32. Wang X, Zhou YX, Qiao W, *et al*. Overexpression of aurora kinase A in mouse mammary epithelium induces genetic instability preceding mammary tumor formation. Oncogene, 2006, 25: 7148–7158.
33. Imen F, Samia SH, Amal B, *et al*. Assessment of Aurora A kinase expression in close neighbour normal tissue with breast cancer.A tool for early diagnosis. Dis Markers, 2013, 34: 63–69.
34. Nadler Y, Camp RL, Schwartz C. Expression of Aurora A (but not Aurora B) is predictive of survival in breast cancer. Clin Cancer Res, 2008, 14: 4455–4462.
35. Ali HR, Dawson SJ, Blows FM. Aurora kinase A outperforms Ki67 as a prognostic markerin ER-positive breast cancer. Br J Cancer, 2012, 106: 1798–1806.
36. Siggelkow W, Boehm D, Gebhard S. Expression of aurora kinase A is associated with metastasis-free survival in node-negative breast cancer patients. BMC Cancer, 2012, 12: 562.
37. Wirapati P, Sotiriou C, Kunkel S, *et al*. Meta-analysis of gene expression profiles in breast cancer:toward a unified understanding of breast cancer subtyping and prognosis signatures. Breast Cancer Res, 2008,10: R65.
38. Mancini M, Leo E, Aluigi M, *et al*. Gadd45a transcriptional induction elicited by the Aurora kinase inhibitor MK-0457 in Bcr-Abl-expressing cells is driven by Oct-1 transcription factor. Leuk Res, 2012, 36: 1028–1034.
39. Vader G, Medema RH, Lens SM. The chromosomal passenger complex: guiding Aurora-B through mitosis. J Cell Biol, 2006, 173: 833–837.
40. Adams RR, Carmena M, Earnshaw WC. Chromosomal passengers and the (aurora) ABCs of mitosis. Trends Cell Biol, 2001, 11: 49–54.
41. Speliotes EK, Uren A, Vaux D, *et al*. The survivin-likeC. elegansBIR-1 protein acts with the Auroralike kinase AIR-2 to affect chromosomes and the spindle midzone. Mol Cell, 2006, 6: 211–223.
42. Sampath SC, Ohi R, Leismann O, *et al*. The chromosomal passenger complex is required for chromatin-induced microtubule stabilization and spindle assembly. Cell, 2004, 118: 187–202.
43. Kimura M, Matsuda Y, Yoshioka T, *et al*. Identification and characterization of STK12/Aik2: a human gene related to aurora of Drosphila and yeast IPL1, Cytogenet. Cell Genet, 1998, 82: 147–152.
44. Zeitlin SG, Shelby RD, Sullivan KF. CENP-A is phosphorylated by Aurora B kinase and plays an unexpected role in completion of cytokinesis. J Cell Biol, 2001, 155: 1147–1157.
45. Morrow CJ, Tighe A, Johnson VL, *et al*. Taylor, Bub1 and aurora B cooperate to maintain BubR1-mediated inhibition of APC/CCdc20. J Cell Sci, 2005, 118: 3639–3652.
46. Giet R, Glover DM. Drosophilaaurora B kinase is required for histone H3 phosphorylation and condensing recruitment during chromosome condensation and to organize the central spindle during cytokinesis, J Cell Biol, 2001, 152: 669–682.
47. Vader G, Medema RH, Lens SM. The chromosomal passenger complex: guiding Aurora-B through mitosis. J Cell Biol, 2006, 173: 833–837.
48. Kanda A, Kawai H, Suto S, *et al*. Aurora-B/AIM-1 kinase activity is involved in Ras-mediated cell transformation. Oncogene, 2005, 24: 7266–7272.
49. Cochran AG. Aurora A: target invalidated? Chem Biol, 2008,15: 525–526.
50. Tang CJ, Lin CY, Tang TK. Dynamic localization and functional implications of Aurora-C kinase during male mouse meiosis. Dev Biol, 2006, 290: 398–410.
51. Sasai K, Katayama H, Stenoien DL, *et al*. Aurora-C kinase is a novel chromosomal passenger protein that can complement Aurora-B kinase function in mitotic cells. Cell Motil Cytoskeleton, 2004, 59: 249–263.
52. Takahashi T, Futamura M, Yoshimi N, *et al*. Centrosomal kinases, HsAIRK1 and HsAIRK3, are overexpressed in primary colorectal cancers. Jpn J Cancer Res, 2000, 91: 1007–1014.
53. Perez EA, Romond EH, Suman VJ, *et al*. Four-year follow-up of trastuzumab plus adjuvant chemotherapy for operable human epidermal growth factor receptor 2-positive breast cancer: joint analysis of data from NCCTG N9831 and NSABP B-31. J Clin Oncol, 2011, 29: 3366–3373.
54. Desmedt C, Haibe-Kains B, Wirapati P, *et al*. Biological processes associated with breast cancer clinical outcome depend on the molecular subtypes. Clin Canc Res, 2008,14: 5158–5165.
55. Prat A, Perou CM. Deconstructing the molecular portraits of breast cancer. Mol Oncol, 2011, 5: 5–23.
56. Diamond JR, Eckhardt SG, Tan AC, *et al*. Predictive biomarkers of sensitivity to the aurora and angiogenic kinase Inhibitor ENMD-2076 in preclinical breast cancer models. Clin Cancer Res, 2013, 19: 291–303.
57. Xu J, Wu X, Zhou WH, *et al*. Aurora-A identifies early recurrence and poor prognosis and promises a potential therapeutic target in triple negative breast cancer. PLoS One, 2013, 8: e56919.
58. Diamond JR, Eckhardt SG, Tan AC. Predictive biomarkers of sensitivity to the aurora and angiogenic kinase inhibitor ENMD-2076 in preclinical breast cancer models. Clin Cancer Res, 2013, 19: 291–303.
59. HR Ali, Dawson SJ, Blows FM. Aurora kinase A outperforms Ki67 as a prognostic marker in ER-positive breast cancer. Br J Cancer, 2012, 106:1798–1806.

60. Burtness B, Bauman JE, Galloway T. Novel targets in HPV-negative head and neck cancer: overcoming resistance to EGFR inhibition. Lancet Oncol, 2013, 14: 302–309.
61. Blows FM, Dawson SJ, Blows FM, *et al*. Aurora kinase A outperforms Ki67 as a prognostic marker in ER-positive breast cancer. Br J Cancer, 2012, 106: 798–806.
62. Miyoshi Y, Iwao K, Egawa C, *et al*. Association of centrosomal kinase STK15/BTAK mRNA expression with chromosomal instability in human breast cancers. Int J Cancer, 2001, 92: 370–373.
63. Siggelkow W, Boehm D, Gebhard S, *et al*. Expression of aurora kinase A is associated with metastasis-free survival in node-negative breast cancer patients. BMC Cancer, 2012,12: 562.
64. Curtis C, Shah SP, Chin SF, *et al*. The genomic and transcriptomic architecture of 2,000 breast tumours reveals novel subgroups. Nature, 2012, 486: 346–352.
65. Renshaw JS, Patnaik A, Gordon M *et al*. A phase I two arm trial of AS703569 (R763), an orally available aurora kinase inhibitor, in subjects with solid tumors: preliminary results. J Clin Oncol, 2007, 25: 14130.
66. Cervantes-Ruiperez A, Elez ME, Rosello S, *et al*. Phase I pharmacokinetic (PK) and pharmacodynamic (PD) study of MLN8237, a novel selective aurora A kinase (AAK) inhibitor, in patients (pts) with advanced solid tumors. J Clin Oncol, 2009, 27: 2565.
67. Infante J, Dees EC, Cohen RB *et al*. Phase I study of the safety, pharmacokinetics (PK), and pharmacodynamics (PD) of MLN8237, a selective aurora A kinase inhibitor, in the United States. Eur J Cancer Suppl, 2008, 6: 280.
68. Kristeleit R, Calvert H, Arkenau H, *et al*. A phase I study of AT9283, an aurora kinase inhibitor, in patients with refractory solid tumors. J Clin Oncol, 2009, 27: 2566.
69. How J, Yee K. ENMD-2076 for hematological malignancies. Expert Opin Investig Drugs, 2012, 21: 717–732.
70. Zhang S, Farag SS. From cell biology to therapy: ENMD-2076 in the treatment of multiple myeloma. Expert Opin Investig Drugs, 2011, 20: 1015–1028.
71. Be X, Moore ES, Zhao Z. LC-MS/MS bioanalytical method development for AMG 900: resolution of an isobaric interference in rodent in vivo studies. J Pharm Biomed Anal, 2013, 74: 171–177.
72. Payton M, Bush TL, Chung G. Preclinical evaluation of AMG 900, a novel potent and highly selective pan-aurora kinase inhibitor with activity in taxane-resistant tumor cell lines. Cancer Res, 2010, 70: 9846–9854.
73. Papayannidis C, Iacobucci I, Soverini S, *et al*. Innovative phase I study of concomitant and consecutive treatment with dasatinib and MK-0457 in refractory PhCML and ALL patients. J Clin Oncol, 2009, 27: 7080.
74. Wang S, Midgley CA, Scaërou F. Discovery of N-phenyl-4-(thiazol-5-yl)pyrimidin-2-amine aurora kinase inhibitors. J Med Chem, 2010, 53: 4367–4378.
75. Shi HB, Li HB, Lu KQ. Synthesis of novel thiazolyl-pyrimidines and their anticancer activity in vitro. Arch Pharm, 2011, 344: 675–683.

DOI 10.1007/s10330-018-0315-5
Cite this article as: Yiliyaer, Yusufu Maimaiti. Aurora kinases: novel anti-breast cancer targets. Oncol Transl Med, 2019, 5: 43–48.

Oncology and Translational Medicine
DOI 10.1007/s10330-018-0319-9
February 2019, Vol. 5, No. 1, P49–P51

CASE REPORT

A case of prostate embryonal rhabdomyosarcoma in an adult patient

Qi Wei (✉), Zhiyong Sun

Department of Urology, East District of First Affiliated Hospital of Anhui Medical University, (Feidong People's Hospital), Hefei 230001, China

Received: 18 November 2018
Revised: 12 December 2018
Accepted: 13 January 2019

Abstract

Prostate embryonal rhabdomyosarcoma (ERMS) is characterized by a high degree of malignancy, both local rapid growth with formation of large pelvic masses, often leading to renal failure due to urethral obstruction, and systemic spread, commonly to the lungs, liver, and bone. ERMS of the prostate is a commonly occurring tumor in infants and children. It is rarely seen in adults. Here, we report on a case of the prostate ERMS in a 27-year-old man.

Key words: prostate; embryonal rhabdomyosarcoma; surgery

Rhabdomyosarcoma (RMS) is a commonly occurring cancer in children, representing more than 50% of all soft tissue sarcomas. However, RMS of the prostate is a very rarely found malignancy in adults [1]. Histologically, three subtypes of RMS have been identified: alveolar histiotypic, pleomorphic, and embryonal growth pattern, including its rare spindle cell variant [2]. To date, there have been few reports on sarcoma manifesting as prostate ERMS. Clinical experience in treating adult RMS is limited to isolated cases reported in literature [3]. Here, we present a case of an adult patient with ERMS of the prostate.

Case report

A 27-year-old male presented with history of progressively increasing dysuria and obstructive voiding symptoms for the past 1 month. Fifteen days ago, he found blood in urine. Hemogram and biochemical parameters were within normal limits, without fever, back pain, nausea, vomiting, and other symptoms. BLD was 200 cells/μL. Prostate specific antigen (PSA) concentration was 1.10 ng/mL. Digital rectal examinations: Touched huge and hard mass, inactivities, boundary touch unclear. Ultrasound examination revealed irregular hypoechoic mass in the prostate area. A pelvic computed tomography (CT) scan was then performed, disclosing a 5.8 cm × 5.0 cm × 4.5 cm heterogeneous soft tissues mass rising from the prostrate, with disruption of the prostate anatomy and suspected infiltration of the bladder base and rectal wall. The patient underwent a transrectal biopsy of the prostate before he underwent suprapubic prostatectomy.

Pathological findings

Transrectal biopsy of the prostate revealed spindle cell malignant tumors, indicating spindle cell rhabdomyosarcoma. Immunohistochemical staining was positive for Vim, SMA, Des, h-caldesmon, Myogenin, CD99, bcl-2, and CD45, but negative for EMA, CK, S100, and CD34. Postoperative pathology showed prostate ERMS. The tumor was composed of small round cells and spindle shaped cells and rhabdomyoblasts were visible. Immunohistochemical staining was positive for Myogenin, Vim, CD99, Des, and WT-1, but negative for MyoD1 and CK.

Therapy and further course

A midline, extraperitoneal, lower abdominal incision was made extending from the umbilicus to the pubis. A huge, solid, and hard tumor, with rough surface, occupying most of pelvic, infiltrated bladder neck and bilateral seminal vesicle without infiltrating the rectum. Surgical

✉ Correspondence to: Qi Wei. Email: michaelqw@126.com

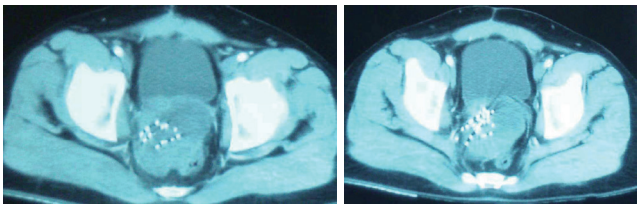

Fig. 1 CT showing radiotherapy (^{125}I seeds implantation)

options consisted of complete excision of the prostate tumor and bilateral seminal vesicle, partial resection of the bladder neck, and monitoring the protection of the rectum. The patient underwent chemotherapy (Vincristine, Actinomycin D, Cyclophosphamide) after surgery. However, after ten months, tumor recurrence was observed by clinical and CT examination. Tumor size was approximately 6.7 cm × 5.5 cm × 4.0 cm. Positron emission tomography-computed tomography (PET-CT) showed that the tumor was limited to the pelvic region without organ metastasis .Then the patient underwent radiotherapy (^{125}I seeds implantation); however, two months later, the tumor mass did not reduce. The patient reported with body pain, dysuria, and constipation. His general condition deteriorated and he had to take oral painkillers and laxative. This patient's condition was followed-up for 2 years.

Discussion

The incidence of prostate sarcoma is reported to be 0.1%–0.2% among primary prostate malignancies in adults; long-term survival for adult patients with prostate sarcoma is poor [4]. It grows rapidly and partially invades adjacent tissues, such as the bladder base or rectal wall. Patients with prostate rhabdomyosarcoma mostly present with dysuria or obstructive micturition problems [5]. In some patients, the compression of the rectum can cause constipation, rectal bleeding, and a sense of rectal fullness [6].

There is no pathognomonic radiological finding for prostate ERMS, and CT scan and MRI study revealed a large soft tissue mass with necrotic regions replacing the whole prostate; however, the radiological differential diagnosis with prostate adenocarcinoma can be very difficult [7]. The diagnosis is usually performed with a transrectal, perineal, or transurethral biopsy. Our patient underwent transrectal biopsy, and the histopathological analysis revealed spindle cell RMS of the prostate. Despite surgical contraindications, he underwent suprapubic prostatectomy. Postoperative pathology showed prostate ERMS. N J Sebire [8] reported that the immunohistochemical staining of pediatric rhabdomyosarcomas, with antibodies against MyoD and myogenin, provides sensitive and specific diagnostic information. Myogenin immunostaining is usually more clinically useful because it is more consistent and is associated with less nonspecific staining. Besides, younger age, normal PSA, large tumor volume, and poorly differentiated tumors help indicate prostate sarcoma.

The prognosis for patients with prostate ERMS is generally poor. In a clinical situation of an organ-confined disease, radical surgical extirpation should be performed [9]. The goal of surgery should be complete removal of disease, which usually requires radical cystoprostatectomy and pelvic extentaration [10]. As an alternative to surgery, radiotherapy and chemotherapy might be useful to achieve local treatment with organ function preservation and good quality of life. The major role of chemotherapy in this tumor location is the reduction of the primary tumor mass in order to assist with local therapy as well as to avoid tumor progression and the development of distant metastases [11]. Radiochemotherapy, alone as a local treatment, seems to be optimal especially in patients with smaller tumors and a good response to neoadjuvant chemotherapy [12]. But there are several relevant concerns about chemotherapy. Fryer reported that radiation therapy contributes to post-treatment morbidity. Another disadvantage is the fact that surgery is even more complicated after radiotherapy [13].

In conclusion, prostate ERMS requires a multidisciplinary treatment approach. At present, there is no standard treatment of prostate RMS in adults due to small number of cases. Some tumors in patients with postradiation sarcoma may be refractory to treatment with chemotherapy[1]. We, therefore, suggest that early radical resection prior to chemotherapy must be considered for such patients. Chemotherapy combined with radiation therapy should be adjunct to surgery to prevent local and distant recurrences. The severity of the disease needs to be informed to the patients and their family members before surgery and the patients need close follow-up after surgery.

References

1. Niimi K, Hashimoto Y, Kurokawa S, *et al*. Embryonal rhabdomyosarcoma of the prostate. Int J Clin Oncol, 2010, 15: 93–96.
2. Mentzel T, Kuhnen C. Spindle cell rhabdomyosarcoma in adults: clinicopathological and immunohistochemical analysis of seven new cases. Virchows Arch, 2006, 449: 554–560.
3. Little DJ, Ballo MT, Zagars GK, *et al*. Adult rhabdomyosarcoma: outcome following multimodality treatment. Cancer, 2002, 95: 377–388.
4. Young MD, Dahm P, Robertson CN. Prostatic sarcoma with rapid tumor progression after nerve sparing radical cystoprostatectomy. J Urol, 2001, 166: 994.
5. Bisceglia M, Magro G, Carosi I, *et al*. Primary embryonal rhabdomyosarcoma of the prostate in adults: report of a case and review of the literature. Int J Surg Pathol, 2011, 19: 831–837.

6. Tannenbaum M. Sarcomas of the prostate gland. Urology, 1975, 5: 810–814.
7. Ciammella P, Galeandro M, D'Abbiero N, *et al*. Prostate embryonal rhabdomyosarcoma in adults: Case report and review of literature. Rep Pract Oncol Radiother, 2013, 18: 310–315.
8. Sebire NJ, Malone M. Myogenin and MyoD1 expression in paediatric rhabdomyosarcomas. J Clin Pathol, 2003, 56: 412–416.
9. Sexton WJ, Lance RE, Reyes AO, *et al*. Adult prostate sarcoma: the M. D. Anderson Cancer Center Experience. J Urol, 2001, 166: 521–525.
10. Nabi G, Dinda AK, Dogra PN. Primary embryonal rhabdomyosarcoma of prostate in adults: diagnosis and management. Int Urol Nephrol, 2002, 34: 531–534.
11. Modritz D, Ladenstein R, Potschger U, *et al*. Treatment for soft tissue sarcoma in childhood and adolescence. Austrian results within the CWS 96 study. Wien Klin Wochenschr, 2005, 117: 196–209.
12. Dantonello TM, Int-Veen C, Harms D, *et al*. Cooperative trial CWS-91 for localized soft tissue sarcoma in children, adolescents, and young adults. J Clin Oncol, 2009, 27: 1446–1455.
13. Fryer CJ. Pelvic rhabdomyosarcoma: paying the price of bladder preservation. Lancet, 1995, 345: 141–142.

DOI 10.1007/s10330-018-0319-9
Cite this article as: Wei Q, Sun ZY. A case of prostate embryonal rhabdomyosarcoma in an adult patient. Oncol Transl Med, 2019, 5: 49–51.

Oncology and Translational Medicine

Aims & Scope

Oncology and Translational Medicine is an international professional academic periodical. The Journal is designed to report progress in research and the latest findings in domestic and international oncology and translational medicine, to facilitate international academic exchanges, and to promote research in oncology and translational medicine as well as levels of service in clinical practice. The entire journal is published in English for a domestic and international readership.

Copyright

Supervised by

Ministry of Education of the People's Republic of China.

Administered by

Tongji Medical College, Huazhong University of Science and Technology.

Submission information

Manuscripts should be submitted to:
http://otm.tjh.com.cn
dmedizin@sina.com

Subscription information

ISSN edition: 2095-9621
CN: 42-1865/R

■ Subscription rates
Subscription may begin at any time. Remittances made by check, draft or express money order should be made payable to this journal. The price for 2017 is as follows: US $ 30 per issue; RMB ￥28.00 per issue.

Database

Oncology and Translational Medicine is abstracted and indexed in EMBASE, Index Copernicus, Chinese Science and Technology Paper Citation Database (CSTPCD), Chinese Core Journals Database, Chinese Journal Full-text Database (CJFD), Wanfang Data; Weipu Data; Chinese Academic Journal Comprehensive Evaluation Database.

Business correspondence

All matters relating to orders, subscriptions, back issues, offprints, advertisement booking and general enquiries should be addressed to the editorial office.

Mailing address
Editorial office of
Oncology and Translational Medicine
Tongji Hospital
Tongji Medical College
Huazhong University of Science and Technology
Jie Fang Da Dao 1095
430030 Wuhan, China
Tel.: +86-27-69378388
Email: dmedizin@sina.com

Printer
Changjiang Spatial Information Technology Engineering Co., Ltd. (Wuhan)
Hangce Information Cartorgraphy Printing Filial, Wuhan, China
Printed in People's Republic of China

Managing director

Executive editors